ACTA FORESTALIA FENNICA

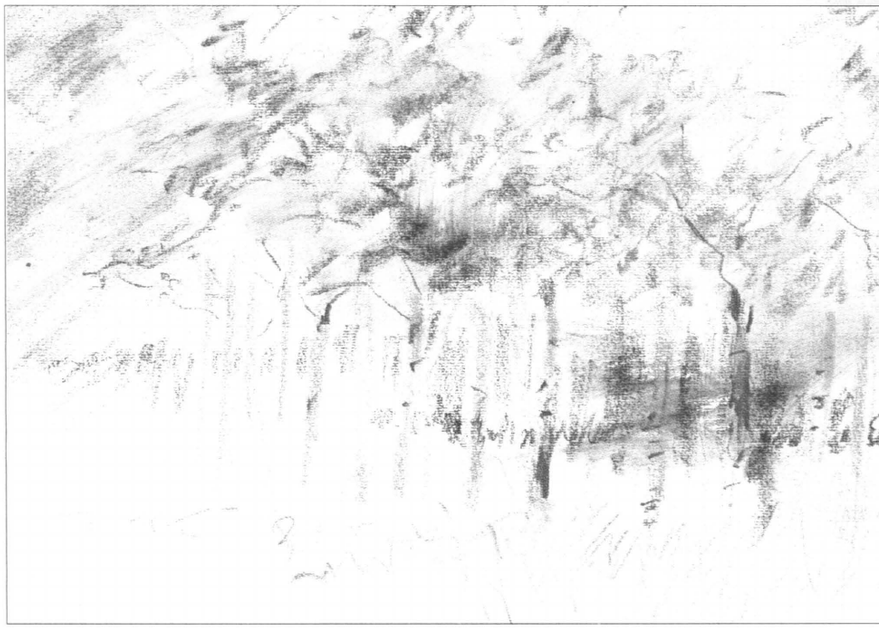

Edited by
Pertti Hari, Juhan Ross and Marja Mecke

Production Process of Scots Pine; Geographical Variation and Models

254 · 1996

ACTA FORESTALIA FENNICA

Publishers The Finnish Society of Forest Science
The Finnish Forest Research Institute

Editors Editor-in-chief Eeva Korpilahti
Production editors Tommi Salonen, Seppo Oja

Editorial Office Unioninkatu 40 A, FIN-00170 Helsinki, Finland
Phone +358 9 857 051, Fax +358 9 625 308, E-mail silva.fennica@metla.fi,
WWW http://www.metla.fi/publish/acta/

Aim and Scope Acta Forestalia Fennica publishes monographs in forest science. These may be original research articles or comprehensive reviews aiming at a synthesis of knowledge in a particular topic. The series covers all aspects of forest science, both basic and applied subjects. Manuscripts are subject to peer review.

ACTA FORESTALIA FENNICA

254 · 1996

Edited by
Pertti Hari, Juhan Ross and Marja Mecke

Production Process of Scots Pine; Geographical Variation and Models

The Finnish Society of Forest Science — The Finnish Forest Research Institute

Hari, P., Ross, J. & Mecke, M. (eds.). 1996. Production process of Scots pine; geographical variation and models. Acta Forestalia Fennica 254. 121 p.

The accompanying collective research report is the result of the research project in 1986–90 between The Finnish Academy and the former Soviet Academy of Sciences. The project was organized around common field work in Finland and in the former Soviet Union and theoretical analyses of tree growth determining processes. Based on theoretical analyses, dynamic stand growth models were made and their parameters were determined utilizing the field results.

Annual cycle affects the tree growth. Our theoretical approach was based on adaptation to local climate conditions from Lapland to South Russia. The initiation of growth was described as a simple low and high temperature accumulation driven model. Linking the theoretical model with long term temperature data allowed us to analyze what type of temperature response produced favorable outcome in different climates. Initiation of growth consumes the carbohydrate reserves in plants. We measured the dynamics of insoluble and soluble sugars in the very northern and Karelian conditions. Clear cyclical pattern was observed but the differences between locations were surprisingly small.

Analysis of field measurements of CO_2 exchange showed that irradiance is the dominating factor causing variation in photosynthetic rate in natural conditions during summer. The effect of other factors is so small that they can be omitted without any considerable loss of accuracy. A special experiment carried out in Hyytiälä showed that the needle living space, defined as the ratio between the shoot cylindric volume and needle surface area, correlates with the shoot photosynthesis.

The penetration of irradiance into Scots pine canopy is a complicated phenomenon because of the movement of the sun on the sky and the complicated structure of branches and needles. A moderately simple but balanced forest radiation regime submodel was constructed. It consists of the tree crown and forest structure, the gap probability calculation and the consideration of spatial and temporal variation of radiation inside the forest.

The common field excursions in different geographical regions resulted in a lot of experimental data of regularities of woody structures. The water transport seems to be a good common factor to analyse these properties of tree structure. There are evident regressions between cross-sectional areas measured at different locations along the water pathway from fine roots to needles. The observed regressions have clear geographical trends. For example, the same cross-sectional area can support three times higher needle mass in South Russia than in Lapland. Geographical trends can also be seen in shoot and needle structure. Analysis of data published by several Russian authors show, that one ton of needles transpire 42 ton of water a year. This annual amount of transpiration seems to be independent of geographical location, year and site conditions.

The produced theoretical and experimental material is utilised in the development of stand growth model that describes the growth and development of Scots pine stands in

ISBN 951-40-1544-4
ISSN 0001-5636
Tampere 1996, Tammer-Paino Oy

Finland and the former Soviet Union. The core of the model is carbon and nutrient balances. This means that carbon obtained in photosynthesis is consumed for growth and maintenance and nutrients are taken according to the metabolic needs. The annual photosynthetic production by trees in the stand is determined as a function of irradiance and shading during the active period. The utilisation of the annual photosynthetic production to the growth of different components of trees is based on structural regularities.

Since the fundamental metabolic processes are the same in all locations the same growth model structure can be applied in the large range of Scots pine. The annual photosynthetic production and structural regularities determining the allocation of resources have geographical features. The common field measurements enable the application of the model to the analysis of growth and development of stands growing on the five locations of experiments.

The model enables the analysis of geographical differences in the growth of Scots pine. For example, the annual photosynthetic production of a 100-year-old stand at Voronez is 3.5 times higher than in Lapland. The share consumed to needle growth (30 %) and to growth of branches (5 %) seems to be the same in all locations. In contrast, the share of fine roots is decreasing when moving from north to south. It is 20 % in Lapland, 15 % in Hyytiälä Central Finland and Kentjärvi Karelia and 15 % in Voronez South Russia. The stem masses (115–113 ton/ha) are rather similar in Hyytiälä, Kentjärvi and Voronez, but rather low (50 ton/ha) in Lapland. In Voronez the height of the trees reach 29 m being in Hyytiälä and Kentjärvi 22 m and in Lapland only 14 m.

The present approach enables utilization of structural and functional knowledge, gained in places of intensive research, in the analysis of growth and development of any stand. This opens new possibilities for growth research and also for applications in forestry practice.

Keywords Scots pine, photosynthesis, annual cycle, irradiance, structure, stand models, geographical features, allocation
Correspondence *Hari* University of Helsinki, Dept. of Forest Ecology, Unioninkatu 40 B, FIN-00014 Helsingin yliopisto
Telefax +358-9-191 7605 **E-mail** pertti.hari@helsinki.fi
Accepted 27 November 1996

Contents

Preface

The increasing use of quantitative methods has been characteritic for the studies of forest functions and growth during the last 30–40 years. Physicists, mathemathicians, meteorologists and peoples from other exact sciences have entered the field.

A research group of phytoactinometrists under the leadership of J. Ross started to work in 1960's in Tartu at the Institute of Astrophysics and Atmospheric Physics of the Academy of Sciences of the Estonian S.S.S.R. This group consisted of physicists and mathemathicians and they studied the radiation regime of plant stands using optical measurements and mathematical modeling of radiative transfer in crops. Later this group started to study the influence of meteorological factors on the leaf photosynthesis and to deal also with mathematical modeling of crop production process.

In late sixties and early seventies, a research group grew in the Department of Silviculture, University of Helsinki. P. Hari had a key role in the group. At first, the main emphasis in the research was towards the basic functions of trees, ie. photosynthesis, transpiration and shoot elongation. Field measurements were analysed using dynamic models. The focus was extended to stand development in the midle of seventies. Later the effects of changing environmental factors on forest functions and growth was also included into the research program. The use of modern measuring instrumentation and modelling was characteristic for the research approach in the group.

Independently from above mentioned groups, a researtch group started to work under the leadership of L. Kaipiainen in 1971 in Petrozavodsk at the Forest Institute of the Karelian Branch, Acadedy of Science,U.S.S.R. The focus in the research was in forest micrometeorology and water movement in the soil-tree-atmosphere system. This group consists also mostly of physicists.

In the year 1975, scientific contacts arose between these groups. Discussion showed that methodological basis and research style of all groups have similar features, namely they

(i) studied the production process of different canopies and the influence of environmental factors on this process
(ii) used mathematical modeling for describing the processes under study
(iii) used modern physical and chemical methods in field study
(iiii) built new instruments and equipments in field study

Active contacts were quickly built despite the complications caused by the soviet system. The research were included for five years in the Finnish Soviet co-operation for science between the academies for the first five yer period 1981–1985 under the tittle "Structure, Radiation and Production in Coniferous Stand". Research report by Hari et al. in 1985 was published as a result cooperation.

In 1986–1990 the project was continued under the title "Growth and Development of Pine Forest". A new organizations joined the project – the Forest Faculty of the University of Joensuu. This monograph is summary of the work during the second period.

The project was established as Finnish Sovjet co-operation and finalized as co-operation between Finland, Estonia and Russia. We want to thank The Finnish Academy, The Estonian Academy of Scieces and The Russian Academy of Sciences who have supported the project.

Pertti Hari, Leo Kaipiainen, Paavo Pelkonen and Juhan Ross

1 Introduction

Pertti Hari

1.1 Background

The range of Scots pine is very large, extending from Lapland in the north where Scots pine grows on the timberline to North Italy and Spain in the south. The area is still wider in an east-west direction, extending from Scotland to areas close to the Pacific Ocean. Poor soils are characteristic of the stands. Scots pine can grow also on fertile sites but there other species are often stronger competitors and replace it, especially in more southern conditions.

The fundamental structure of Scots pine is the same over the whole growing area as is natural for a single species. The needles are in a pair or sometimes in triplets, the structure of woody components and of the root system are the same. Similarities can be found also in the fine structure of each organelle.

The main metabolic processes function in a similar manner over its entire range. The basic processes, such as photosynthesis and nutrient uptake are carried out by similar biochemical and tissue structures in all Scots pine trees. Thus the linkage between environment and production or consumption of materials in metabolic processes should be, at least intuitively, qualitatively similar for all Scots pines.

The appearance of pine trees in the southern stands, however, differs clearly from that in northern ones. The southern pines have thick branches, the stem is not straight and the canopy is thin, while the northern trees have thin branches, a straight stem and deep canopy. The details of fine structure may also differ from each other. For example, the cell size and thickness of cell walls can differ in the north from those in the south, showing adaptability in the structure within the same tree species.

There are also great qualitative differences in the functioning of pine trees within this wide range. The southern pines blossom when the northern ones are still dormant and all metabolism is greatly reduced. This is caused by the warmer climate in the south. There are also evident differences in the water metabolism between the southern and northern sites, caused to great extent by the differences in the environment.

The pines have adapted after the ice age to the prevailing climate within their range. Thus the differences in the structures and functions may reflect the climatic conditions of the particular region after the ice age, but may also be acclimatization to the present environment.

The growth and development of pine stands are based on the structures of trees and on the functioning of the structure. Since the fundamental structure is the same, same type of analysis can be utilised in growth and development studies of all Scots pine stands. The differences in the details of structure and in functions should also be incorporated into the analysis. This arises the methodological questions of how the common features and differences can be utilised in the analysis of the growth and development of Scots pine stands.

The methodological aim of the present study is to develop tools to utilise the common structural and metabolic features of Scots pine stands in the analysis of their growth. The general methodological aim is twofold. a) Analysis of the regularities and their geographical variation, b) utilisation of the observed regularities and their geographical aspects in the analysis of stand development.

1.2 Research Tasks

Carbon compounds are accumulated in woody structures during stand development. A mature pine stand often has more than 200 m^3/ha of stem wood which makes over 100 tons of dry matter

per hectare. The needles and roots also contribute to the total mass of trees in a stand, although their mass is small when compared with woody structures. The organic materials also include some elements which are necessary for the formation of chemically active compounds. In addition, the forest functions require large amounts of water which is not accumulated in the tree structure.

The carbon compounds are formed by solar energy from atmospheric carbon dioxide and from water originating from the soil. The CO_2 enters the leaves through the stomata. The photosynthesis occurs in chloroplasts where energy-rich carbon compounds are formed using solar energy. The availability of solar energy for photosynthesis is markedly reduced in the lower part of canopy, which makes studies of the reduction of irradiance important.

The trees do not tolerate low temperatures in summer time when the photosynthetic functions are active. To achieve the necessary cold tolerance the trees go into a dormant state, the change from one state to another being a difficult regulation problem. If trees become dormant easily and recover from the winter state slowly they avoid cold damage very effectively but they also lose photosynthetic production. On the other hand, if trees go into the winter state late and leave it rapidly they gain in photosynthetic production but the cold damage may be overwhelming.

Photosynthetic production is extremely variable, both temporally and spatially, since the availability of energy for the process and the activity of the photosynthetic system vary. It is thus difficult to determine the annual photosynthetic production. *First research aim is to determine the annual photosynthetic production of a tree in a stand.* The effects of the availability of light on photosynthetic production and geographical aspects of production particularly should be better understood.

Photosynthetic production is utilised for the formation of new structures. Strong functional, geometrical and physical constraints determine the properties of an effective tree structure. If these constraints are lacking, then the system may overproduce some metabolites and underproduce others. It is also possible that the structure may fail to fulfil the strength requirements.

The tree structure can be analysed on the understanding that each organelle has a metabolic task and that each organelle has evolved to carry out its principal metabolic task effectively. We may even assume that the main parts of a tree are optimal to carry out their metabolic tasks within the limitations imposed on their structure and the environment.

The structural regularities which exist in trees due to functional, physical and geometrical constrains determine the pattern of trees. *Second research aim is to analyse the structural regularities of pine trees and the geographical aspects of the regularities observed.*

The growth of a tree is a result of photosynthetic production, nutrient uptake and their utilisation for formation of new tissues. If the annual photosynthetic production, nutrient uptake of a tree and the rules of utilisation of the production are known, then the growth of the tree can be determined. Thus the annual photosynthetic production, nutrient uptake and the rules of its utilisation are the cornerstones of stand development, enabling utilisation of mathematical methods in construction of a stand model.

The annual photosynthetic production varies considerably according to the geographical location and according the position of the tree in the stand. The regularities in the tree structure of pine trees may also have geographical aspects as well depending on the position of the tree in the stand. *Third research aim is to develop dynamic models for growth and development of Scots pine stands within the range of Scots pine based on photosynthetic production and regularities in the tree structure.*

The present monograph is the outcome of international research co-operation. Separate research tasks within the general framework of the group were allocated to rather independent subgroups. This fact is reflected in the relatively independent chapters of this monograph. The first three deal with the functional basis of trees and Chapter 5 describes regularities in the tree structure. The separate parts are combined together in the stand model described in Chapter 6. Finally, the geographical aspect is introduced into the model. General concluding remarks bring the monograph to a close.

2 Annual Cycle

2.1 The Implications of Geographical Variation in Climate for Differentation of Bud Dormancy Ecotypes in Scots Pine

Heikki Hänninen and Pertti Hari

2.1.1 Introduction

The climate in the cool and temperate regions is characterized by a pronounced annual cycle in which the air temperature typically ranges over about 70°C. The annual cycle of trees native to the cool and temperate regions is adapted to the annual climatic cycle, ie., the alternation of active growth state (*capacity adaptation*) and frost tolerant dormant state (*survival adaptation*) is synchronized with the annual climatic cycle prevailing at the growing site (Sarvas 1972, 1974, Fuchigami et al. 1982, Heide 1985). Timing of growth onset is essential in the annual cycle of the trees. Early growth onset involves a high risk of frost damage (insufficient survival adaptation), whereas late growth onset involves loss of utilization of the growth resources resulting in a low competition potential (insufficient capacity adaptation) (Weiser 1970, Lockhart 1983, Sakai and Larcher 1987, Häkkinen and Hari 1988).

The prevailing theory suggests that the timing of growth onset of trees from the cool and temperate regions is regulated by air temperature (Romberger 1963, Perry 1971, Sarvas 1972, 1974, Fuchigami et al. 1982). After growth cessation, long-term exposure to chilling temperatures (e.g. $-5°C < T < +10°C$) is first required for the process of rest break, which removes the growth-arresting physiological conditions in the dormant buds. Long-term exposure to high temperatures (e.g. $T > 0°C$) is then required for the ontogenetic development leading to onset of visible growth. The prevailing theory has given rise to various simulation models (for reviews, see Fuchigami et al. 1982, Cannell 1989, 1990, Hänninen 1990a, 1995, Kramer 1994a). In the modelling approach, the tree genotype is characterized by the logical structure of the model and by the values of the model parameters. The growing environment is characterized by air temperature data. Model predictions for timing of growth onset for each year during the simulation period are obtained as results.

Scots pine (*Pinus sylvestris* L.) grows naturally over a wide geographical range within which the climate varies from maritime to continental (see also Chapter 1). Various provenances of Scots pine are thus exposed during cold season to different regimes of rest breaking chilling temperatures, ontogenetic development promoting high temperatures, and potentially damaging frost temperatures at their natural sites. It may be assumed that this geographical variation in climate has resulted in ecotypical differentiation in Scots pine with respect to the air temperature regulation of timing of growth onset.

The purpose of the present study is to examine theoretically what kind of ecotypical variation is likely to be found among Scots pine populations with respect to air temperature responses of rest break and ontogenetic development leading to onset of visible growth.

2.1.2 Materials and Methods

2.1.2.1 Outline of the Analysis

First, it is postulated that the model developed for Finnish forest trees (Sarvas 1972, 1974, Hänninen 1990b, 1995) provides a realistic description of the regulation of growth onset in Scots pine. With the exception of reference to earlier empirical studies, any use of biological concepts later refers to the theoretical entities and phenomena inherent in the model or implied by it. Conse-

quently, the tree genotype is determined by the combination of the values of two genotype-specific parameters (Chap. 2.1.2.2).

Second, the timing of growth onset is predicted by the model for each genotype, year, and location involved in the study.

Third, the survival adaptation of the different genotypes at the various locations is analysed by examining minimum temperatures appearing after the growth onset. Genotypes with sufficient survival adaptation are identified for each location by a criterion for minimum temperatures.

Fourth, the capacity adaptation of the different genotypes at the various locations is analysed by examining the accumulation of high temperature units (temperature sum) after the growth onset. Genotypes with sufficient capacity adaptation are identified for each location by a criterion for the accumulated high temperature units. This is carried out only in the case of genotypes with sufficient survival adptation; thus, the genotypes identified are the optimal ones, combining sufficient survival and capacity adaptation at the location.

Fifth, the performance of the genotypes is compared among the locations.

2.1.2.2 Model of Growth Onset

The process of rest break involves biochemical changes that remove the growth arresting conditions in the bud (Smith and Kefford 1964, Dennis 1987, Powell 1987, Rinne et al. 1994a, b). Rest break leads to rest completion, ie., to the attainment of full growth competence of the bud (Hänninen 1990a, 1995, Kramer 1994a, b). The variable state of rest break, S_r, is used to describe the process on a relative dimensionless scale from 0 (rest initiation, none of the biochemical changes occurred) to 100 (rest completion). The value of S_r at any given moment indicates the proportion of biochemical changes occurred to those required for rest completion (Hänninen 1995).

The process of ontogenetic development involves a sequence of microscopic structural changes in the bud preceding onset of visible growth (Sarvas 1972, 1974). The variable state of ontogenetic development, S_o, is used to describe the process on a relative dimensionless scale from 0 (formation of bud completed, no ontogenetic development towards growth onset) to 100 (growth onset). The value of S_o at any given moment indicates the proportion of structural changes occurred to those required for growth onset (Hänninen 1995).

Sarvas's model (1972, 1974) as formulated by Hänninen (1990b, 1995) was used in the present study. The model involves the assumption that regardless of the prevailing temperature conditions, no ontogenetic development takes place before rest completion. Thus the effects of chilling on rest break and the effects of high temperatures on ontogenetic development are described sequentially in the model.

It is assumed that the temperature dependence of rate of rest break, $M_{rT}(T(t))$, is similar among the different genotypes, ie. (Fig. 2.1a):

$$M_{rT}(T(t)) = \begin{cases} 0 \quad CU\ day^{-1}, & T(t) \le -3.4°C \\ a_1\ T(t) + a_2, & -3.4°C < T(t) \le 3.5°C \\ a_3\ T(t) + a_4, & 3.5°C < T(t) \le 10.4°C \\ 0 \quad CU\ day^{-1}, & T(t) > 10.4°C \end{cases} \tag{2.1}$$

where $T(t)$ = prevailing air temperature, $a_1 = 0.16$ *CU* day^{-1} °C^{-1}, $a_2 = 0.5$ *CU* day^{-1}, $a_3 = -0.16$ *CU* day^{-1}°C^{-1}, and $a_4 = 1.6$ *CU* day^{-1}. Differences among genotypes are assumed in the rate of rest break at any temperature in the rest-breaking temperature range. These differences are taken into account by the genotype-specific parameter *chilling requirement of rest completion*, C_{crit}, which in mathematical terms is the time integral of Eq. (2.1) at the time of rest completion. The rate of rest break, M_r, is calculated as

$$M_r(T(t)) = 100\ M_{rT}(T(t)) / C_{crit} \tag{2.2}$$

where $M_{rT}(T(t))$ is the temperature dependence of rate of rest break (Eq. 2.1). M_{rT} is expressed in arbitrary chilling units, *CU*, per unit of time, C_{crit} in the corresponding chilling units, and M_r in the dimensionless units of state of rest break per unit of time. Following the definitions in Eqs. (2.1) and (2.2), the rate of rest break is highest with all genotypes at a temperature of 3.5°C (Eq. 2.1, Fig. 2.1a), the rate of rest break of a genotype with C_{crit} = 20 *CU* for instance being twice that of a genotype with C_{crit} = 40 *CU* at any temperature between –3.4°C and +10.4°C (Eq. 2.2).

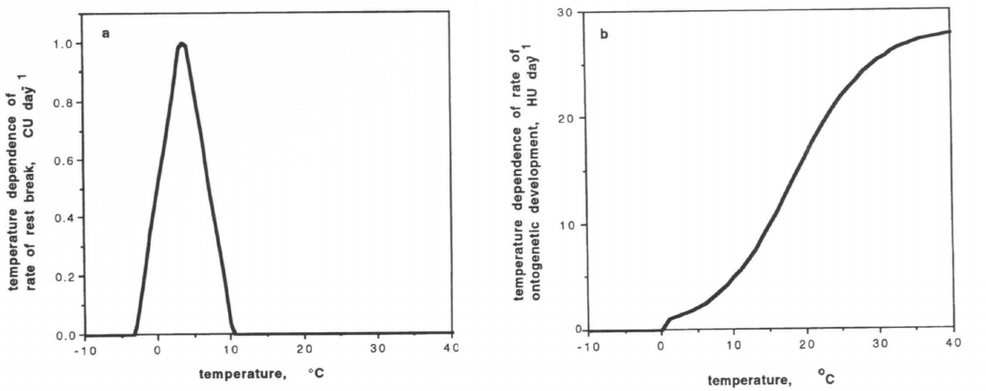

Fig. 2.1. Temperature dependence of (a) rate of rest break, and (b) rate of ontogenetic development, in the model of growth onset used in the study. Response functions fitted by Hänninen (1990b) to Sarvas's data (1972, 1974). Chilling unit (*CU*) and high temperature unit (*HU*) are arbitrary developmental units for rest break and ontogenetic development, respectively.

The state of rest break at a given moment t, $S_r(t)$, is obtained by integrating the rate of rest break (Eq. 2.2) from the moment of rest initiation, t_{RI}, up to moment t (Hari 1968, 1972):

$$S_r(t) = \int_{t_{RI}}^{t} M_r(\tau)\, d\tau \tag{2.3}$$

Following the definitions in Eq. 2.2, rest completion takes place when S_r attains a value of 100.

After rest completion, ontogenetic development takes place at temperatures above zero. As with the rest break it is assumed that the temperature dependence of the rate of ontogenetic development, $M_{oT}(T(t))$, is common to different genotypes (Fig. 2.1b):

$$M_{oT}(T(t)) = \begin{cases} 0 \quad HU\ day^{-1}, & T(t) \le 0°C \\ \dfrac{a_5}{1 + \exp(a_6\,(T(t) - a_7))}, & T(t) > 0°C \end{cases} \tag{2.4}$$

where $T(t)$ = daily mean air temperature, $a_5 = 28.4$ *HU* day^{-1}, $a_6 = -0.185$ °C^{-1}, and $a_7 = 18.4$°C. As with the rest break, differences among genotypes in the rate of ontogenetic development are described by a genotype-specific parameter *high temperature requirement of growth onset*, H_{crit}, which is the time integral of Eq. (2.4) at the time of growth onset in mathematical terms. Rate of ontogenetic development, M_o, is calculated as:

$$M_o(T(t)) = 100\ M_{oT}(T(t)) / H_{crit} \tag{2.5}$$

where $M_{oT}(t)$ is the temperature dependence of the rate of ontogenetic development (Eq. 2.4). M_{oT} is expressed in arbitrary high temperature units, *HU*, per unit of time, H_{crit} in the corresponding high temperature units, and M_o in the dimensionless units of state of ontogenetic development per unit of time. Following the definitions in Eqs. (2.4) and (2.5), the rate of ontogenetic development of all genotypes increases sigmoidally with increasing temperature (Eq. 2.4, Fig. 2.1b), the rate of ontogenetic development of a genotype with H_{crit} = 100 *HU* for instance being twice that of a genotype with H_{crit} = 200 *HU* at any temperature above zero (Eq. 2.5).

The state of ontogenetic development at a given moment t, $S_o(t)$, is obtained by integrating the rate of ontogenetic development (Eq. 2.5) from the moment of rest completion, t_{RC}, up to the moment t (Hari 1968, 1972):

$$S_o(t) = \int_{t_{RC}}^{t} M_o(\tau)\, d\tau \tag{2.6}$$

Following the definitions in Eq. 2.5, growth onset takes place when S_o attains a value of 100.

2.1.2.3 Temperature Data

Temperature data from four locations in the natural geographical range of Scots pine were used in the study (Fig. 2.2). Temperature records were made in standard meteorological screens at each of the four locations. For Jyväskylä the temperature data covered the years 1902–1980, except 1912–1916 for which were observations missing. For the other three locations the temperature data covered the period 1966–1980. In order to facilitate comparisons, the calculations were carried out with all four locations for this period (14 years). For Jyväskylä, however, the calculations were first carried out with the longer temperature data series available for that location (73 years).

Temperature conditions on a given day were described in the calculations by daily mean and minimum temperatures. Unfortunately, these were determined slightly differently among the data sets available for the different locations. For Eskdalemuir, the daily minimum temperature was determined as the observed daily minimum, and the daily mean temperature as the mean of the observed daily minimum and maximum. For Jyväskylä, the daily minimum temperature was determined as the observed daily minimum, and the daily mean temperature as the mean of the records made at 0800 h, 1400 h and 2000 h. For Murmansk and Voronez, the daily minimum temperature was determined as the minimum among the eight daily temperature records made at three-hourly intervals, and the daily mean as the mean of these records.

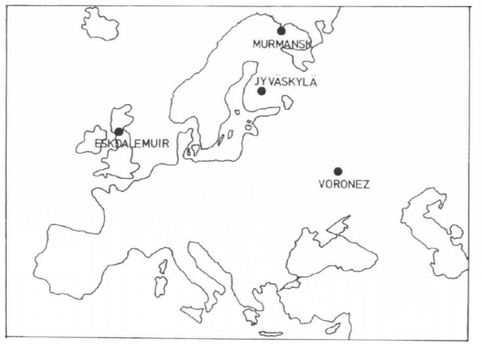

Fig. 2.2. Locations in the natural range of Scots pine considered in the study.

2.1.2.4 Calculations

Timing of Growth Onset

The timing of growth onset was calculated for each genotype (combination of C_{crit} and H_{crit}), location, and year by the model defined by Eqs. 2.1–2.6, using numerical approximation with a time step of one day in the integrations, and by defining the date of rest initiation, (t_{RI}, Eq. 2.3) each year as September 1st (Hänninen 1990a, 1991). The genotype-specific value of C_{crit} was varied by a step of five chilling units, the minimum value used being five *CU*. The maximum value of C_{crit} used in the calculations at a given location was determined according to the minimum accumulation of chilling units between September 1 and May 31 during the simulation period at the location. In this way 10 to 22 values of C_{crit} were used in the calculations depending on the location. Thirty genotype-specific values of H_{crit} were used in the calculations with all four locations (from 10 to 300 high temperature units, step 10 *HU*). By combining the values of C_{crit} and H_{crit}, a population between 300 (10×30) and 660 (22×30) genotypes was considered in the calculations, the size of the population depending on the location.

Survival Adaptation

For a given genotype at a given location, the annual post-dormant minimum temperature, T_{min}, was determined from the air temperature data as the minimum among the daily minimum temperatures between the day of growth onset and August 1. The cumulative frequency distribution of the values of T_{min} was subsequently constructed over the simulation years, and the survival adaptation was examined using the distribution (Fig. 2.3). For sufficient survival adaptation it was required that the probability of a killing frost, P_{kil}, be zero, ie.

$$P(T_{min} \leq T_{kil}) = 0 \qquad (2.7)$$

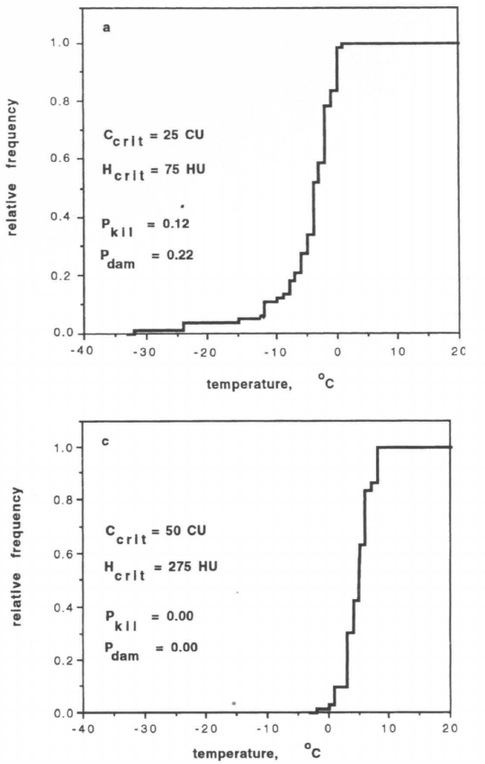

Fig. 2.3. Cumulative frequency distribution of annual post-dormant minimum temperature, T_{min}, obtained with three genotypes (combinations of values of the model parameters C_{crit} and H_{crit}). Probabilities of killing (P_{kil}) and damaging frost (P_{dam}) are also indicated. Simulations with 73-year temperature data from Jyväskylä, central Finland (Fig. 2.2).

and that the probability of a damaging frost, P_{dam}, be less than 0.1, ie.

$$P(T_{kil} < T_{min} \leq T_{dam}) < 0.1 \qquad (2.8)$$

The values $T_{kil} = -10$°C and $T_{dam} = -5$°C were used in the calculations (Repo and Pelkonen 1986, Rikala and Repo 1987, Repo 1992). As an example, at Jyväskylä (Fig. 2.2), the genotype with C_{crit} = 40 *CU* and H_{crit} = 125 *HU* and the genotype with C_{crit} = 50 *CU* and H_{crit} = 275 *HU* were found to have sufficient survival adaptation (Figs. 2.3b, c), whereas the genotype with C_{crit} = 25 *CU* and H_{crit} = 75 *HU* was found to have insufficient survival adaptation (Fig. 2.3a).

Capacity Adaptation

For a given genotype with sufficient survival adaptation at a given location, the annual post-dormant accumulation of high temperature units, HU_{pd}, at the location was calculated by integrating Eq. 2.4 from the date of growth onset to 1 August. The frequency distribution of the values of HU_{pd} was subsequently constructed over the simulation years, and the mean post-dormant accumulation of high temperature units, $\overline{HU}_{pd}$, at the location for the genotype was calculated (Fig. 2.4). As this was done for all of the genotypes with sufficient survival adaptation at the location, the maximal mean post-dormant accumulation of high temperature units, $\overline{HU}_{pdmax}$, was determined as the maximum value of $\overline{HU}_{pd}$ among the genotypes. For Jyväskylä, a value of

$\overline{HU}_{pdmax}$ = 898 *HU* was obtained. The genotype corresponding to that value maximizes the utilization of growth resources (capacity adaptation) without being seriously damaged by frost (survival adaptation) for that location. It was required that the mean post-dormant accumulation of high temperature units be more than 90 per cent of the maximal mean post-dormant accumulation of high temperature units for a sufficient capacity adaptation of a given genotype at a given location, ie.

$$\overline{HU}_{pd} > 0.9\ \overline{HU}_{pdmax} \qquad (2.9)$$

As an example, at Jyväskylä (Fig. 2.2), the genotype with C_{crit} = 40 *CU* and H_{crit} = 125 *HU* was found to have sufficient capacity adaptation (Fig. 2.4a), whereas the genotype with with C_{crit} = 50 *CU* and H_{crit} = 275 *HU* was found to have insufficient capacity adaptation (Fig. 2.4b).

The genotypes with sufficient capacity adaptation are simultaneously the optimal genotypes for the location, since the capacity adaptation was examined only in the case of genotypes with sufficient survival adaptation. In the case of the three example genotypes, that with C_{crit} = 40 *CU* and H_{crit} = 125 *HU* belongs to the optimal genotypes (Figs. 2.3b, 2.4a), whereas the other two genotypes do not (Figs. 2.3a, c, 2.4b).

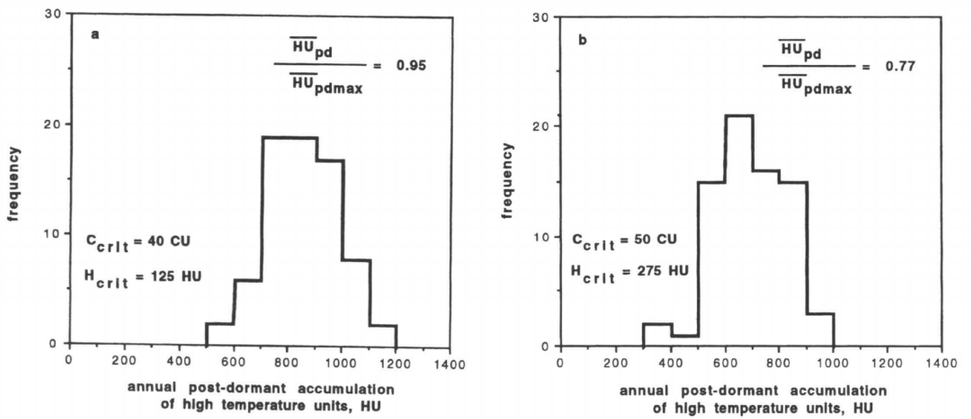

Fig. 2.4. Frequency distributions of annual post-dormant accumulation of high temperature units (HU_{pd}), obtained with two genotypes (combinations of values of the model parameters C_{crit} and H_{crit}). Mean values of the distributions ($\overline{HU}_{pd}$), and the proportions of $\overline{HU}_{pd}$ to the maximal mean post-dormant accumulation of high temperature units, $\overline{HU}_{pdmax}$, indicated in the figures. Simulations with 73-year temperature data from Jyväskylä, central Finland (Fig. 2.2).

2.1.3 Results

2.1.3.1 Performance of Genotypes in Jyväskylä

Genotypes with a low chilling requirement for rest completion (low C_{crit}) and low high temperature requirement for growth onset (low H_{crit}), were associated with early growth onset and high risk of frost damage (Fig. 2.3a), and thus insufficient survival adaptation (Fig. 2.5). On the other hand genotypes with high C_{crit} and high H_{crit} were associated with late growth onset and a loss of the growing season favourable for growth (Fig. 2.4b), and thus with insufficient capacity adaptation (Fig. 2.5). The optimal genotypes were the intermediate ones (intermediate C_{crit} and H_{crit}, Fig. 2.5), since they allowed efficient utilization of the growing season (Fig. 2.4a), without being seriously damaged by frost (Fig. 2.3b).

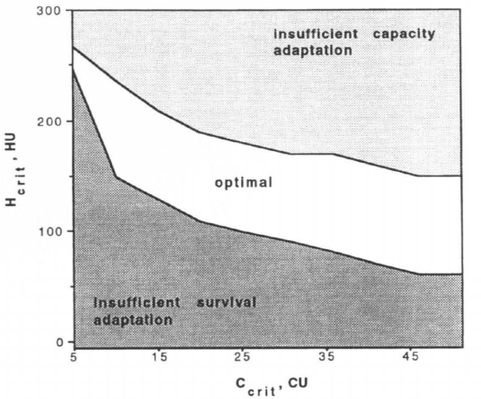

Fig. 2.5. Performance of tree genotypes with respect to survival and capacity adaptation. Each genotype is represented by a combination of the values of the model parameters C_{crit} and H_{crit}. Simulations with 73-year temperature data from Jyväskylä, central Finland (Fig. 2.2).

2.1.3.2 Performance of Genotypes at Four Locations

Effects of Temperature Conditions During Winter

In the maritime climate of Eskdalemuir, considerable accumulation of both chilling units and high temperature units took place during autumn, winter, and early spring, when heavy frosts were also frequent. In these conditions, relatively high values for C_{crit} and H_{crit} were required to obtain sufficient survival adaptation (Fig. 2.6a).

At locations with a continental climate, relatively minor accumulation of both chilling units and high temperature units took place during autumn, winter, and early spring. In these conditions, only relatively low values of C_{crit} and H_{crit} were required to obtain sufficient survival adaptation. Compared with Eskdalemuir (Fig. 2.6a), all of the other three locations were continental in this respect (Figs. 2.6b, c, d).

Effects of Temperature Conditions During Summer

In a maritime climate, relatively minor accumulation of high temperature units took place during spring and summer after the last heavy frosts. Thus any delay of growth onset after that corresponding to a given accumulation of high temperature units caused a relatively large loss in the post-dormant accumulation of high temperature units. This was the case with Eskdalemuir where a relatively small increase in the values of C_{crit} and H_{crit} from those values that were just great enough for sufficient survival adaptation caused insufficient capacity adaptation. The range of optimal genotypes is thus relatively small (Fig. 2.6a). Similarly, the range for optimal genotypes was relatively small in Murmansk (Fig. 2.6b), since the summer at this northern location is short and cold, implying low accumulation of high temperature units.

In a continental climate as against maritime climates, a relatively large accumulation of high temperature units took place during spring and summer after last heavy frosts. A great increase in the values of C_{crit} and H_{crit} from those values just sufficient for survival adaptation being needed to cause insufficient capacity adaptation, ie. the range of optimal genotypes is relatively large. This was the case especially in Voronez (Fig. 2.6d), and to a lesser extent in Jyväskylä (Fig. 2.6c).

2.1.4 Discussion

In the present study the effects of air temperature on growth onset timing were described by a model developed earlier for Finnish forest trees (Sarvas 1972, 1974, Hänninen 1990b, 1995). The model still requires further development, in spite of the fact that it accounts for two main phenomena involved in the regulation of growth onset (Hänninen 1990a, 1995, Hänninen et al. 1993, Hänninen and Backman 1994). Furthermore, values of part of the parameters related to survival and capacity adaptation were determined in the present study without sound empirical evidence. In order to determine the threshold probability for the occurrence of damaging frost (0.1 in Eq. 2.8), for instance, it should ideally be known how much a

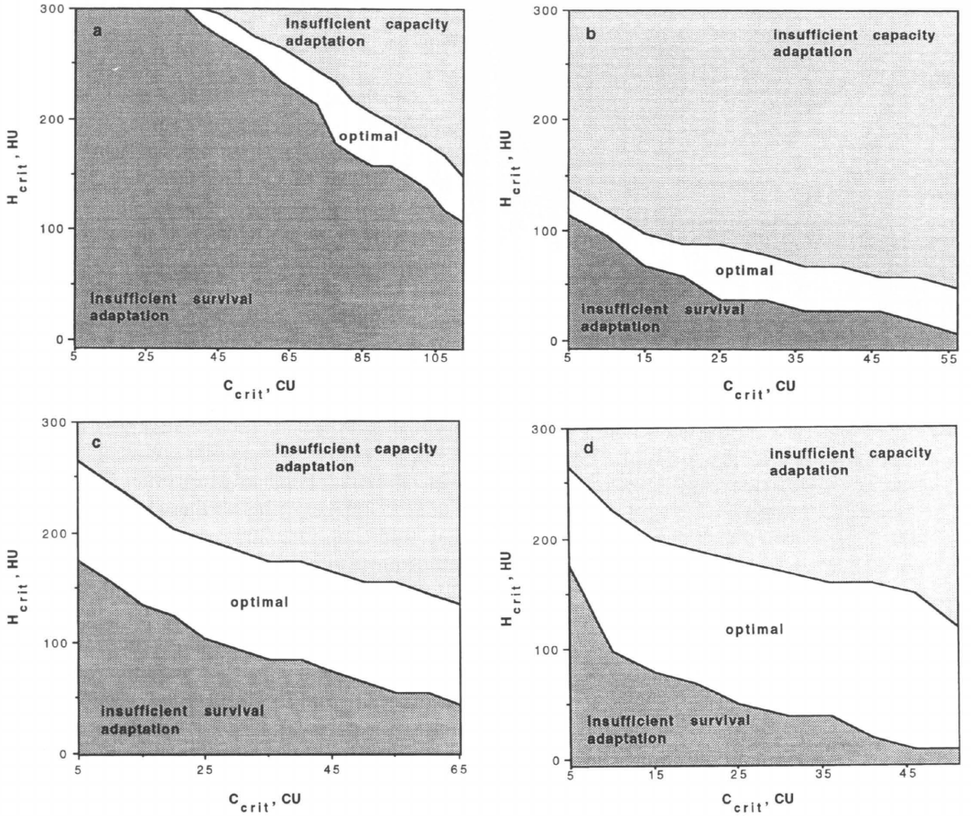

Fig. 2.6. As Fig. 2.5, but simulations with 14-year temperature data from (a) Eskdalemuir, Scotland; (b) Murmansk, north-eastern Russia, (c) Jyväskylä, central Finland; and (d) Voronez, southern Russia. See Fig. 2.2 for the locations. Note the different scales of the x-axes.

damaging frost reduces subsequent growth.

It was possible to carry out a rough comparison of the performances of the different genotypes in the climatic conditions of the four locations using the temperature data for 14 years, since these were long enough to reveal the main differences among the climates (Fig. 2.6). The results at each location, however, should be interpreted with care, since the 14-year period does not necessarily contain the critical years which ultimately determine the identification of the optimal genotypes. This was clearly demonstrated in the Jyväskylä results where the range of optimal genotypes was smaller in the simulation with the 73-year data (Fig. 2.5) than in the simulation with the 14-year data (Fig. 2.6c).

Despite the shortcomings in detailed biological and climatological information, the present study revealed the importance of the variations in the annual temperature conditions among the different geographical locations in the natural range of Scots pine on the differentiation of bud dormancy ecotypes in that species. The results suggest that ecotypes from maritime regions should have a greater chilling requirement for rest completion and / or greater high temperature requirement for growth onset than ecotypes from more continental regions (Fig. 2.6).

In the case of chilling requirement for rest completion, the theoretical ecotypical pattern of the present study was experimentally observed for Scots pine by Leinonen (1996), who also found a similar pattern for *Betula pendula* Roth. The pattern had previously been documented for *Pseudotsuga menziesii* var. *menziesii* (Mirb.) Franco by Campbell and Sugano (1979).

The ecotypical variation in high temperature requirement for growth onset has been found to be related to the latitude of the location, rather than to its distance from the ocean, ie., the requirement is generally lower in the case of provenances from cold northern areas than in the provenances from warm southern areas (Kriebel and Wang 1962, Worrall and Mergen 1967, Dormling et al. 1968, Dormling 1982). The theoretical results of the present study are in accordance with this empirical pattern (Figs. 2.6b, c).

In the present study, computer simulations were used to study the implications of geographical variation in climate for differentiation of climatic ecotypes in trees theoretically. Similar calculations, however, can also be used for applied purposes where a proven growth onset model is available. Models of growth onset can be applied for instance for planning of provenance transfers (Campbell 1974, Cannell and Smith 1984), or assessing the effects of climatic warming on the survival and growth of trees (Cannell and Smith 1986, Kellomäki et al. 1988, 1995, Murray et al. 1989, Hänninen 1991, 1996, Kramer 1994b, 1995).

Acknowledgments

We thank Seppo Kellomäki, Paavo Pelkonen, Tapani Repo, and Heikki Smolander for their constructive criticism, and Risto Häkkinen, Leo Kaipiainen, Tiit Nilson, Juhan Ross, and Ron Smith for help with the temperature data.

References

Campbell, R. K. 1974. Use of phenology for examining provenance transfers in reforestation of Douglas-fir. Journal of Applied Ecology 11: 1069–1080.

— & Sugano, A. I. 1979. Genecology of bud-burst phenology in Douglas-fir: response to flushing temperature and chilling. Botanical Gazette 140(2): 223–231

Cannell, M. G. R. 1989. Chilling, thermal time and the date of flowering of trees. In: Wright, C. J. (ed.). Manipulation of fruiting. Butterworths, London. p. 99–113.

— 1990. Modelling the phenology of trees. In: Jozefek, H. (ed.). Modelling to understand forest functions. Silva Carelica 15: 11–27. (University of Joensuu).

— & Smith, R. I. 1984. Spring frost damage on young Picea sitchensis 2. Predicted dates of budburst and probability of frost damage. Forestry 57(2): 177–197.

— & Smith, R. I. 1986. Climatic warming, spring budburst and frost damage on trees. Journal of Applied Ecology 23: 177–191.

Dennis, F. G. Jr. 1987. Two methods of studying rest: temperature alternation and genetic analysis. HortScience 22(5): 820–824.

Dormling, I. 1982. Frost resistance during bud flushing and shoot elongation in Picea abies. Silva Fennica 16(2): 167–177.

— , Gustafsson, Å & von Wettstein, D. 1968. The experimental control of the life cycle in Picea abies (L.) Karst. I. Some basic experiments on the vegetative cycle. Silvae Genetica 17: 44–64.

Fuchigami, L. H., Weiser, C. J., Kobayashi, K., Timmis, R. & Gusta, L. V. 1982. A degree growth stage (°GS) model and cold acclimation in temperate woody plants. In: Li, P. H. and Sakai, A. (eds.). Plant cold hardiness and freezing stress. Mechanisms and crop implications. Vol. 2. Academic Press, New York. p. 93–116.

Häkkinen, R. & Hari, P. 1988. The efficiency of time and temperature driven regulation principles in plants at the beginning of the active period. Silva Fennica 22(2): 163–170.

Hänninen, H. 1990a. Modelling bud dormancy release in trees from cool and temperate regions. Acta Forestalia Fennica 213. 47 p.

— 1990b. Modeling dormancy release in trees from cool and temperate regions. In: Dixon, R. K., Meldahl, R. S., Ruark, G. A. and Warren, W. G. (eds.). Process modeling of forest growth responses to environmental stress. Timber Press, Portland. p. 159–165.

— 1991. Does climatic warming increase the risk of frost damage in northern trees? Plant, Cell and Environment 14: 449–454.

— 1995. Effects of climatic change on trees from cool and temperate regions: an ecophysiological approach to modelling of bud burst phenology. Canadian Journal of Botany 73: 183–199.
— 1996. Effects of climatic warming on northern trees: testing the frost damage hypothesis with meteorological data from provenance transfer experiments. Scandinavian Journal of Forest Research 11: 17–25.
— & Backman, R. 1994. Rest break in Norway spruce seedlings: test of a dynamic temperature response hypothesis. Canadian Journal of Forest Research 24: 558–563.
— , Kellomäki, S., Laitinen, K., Pajari, B. & Repo, T. 1993. Effect of increased winter temperature on the onset of height growth of Scots pine: a field test of a phenological model. Silva Fennica 27: 251–257.
Hari, P. 1968. A growth model for a biological population, applied to a stand of pine. Communicationes Instituti Forestalis Fenniae 66(7). 16 p.
— 1972. Physiological stage of development in biological models of growth and maturation. Annales Botanici Fennici 9: 107–115.
Heide, O. M. 1985. Physiological aspects of climatic adaptation in plants with special reference to high-latitude environments. In: Kaurin, Å., Junttila, O. & Nilsen, J. (eds.). Plant production in the north. Norwegian University Press, Tromso. p. 1–22.
Kellomäki, S., Hänninen, H. & Kolström, M. 1995. Computations on frost damage to Scots pine under climatic warming in boreal conditions. Ecological Applications 5(1): 42–52.
— , Hänninen, H. & Kolström, T. 1988. Model computations on the impacts of the climatic change on the productivity and silvicultural management of the forest ecosystem. Silva Fennica 22(4): 293–305.
Kramer, K. 1994a. Selecting a model to predict the onset of growth of Fagus sylvatica. Journal of Applied Ecology 31: 172–181.
— 1994b. A modelling analysis of the effects of climatic warming on the probability of spring frost damage to tree species in The Netherlands and Germany. Plant, Cell and Environment 17: 367–377.
— 1995. Phenotypic plasticity of the phenology of seven European tree species in relation to climatic warming. Plant, Cell and Environment 18: 93–104.
Kriebel, H. B. & Wang, C-W. 1962. The interaction between provenance and degree of chilling in budbreak of Sugar maple. Silvae Genetica 11: 125–130.
Leinonen, I. 1996. Dependence of dormancy release on temperature in different origins of Pinus sylvestris and Betula pendula seedlings. Scandinavian Journal of Forest Research 11: 122–128.
Lockhart, J. A. 1983. Optimum growth initiation time for shoot buds of deciduous plants in a temperate climate. Oecologia 60: 34–37.
Murray, M. B., Cannell, M. G. R. & Smith, R. I. 1989. Date of budburst of fifteen tree species in Britain following climatic warming. Journal of Applied Ecology 26: 693–700.
Perry, T. O. 1971. Dormancy of trees in winter. Science, (N.Y.) 171: 29–36.
Powell, L. E. 1987. Hormonal aspects of bud and seed dormancy in temperate-zone woody plants. HortScience 22(5): 845–850.
Repo, T. 1992. Seasonal changes of frost hardiness in Picea abies and Pinus sylvestris in Finland. Canadian Journal of Forest Research 22: 1949–1957.
— & Pelkonen, P. 1986. Temperature step response of dehardening in Pinus sylvestris seedlings. Scandinavian Journal of Forest Research 1: 271–284.
Rikala, R. & Repo, T. 1987. Frost resistance and frost damage in Pinus sylvestris seedlings during shoot elongation. Scandinavian Journal of Forest Research 2: 433–440.
Rinne, P., Saarelainen, A., & Junttila, O. 1994a. Growth cessation and bud dormancy in relation to ABA level in seedlings and coppice shoots of Betula pubescens as affected by a short photoperiod, water stress and chilling. Physiologia Plantarum 90: 451–458.
— , Tuominen, H., & Junttila, O. 1994b. Seasonal changes in bud dormancy in relation to bud morphology, water and starch content, and abscisic acid concentration in adult trees of Betula pubescens. Tree Physiology 14: 549–561.
Romberger, J. A. 1963. Meristems, growth, and development in woody plants. United States Department of Agriculture, Forest Service, Technical Bulletin 1293. 214 p.
Sakai, A. & Larcher, W. 1987. Frost survival of plants. Responses and adaptation to freezing stress. Springer-Verlag, Berlin. 321 p.
Sarvas, R. 1972. Investigations on the annual cycle of forest trees. Active period. Communicationes Instituti Forestalis Fenniae 76(3). 110 p.
— 1974. Investigations on the annual cycle of forest trees. II. Autumn dormancy and winter dormancy. Communicationes Instituti Forestalis Fenniae 84(1). 101 p.

Smith, H. & Kefford, N. P. 1964. The chemical regulation of the dormancy phases of bud development. American Journal of Botany 51(9): 1002–1012.
Weiser, C. J. 1970. Cold resistance and injury in woody plants. Science, (N.Y.) 169: 1269–1278.
Worrall, J. & Mergen, F. 1967. Environmental and genetic control of dormancy in Picea abies. Physiologia Plantarum 20(3): 733–745.

2.2 Dynamics of Carbohydrate Distribution in Scots Pine

Galina Sofronova and
Leo Kaipiainen

2.2.1 Background

Height growth of Scots pine is to large extend based on carbohydrates from photosynthetic production of preceding year. Cambial growth and growth of needles are partially provided by the assimilates of the current year and partially by reserve carbohydrates (Kozlowski and Ward 1957, Kramer and Kozlowski 1980, Jushkov P. 1970, Jushkov V. 1970, Sudachkova et al. 1973, Jushkov and Jushkov 1974).

Trees have a carbohydrarate pool which balances the discrepancies between photosyntetic production and consumption in growth. Systematic monitoring of carbohydrate pool in the conifers during a year is, however, rather scare in the literature (Sofronova 1985, Puttonen 1986, Saranpää et al. 1989, Langström et al. 1990, Romanova and Sudachkova 1990, Sundberg et al. 1993). Thus, our knowledge on the role of stored carbon in the growth of trees is still somewhat scarce.

The aim of this chapter is to study the within year dynamics of the concentrations of different forms of carbohydrates in different parts of Scots pine trees. The hypotheses is that the use of stored carbohydrates for growth should show up in the variation in the levels of different forms of carbohydrates in different tree tissues. We also hypothesized that the geographic location from north to south should influence the dynamics of the carbohydrate pool because of the different intensities of tree growth relative to growing season length.

2.2.2 Materials and Methods

Studies of carbohydrate concentrations in Scots pine trees was carried out in a lichen type pine stand 50 km to the North of Petrozavodsk (63°13´N, 34°10´E) from 1976 to 1984. At each year 25 trees were sampled randomly from the stand. A representative sample of foliage from different positions, fine roots (diameter <3 mm) twig and stem phloem, twig and stem xylem and root phloem and xylem from roots were taken at different times of the year. The twig and transport root size varied between 3 and 10 mm.

The effect of trees position in the stand on the carbohydrate dynamics was studied at comparable sites in the same region in 1977, 1978 and in 1982 and 1984. Dominant and depressed trees were chosen for the study. Investigations were carried out during shoot elongation when the intensity of metabolic processes reaches their peak. The selection of samples from each tree was similar to that of the previous study.

Additional studies were performed to analyse the effect of nothern location on the carbonhydrate pool. The dynamics of carbohydrate pool were compared between a lichen type pine stand in Murmansk region (Apatites, Khibines) and Karelien at the time of the shoot growth (June 22–25) and after termination of growth (August 22–23).

The carbohydrates were divided in two fractions, ie. soluble carbohydrates (sugars) and insoluble carbohydrates (polysaccharides). Sugars were formed by monosaccharides and polygosaccharides and polysaccharides by starch and gemycelluloses. Celluloses were separated from the polysaccharides in the analyses.

Average sample from 25 trees was fixed by hot steam. Air-dry samples were grined to small particles with electric mill. Separation of dissoluble and insoluble carbohydrate fractions was based on their different solubility and their resistance to acid hydrolysis (Jastrembovitch and Kalinin 1962, Sofronova et al. 1978). The amount of carbohydrates in each fraction was determined by coloremeter following the preliminary hydrolysis of polysaccharides. (Jastrembovitch and Kalinin 1962, Sofronova et al. 1978). The carbohydrate concentration in the material under study was expressed per dry matter.

2.2.3 Results

In needles, current year shoots and roots (diameter<3 mm) the cellulose content is approximately equivalent to the total amount of other carbohydrates, and in the living xylem of stem, 1–2-year twigs and roots the amount of celluloses exceeds the total amount of other carbohydrates 1.5–2 times (Fig. 2.7).

Sugar concentrations in the tissues of Scots pine are rather high and stable during one year (Fig. 2.8), in the needles, phloem and fine roots the average value is around 10 %, and in xylem about 5 %. Only needles and perhaps stem xylem have a clear annual pattern in the sugar concentrations. The variation in sugar concentrations in the other organs seem to be rather random fluctuation.

The concentrations of polysaccharides are higher that those of sugars (Fig 2.9). Otherwize their behaviour is rather similar to that of sugars. The needle concentrations have a clear annual pattern, while the others mostly vary more or less randomly arround the mean value. The concentrations of polysaccharides in the xylem are also more variable than in the other organels. Also, sugar concentrations in Scots pine are larger in winter then summer, and on the contrary polysaccharide concentrations have maximum during the growth period.

Qualitative correlations between separate carbohydrate fractions is subject to change depending on the physiological state of trees and environmental conditions that influence the presence of specific enzymes catalizing synthesis, hydrolysis and interconversion of sugars and polysaccharides. For this reason also the total content of the carbohydrate pool in trees is interesting. The mean values of carbohydrate content in pine tissues without celluloses are as follows (percent of dry matter): needle they range from 18.1+1.1 to 38+1.4, in buds from 19.8+1.0 to 26.2+0.9; in branch, stem and root bark from 29.9+1.9 to 35.5+0.8; in branch, stem and root wood from 24.1+1.5 to 27.5+0.7 and in thin roots (< 3 mm in diameter) from 27.9+0.4 to 39.9+1.2.

There exist a close interrelation between growth and carbohydrate metabolism, but is there always a sufficiently carbohydrates favailable for growth? To answer this question comparative investigations of carbohydrate metabolism were undertaken in trees, that had different annual productivity

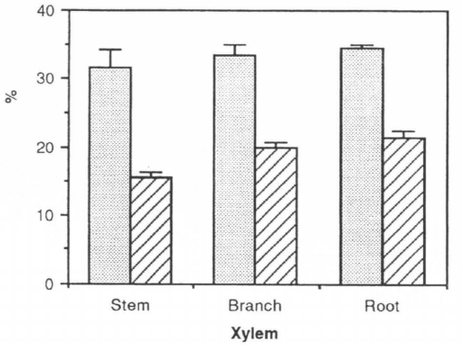

Fig. 2.7. Percentage of celluloses (grey) and carbohydrates (lined) in the xylem of Scots pine (% of dry matter).

and position within a stand. The co-dominant (class II) trees had rapid heigth growth (on an average 40 cm) and depressed (class IV) trees had poor height growth (on an average 7 cm). According to our results, the tree position did not influence the carbohydrate concentration in bud, shoot and needles (Table 2.1). Table 2.2. represents the lenght of shoots of trees.

Trees occuping different positions in stands and their height growths differ substantially from each other. This variation does not, however, reveal distinctively in carbohydrate content of growing shoots and needles (Table 2.1).Similar results from the same objects of study were obtained in 1984, although the shoot growth that year started and ended earlier in more favorable temperature conditions.

The length of leading pine shoots reached 42.9–46.7 % of their terminal length by June 22–25 in the Kola peninsula and in Karelia by June 9–10. Despite of the big differences in the growth rates the pines from Karelia and Kola do not reveal distinctive variations in carbohydrate content in different tissues and parts (Fig. 2.10). This would suggest that the required level of carbohydrates in tree tissues can be maintained with both high and low intensity of physiological and biochemical processes since the system of inner regulation balances the intensity of growth with the carbon sources available.

The size of the carbonhydrater pool was observed to be rather large and stable. The variation

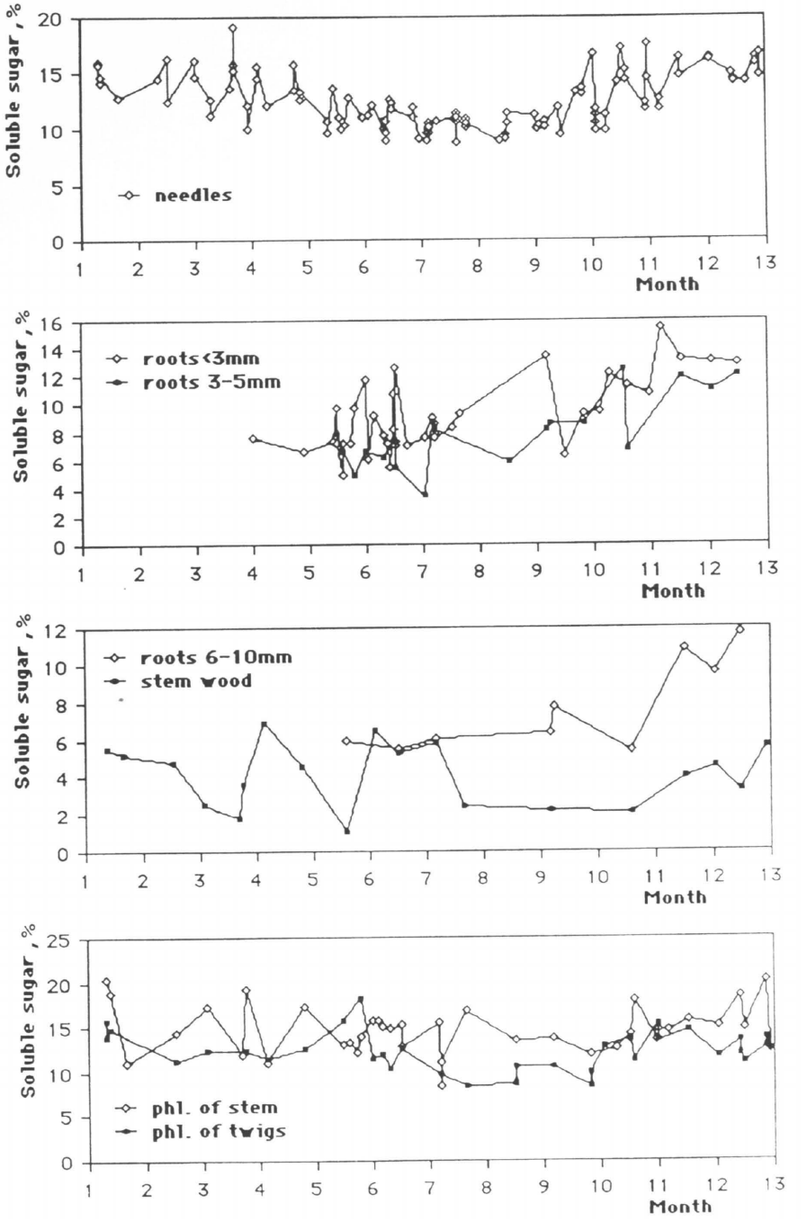

Fig. 2.8. Annual dynamics of sugar concentrations in organs and tissues of Scots pine. Dates was transformed in a row of figures from 1 (1 March) to 366 (29 February).

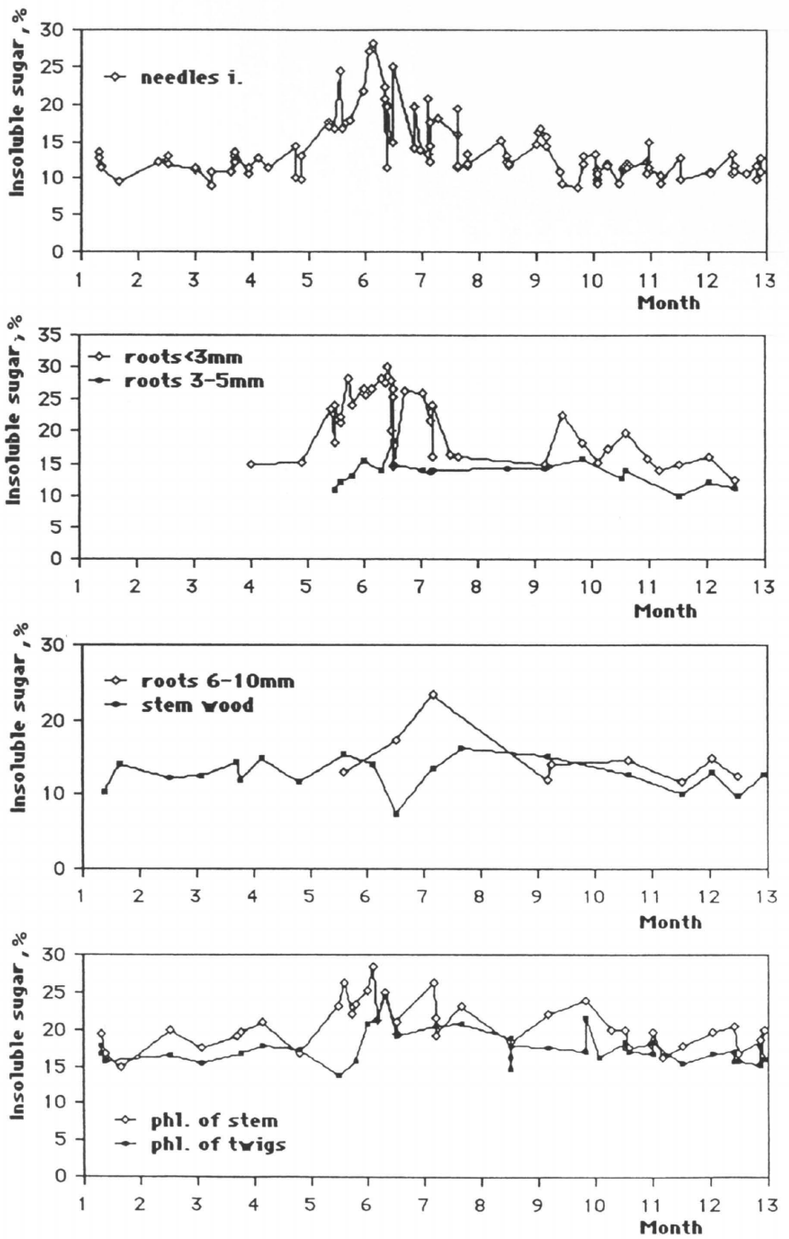

Fig. 2.9. Annual dynamics of polysaccharide concentrations in organs and tissues of Scots pine. Dates was transformed in a row of figures from 1 (1 March) to 366 (29 February).

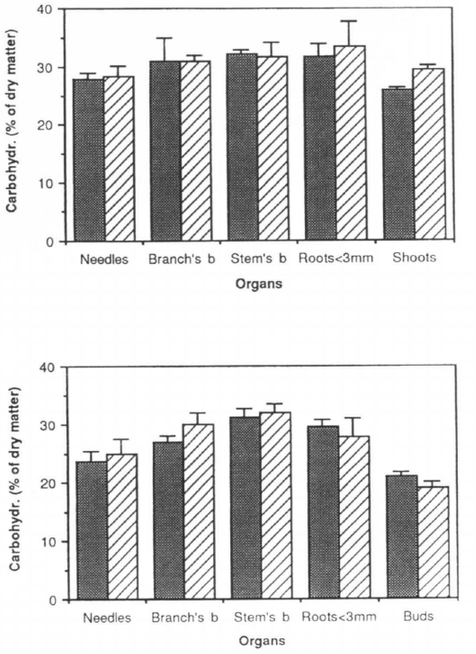

Figure 2.10. The carbohydrate content of different tissues in Murmansk Region (Kola Peninsula, black bars) and Russian Karelia (lined bars).

Tabl. 2.1. Carbohydrate concentrations in Scots pine organs in during growth period (Derevjannoe).

Organs	Class	Sugar (% dry matter) Date 05.17	06.09	Polysaccharides (% dry matter) Date 05.17	06.09
Buds	II	8.4	–	18.0	–
	IV	8.6	–	17.5	–
Shoots	II	–	8.6	–	18.8
	IV	–	9.7	–	18.9
Needles	II	10.4	9.2	17.8	24.1
	IV	9.3	9.0	16.1	20.5

Table 2.2. Carbohydrate concentrations in shoots of the Scots pine during growth period.

Dates	Dominant trees Shoot's length, mm	Carbohydrates % dry matter	Depressed trees Shoot's length, mm	Carbohydrates % dry matter
05.17	30	26.6 ± 1.1	9	25.4 ± 1.1
06.01	85	29.5 ± 1.1	26	28.0 ± 1.1
06.14	178	30.9 ± 1.2	47	33.0 ± 1.3
06.22	252	36.9 ± 0.7	66	34.2 ± 0.8
07.06	342	29.6 ± 1.1	86	27.2 ± 1.0

caused by season, position in the stand and geographical location was small when compared with the size of the pool. These observations agree with the observations that carbohydrate pool as such is rarely limiting growth of secondary meristems(e.g. Savidge 1991).

The large pool of carbohydrates should be taken in consideration when modelling the linkage between photosynthetic production and growth. According the present results there seems to be a balance between carbon consumption in growth and photosynthetic production if the phenomenon is studied during prolonged periods. During unbalanced periods the pool is evidently cabable to balance the discrepancy between consumption and production.

References

Jastrembovich, N.I. & Kalinin, F.L. 1962. Opredelenie uglevodov I rastvorimyh soedinenii azota v odnoi naveske rastitelnogo materiala. Nauchnye trudy Ukrainskoi selsko-hozjaistvennoi akademii. 23: 119–126.

Jushkov, P.I. 1970. Ob uglerodnom pitanii molodyh cocen Pinus sylvestris. III Uralskoe soveschanie po fiziologii drevesnyh rastenii. Ufa: 101–102.

— & Jushkov, V.I. 1974. Radialnoe peredvijshenie assimilatov v osevyh organah sosny obyknovennoi. Problemy fiziologii i biohimii drevesnyh rastenii. Krasnojarsk.: 82–83.

Jushkov, V.I. 1970. Sezonnaja dinamica mechenyh assimiljatov u sosny obyknovennoi. III Uralskoe soveschanie po fiziologii drevesnyh rastenii. Ufa: 100–101.

Kozlowski, T.T. & Ward, R.C. 1957. Seasonal height growth of conifers. Forest Science 3: 167–174.

Kramer, P.J. & Kozlovski, T.Y. 1980. Physiology of trees.

Langström, B., Tenow, O., Ericsson, A., Hellqvist, C. & Larsson, S. 1990. Effects of shoot pruning on stem growth, needle biomass, and dynamics of carbohydrates and nitrogen in Scots pine as related to season and tree age. Can. J. For. Res. 20(5): 514–523.

Puttonen, P. 1986. Carbohydrate reserves in Pinus sylvestris seedling needles as an attribute of seedling vigor. Scand J. For. Res. V.1(2). Stockholm: 181–193.

Romanova, L.I. & Sudachkova, N.E. 1990. Effect of defoliation on the carbohydrate level and structure of the annual ring of Scots pine. Sov. For. Sci. New York: 48–54.

Saranpää, P. & Holl, W. 1989. Soluble carbohydrates of Pinus sylvestris L. sapwood and heartwood. Trees 3: 138–143.

Savidge, R.A. 1991. Seasonal cambial activity in Larix lariciana saplings in relation to endogenous Indol-3-ylacetic Acid, Sucrose and Coniferin. Forest Science 37(3): 953–958.

Sofronova, G.I. 1985. Uglevodnyi obmen. Fiziologo-biohimicheskie osnovy rosta i adaptacii sosny na Severe. Nauka. Leningrad: 30–57.

— , Trubino, G.I., Shreders, S.M. & Makarevskii, M.F. 1978. K metodike kolichestvennogo opredelenija uglevodov v vegetativnyh organah sosny obyknovennoi. Fiziologo-biohimicheskie issledovania sosny na Severe. Petrozavodsk:119–133.

Sudachkova, N.E., Osetrova, G.A. & Semenova, G.P. 1973. Biohimicheskie izmenenija v processe formirovanija godichnogo sloja drevesiny sosny obyknovennoi. Metabolizm hvoinyh v cvjazi s periodichnostju ih rosta. Krasnojarsk:5–15.

Sundberg, B., Ericsson, A., Little, C. H. A., Näsholm, T. & Gref, R. 1993. The relationship between crown size and ring width in Pinus sylvestris L. stems: dependence on indole-3-acetic acid, carbohydrates and nitrogen in the cambial region. Tree-physiology 12(4): 347–362.

3 Photosynthesis

3.1 The Photosynthetic Production of a Tree

Pertti Hari

3.1.1 Introduction

The growth is based on photosynthetic products. This fact makes possible to introduce the causal relationships underlying growth into the analysis. The key questions in the present monograph are a) How can the geographical variation in photosynthesis be introduced into the analysis? and b) How can the position of a tree in the stand be analysed using photosynthesis as an indicator? The solution to these two questions requires consideration of the photosynthetic process.

The study of photosynthesis, however, involves several methodological problems arising from the fact that it is impossible to measure a tree's photosynthetic production during a prolonged period. Indirect methods have to be applied. These methodological considerations are frequently omitted, which has resulted in confusion and misunderstandings.

The relationship between the photosynthetic process and the environment plays a key role in the study of photosynthetic production, which requires the identification of the functional unit of the process determining the level of basic analysis. The variation in irradiance within a leaf in the canopy is often pronounced. If the shading object is close, irradiance may increase more than tenfold within a distance of less than one millimetre. On the other hand, the transport of gases within a leaf is very ineffective, so that the functional unit is very small.

The surface of a leaf is covered by stomata which feed CO_2 to the surrounding cells. The distance between stomata is small, often of the magnitude of 50 μm. Diffusion is the gas transport mechanism within a leaf, a very ineffective process over longer distances. Thus the transport of CO_2 from the intercellular space under one stoma to the next one is of lesser importance. The spatial functional unit of photosynthesis in a leaf is evidently the area which one stoma feeds with CO_2, which is referred to in the present contex as the stomatal domain of the photosynthetic process.

Photosynthesis is also a rapid process. The pools of compounds and captured energy, which operate on a time scale shorter than 10 seconds are only able to filter very rapid oscillation (Hari et al. 1988). Rapid variation in photosynthetic production is noise in analysis over prolonged periods.

There are two levels of hierarchy involved in the analysis of photosynthetic production over prolonged periods. The fundamental phenomena occur on a micro scale, both spatially and temporally. The basic interest is focussed on the macro scale, annual and tree level. The transition from the micro hierarchy to macro is the key question in the analysis.

Several different models for photosynthesis have been presented in the literature. The kinetic approach describes the photosynthetic process using biochemical steps (Hari, Kaitala, et al. 1988, Laisk and Eichelman 1989, Laisk and Walker 1986). Several reactions have been detected in the dark reactions of the Calvin cycle. If all these known steps are introduced into the analysis then the model structure becomes very complicated. More aggregated approaches, in which only main phenomena or most important phenomenon is considered have also been used (Kaitala et al. 1982, Thornley 1976). The assumptions underlying such models are often poorly formulated and their functional basis is often unclear.

The aim of the present paper is to a) derive a simple model to link photosynthesis with environment, b) analyse the feasibility of testing the model and c) develop methods to estimate a tree's annual photosynthetic production.

3.1.2 A Dynamic Model of Photosynthesis

Photosynthesis involves several processes, whose distinction is to some extent arbitrary. The main steps may be 1. capture of light energy (light reactions), 2. formation of stable and energy-rich carbon compounds (dark reactions), 3. diffusion of carbon dioxide in mesophyl, 4. disolution of carbon dioxide in the water on mesophyl walls and 5. diffusion of carbon dioxide into the mesophyl space. These processes and flows of carbon dioxide determine the intercellular CO_2 concentration, since the ambient concentration is relatively constant. The basic gas flows occur at the stoma level.

Let A denote the area (m^2) which a stoma feeds with CO_2, C_i the intercellular CO_2 concentration ($g(CO_2)$ m^{-3}) and C_a the ambient CO_2 concentration ($g(CO_2)$ m^{-3}), p_s the photosynthetic rate ($g(CO_2)$ $s^{-1}m^{-2}$), r_s the respiratory rate ($g(CO_2)$ $s^{-1}m^{-2}$) and h the mean thickness (m) of the intercellular space of the stoma.

The amount of CO_2 in a stoma in the intercellular space is volume multiplied by concentration ie. $h\,A\,C_i$. The volume of intercellular space can be considered constant. The inflow of CO_2 and respiration produces and photosynthesis consumes the intercellular CO_2. The normal principle of constructing dynamic models is that the time derivative of the amount in a given volume equals the inflows minus outflows. This method yields

$$h\,A\frac{dC_i}{dt} = A[g\,(C_a - C_i) - p_s + r_s] \qquad (3.1)$$

where the term $g(C_a–C_i)$ describes the inflow and g is a parameter called stomatal conductance.

Photosynthesis involves several processes, each of them having its own dependence on environmental factors and on the state of the leaf element. The principle of simplicity has proved to be important in constructing models. For the sake of simplicity, assume that photosynthesis is proportional to the product of the two limiting factors, irradiance and intercellular CO_2 concentration

$$p_s = \alpha\,I\,C_i \qquad (3.2)$$

where α is a parameter.

This simple model describes the total effect of dissolution of CO_2 into the water on mesophyl walls, of diffusion in the mesophyl, of light and dark reactions. This assumption is a simplification of that presented by Marshal and Biscoe (1980). The time constant of intercellular CO_2 concentration seems to be a few seconds (Hari et al. 1988).

Assuming that for short intervals the intercellular CO_2 concentration is in a steady state, the time derivative equals zero and Eq. (3.1) results in

$$A[g\,(C_a - C_i) - p_s + r_s] = 0 \qquad (3.3)$$

The intercellular CO_2 concentration, C_i can be solved as

$$C_i = \frac{g\,C_a + r_s}{g + \alpha\,I} \qquad (3.4)$$

The dependence of the photosynthetic rate, p_s, on irradiance and ambient CO_2 concentration can be determined using Eqs. (3.2) and (3.4).

$$p_s = \frac{\alpha\,I\,(g\,C_a + r_s)}{g + \alpha\,I} \qquad (3.5)$$

For steady state conditions the resulting function is of the Michaelis-Menten type for irradiance and is linear for ambient CO_2.

The main emphasis in photosynthetic studies is at the tree level over prolonged periods. Irradiance depends on time and space within a canopy. This variation also generates variation in photosynthesis, which means that testing model (3.5) has to be based on data including variation in the environment, ie.

$$p_s(x,t) = \frac{a\,I(x,t)}{I(x,t) + b} \qquad (3.6)$$

The interpretation of the parameters is according to Eq. (3.5) $a = g\,C_a + r$ and $b = g/\alpha$.

3.1.3 Requirements for a Measuring System

The testing of this model is, however, problematic, since it is impossible to measure the photosynthetic rate of a single stoma. Only the CO_2 exchange of a large group of stomata over a prolonged period, say 10 s, can be measured. This transition from detailed stomatal level to a more aggregated level is a major methodological problem.

A small branch is closed into a measuring cuvette in the field system for measuring photosynthesis. The CO_2 concentration in the cuvette is changed by the CO_2 metabolism of the branch and by the inflow of air into the cuvette replacing the gas needed for the gas analyser. Let C denote the CO_2 concentration in the cuvette, C_a the ambient CO_2 concentration, p_b the photyosynthetic rate of the branch in the cuvette, r_b the respiratory rate of the branch, q the inflow rate of air into the cuvette and V the volume of the cuvette. The method of constructing a dynamic model using inflows and outflows can again be applied

$$V\frac{dC}{dt} = -p_b + r_b + q\,(C_a - C) \qquad (3.7)$$

When the above equation is integrated from the moment of the closure of the cuvette, t_i, to the moment of its opening, $t_i + \Delta$, then

$$-\int_{t_i}^{t_i+\Delta}(p_b(t) - r_b(t))\,dt = V\,(C(t_i+\Delta) - C(t_i)) - \int_{t_i}^{t_i+\Delta} q(t)\,(C_a - C(t))dt \qquad (3.8)$$

This equation enables the measurement of the gas exchange (photosynthesis – respiration) of a branch during an interval as the change in the amount of carbondioxide in the cuvette during closure and a small correction term describing the effect of inflow into the cuvette replacing the gas for the analyser. The cuvette concentration is usually measured 10–100 seconds after closing the cuvette.

The measurements produce data on the branch and 10–100 second interval levels. This is why the analysis of data has to be carried out at branch and interval level, although the fundamental model describes stomatal domain and rate level. Let $P_b(t_i,t_i+\Delta)$ denote the photosynthetic production during the ith measurement, $R_b(t_i,t_i+\Delta)$ the corresponding amount of respiration and $M(t_i,t_i+\Delta)$ the outcome of the ith measurement of gas exchange. Then

$$M(t_i,\ t_i+\Delta) = V(C(t_i+\Delta) - C(t_i)) + \int_{t_i}^{t_i+\Delta} q(t)(C_a - C(t))dt \qquad (3.9)$$

The problem now is that the measurements of photosynthetic production and the model describing photosynthesis are at different levels of hierarchy, ie. branch level during prolonged periods and momentary domain level.

The transition from domain level to branch level occurs by adding the photosynthesis of stomata, and temporal transition occurs by adding the photosynthetic production by the branch over short intervals. Mathematically this means integration of the product of stomatal photosynthesis and leaf area density ρ_A over the volume of the branch and over the period of measurement

$$P_b(t_i,\ t_i+\Delta) = \int_{t_i}^{t_i+\Delta}\int_V \rho_A(x)\ p_s(x,t)\,dV\,dt \qquad (3.10)$$

Let $\hat{P}_b$ denote photosynthetic production by the twig calculated according the model in the Eqs. (3.6) and (3.10). Thus

$$\hat{P}_b(t_i,\ t_i+\Delta,\ a,\ b) = \int_{t_i}^{t_i+\Delta}\int_V \rho_A(x)\frac{a\,I(x,t)}{I(x,t)+b}\,dV\,dt \qquad (3.11)$$

The above equation is not operational in arrangements of measurements within a canopy. In principle, there are two alternatives for determining the dependence of photosynthesis of a stoma on irradiance, either to carry out the measurements in a homogenous environment or to measure the dependence of irradiance on space and time. Since the later method requires special measuring arrangements which are rather complicated, the homogenization method has been chosen for further consideration.

Because the great variability of irradiance within a canopy is caused by shading, the uppermost branches sustain a more homogenous irradiance. Choose top branches in the canopy for study objects. It can then be assumed that within the cuvette the irradiance is spatially and temporally constant during the closure of the cuvette, ie.

$$I(x,t) = I(x_0,t_i) \qquad (3.12)$$

where x_o is a point above the canopy and t_i is the moment of the closure of the cuvette.

When the constancy assumption is introduced into the integration, then

$$\hat{P}_b(t_i+\Delta,a,b) \approx \frac{aI(x_0,t_i)}{I(x_0,t_i)+b}\int_V \rho_A(x)dV\ \ \Delta t = \frac{aI(x_0,t_i)}{I(x_0,t_i)+b}\Delta A\ \ \Delta t \qquad (3.13)$$

where ΔA is the leaf area in the cuvette.

The CO_2 exchange is an outcome of two processes, ie. photosynthesis and respiration. The effects of both processes have to be included in models in analysing CO_2 exchange data since these two processes can not be measured separately.

The respiration term is usually rather small. It can be introduced using a model linking temperature and respiration. This dependence is exponential.

$$r(x,t) = r_0 \; e^{\beta T(x,t)} \tag{3.14}$$

The above equation describes phenomena at the momentary and stomatal domain level. It has to be converted to interval and branch level by integration over time and space as in the case with photosynthesis. The variation in temperature is so small that it can be omitted without introducing disturbing error. Let $\hat{R}$ denote the approximated respiration, which can be obtained by integration as with the treatment of photosynthesis

$$\hat{R}_b(t_i,\; t_i+\Delta, r_0, \beta) \approx r_0 \, e^{\beta \; T(x_0,t_i)} \Delta A \;\; \Delta t \tag{3.15}$$

The values of the parameters are estimated using normal statistical procedures, such as the method of least squares, which solves the following minimization problem.

$$\min_{g_0,\alpha,r_0,\beta} \left\{ \sum_i (M_i - \hat{P}_b(t_i, t_{i+\Delta}, g_0, \alpha) + \hat{R}_b(t_i, t_{i+\Delta}, r_0, \beta))^2 \right\} \tag{3.16}$$

The utilization of the approach above requires measurements of CO_2 exchange, irradiance in unshaded conditions, and of temperature.

3.1.4 The measuring System

A measuring system was constructed in 1991 to test model (3.6) and to determine the values of its parameters at Värriö Research Station, Helsinki University (67°45'15"N, 29°36'17"E, 400 a.s.l.). The system consists of measuring cuvettes, a tubing system for air flow, magnetic valves for selecting the cuvette to be measured, as well as for opening and of closing cuvettes, a control system for air flow rate, a gas analyser (CO_2), sensors for irradiance, temperature, and air pressure, a data logger and a microcomputer.

The trap type cuvette, which is normally open but closed for measurement, was selected, since its disturbing effect on the functions of the object measured is small. The cuvette has several desirable properties. These are that:

1. The spatial variation of CO_2 concentration within the cuvette should be as small as possible.
2. When the cuvette is open, the leaves should have the same environmental conditions as neighbouring leaves outside the cuvette.
3. When closed, the cuvette should be as tight as possible, without any uncontrolled inflow of gas.
4. The cuvette should not change light conditions.

These demands cannot be fulfilled simultaneously since they conflict with each other to some extent. The requirements of gas tightness and of homogeneity of the CO_2 concentration were considered to be crucial.

In order to make the cuvette gastight, only the top and a hole in its lower part can open and close. A fan in the hole in the lower part generates a constant air flow through the cuvette when it is open and homogenizes the CO_2 concentration inside the cuvette when closed for measurements. The cuvette is made of plexiglass and the area of shade-casting metal parts is minimized. Closing and opening of the cuvettes is accomplished using pneumatic cylinders and magnetic valves.

The cuvette is placed for measurement in such a way that the pine shoot to be measured is parallel to the axis of the globe. The advantage of this arrangement is that the angle between the sun and the shoot does not vary during the day. The variation during the growing season, say from first of May to 23 September, is also rather small, from 66° to 90° so that shading by needles in the same shoot is as small as possible.

There is no artificial cooling system in the cuvette. The energy input caused by irradiance is transported from the cuvette by the air flow through it when open or is consumed in transpiration. The velocity of air in the open cuvette is about 50 cm s^{-1}. This is nearly the wind speed within the canopy on calm days. During closure, the temperature in the cuvette increases due to

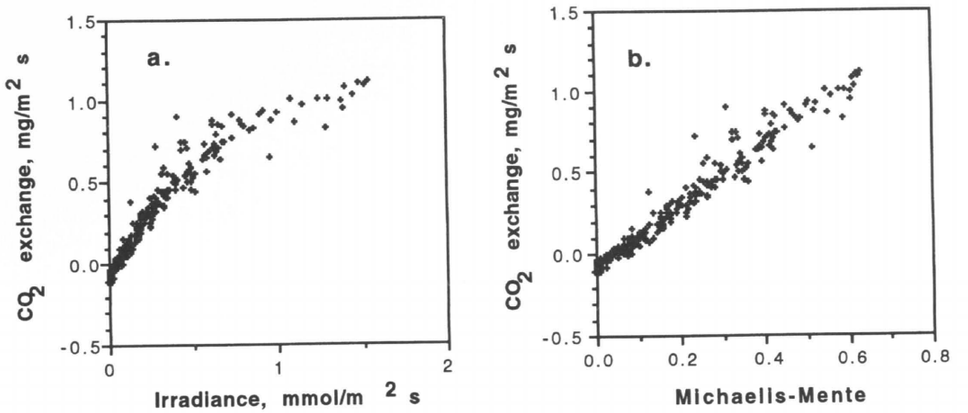

Fig. 3.1 The dependence of measured gas exchange on irradiance (a) and the relationship between I / (I + 900) and measured gas exchange (b). The measurements from 16 July to 19 July 1992.

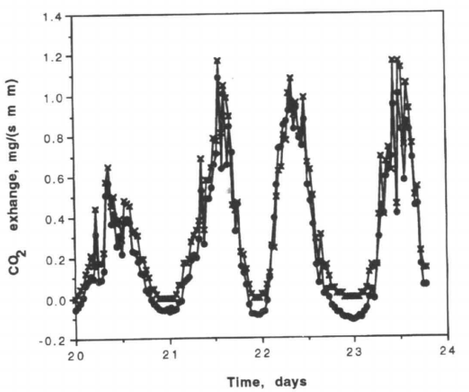

Fig. 3.2. The measured (filled circle) and predicted (cross) CO_2 exchange 20–23 July 1992.

radiative energy input. The maximum increase rate is about 0.1°C s^{-1} when the irradiance is high.

The tubing system was constructed of polyethene pipes (6 mm/4.4 mm). The flow of gas in the tubes generates a time lag, about 30 s, between the concentration in the cuvette and the moment of its measurement. Because the CO_2 concentration changes rapidly in the cuvette, any variation in the flow rate of gas in the tubing system generates inaccuracies. For this reason special emphasis was given to the control of flow rate, which was measured and regulated by a mass flow controller (5850 TR, Brooks Instrument B.V. Netherlands) which is able to maintain the preset flow rate within ±1.5 % of the desired rate.

The CO_2 concentration is measured with an IRGA (URAS 3G, Hartmann & Braun, BRD). Temperature is monitored using copper constantane thermo pairs. Ambient air pressure and the air pressure difference between the IRGA and the ambient air is monitored with pressure transducers (Schaevitz P-3061, Shaevitz engineering, U.S.A.).

The measuring system is controlled and the readings taken are stored on a microcomputer. Magnetic valves are employed for the closing and opening of the cuvettes. The microcomputer and data logger together regulate the opening and closing of the magnetic valves, as well as the selection of the cuvette for measurement. The construction of the photosynthesis measuring system is very similar to that in the Forestry Field Station, Helsinki University (Hari et al. 1990).

3.1.5 Analysis of Field Measurements

Two branches in our experimental stand were selected for the measurements in early summer 1992. The mean diameter of the trees in the stand is 10 cm, mean height 6 m, and leaf area 4 m^2(leaf)/m^2(soil).

Photosynthesis is the dominant gas exchange process, often being ten times respiration. Thus

rather rough estimates of the parameters in the model describing respiration are needed in order to determine the values of the parameters of the photosynthetic model. The estimation can be done stepwise; first, estimation of respiratory parameters and secondly, photosynthetic parameters. The value of the level parameter of respiration r_o can be estimated from night-time measurements and the value of temperature dependence parameter β can be based on the literature. These produce: $r_o = 0.065$ mg m^{-2} s^{-1} and $\beta = 0.036$°C (Korpilahti 1988).

In the first phase of the analysis the dependence of gas exhange measurements on the integrals $\hat{P}_b$ was investigated using different values for the non-linearity parameter of Michaelis-Menten function, b in Eq. (3.6). The parameter value which produces the smallest residual between $\hat{P}_b$ and measured gas exchange is the result of the estimation. The estimation procedure is not very sensitive to the non-linearity parameter because the magnitude parameter can to great extent compensate the error in the value of the non-linearity parameter.

The gas exchange of the branch in the cuvette was predicted for the days from 20 to 23 July using light measurements and the model using parameter values estimated from the data 16–19 July. Consequently, the parameters in the model had fixed values. The comparison between observed and predicted gas exchanges can be seen in Fig. 3.2. The model is evidently capable of predicting the gas exchange quite accurately. The same type of result has been obtained earlier (Hari et al. 1981, Korpilahti 1988, Lohammar et al. 1980).

3.1.6 The Effect of Stage of Development on Photosynthesis

The experimental results in Figs. 3.1. and 3.2. consern photosynthesis when the trees are in their active summer state. A slow transition from the dormant winter state to the active summer state occurs in the spring and a corresponding return to the winter state in autumn. These changes in the biochemical control system are weather driven. The favourable summer conditions begin earlier in the south enabling a longer photosynthetically active period and larger annual photosynthetic production.

Assume as in Chapter 2 that the state of the biochemical control system can be introduced with one scalar variable called stage of development, denoted by M. According to Pelkonen (Pelkonen 1980, Pelkonen 1981) the photosynthetic rate in the spring depends on irradiance and annual stage of development and a multiplicative model

$$p(I,M) = f_I(I)\ f_M(M) \tag{3.17}$$

where f_I describes the effect of irradiance and f_M the effect of stage of development can be used. The dependence on irradiance is the same as previously, ie. in Eq. 3.6. Model Eq. 3.17 should give the same results as Eq. 3.6. during the active period. Thus the function f_M should equal one during the active period. Since photosynthesis is blocked during dormancy, f_M should be zero in winter. These requirements are fulfilled by the following function

$$f_M(M) = \begin{cases} 0 \text{ when } M \le 0 \\ M / d_1 \text{ when } 0 < M < d_1 \\ 1 \text{ when } M \ge d_1 \end{cases} \tag{3.18}$$

where d_1 is a parameter.

The rate of development, m, is defined as the time derivative of the annual stage of development. Warm weather moves the biochemical control system towards its summer state and extremely cold weather back to the dormant state. These phenomena are introduced into the analysis with the temperature dependence of the rate of maturation. The annual stage of development also has an effect on the rate of development. The following approximation seems to be in satisfactory agreement with field measurements (Pelkonen 1980)

$$\frac{dm}{dt} = m(T,M) = \frac{100}{1+100\, d_2^{-(T-M/d_3)}} - \frac{100}{1+100\, d_2^{+(T-M/d_3)}} \tag{3.19}$$

where d_2 and d_3 are parameters.

Since the model defined by Eqs. 3.17–3.19 describes photosynthesis during the recovery in the spring quite accurately (Pelkonen 1980, Pelkonen 1981), the photosynthetic rate of a stoma can be predicted at any time using weather information. If continous temperature and irradiance measurements are available then the photosynthetic rate of a stoma in unshaded conditions can be determined.

3.1.7 The Photosynthetic Production of a Tree

The models of photosynthesis including the status of biochemical control systems have the advantage that the photosynthetic rate can be predicted accurately using only environmental variables, ie. irradiance and temperature, although this model has the disadvantage that the structure of the system is characterized by an aggregated variable, the stage of annual development.

Information concerning the functions of a single stoma can be converted to tree level by summing the gas exchange of each stoma. Mathematically this means integration over space. The transition from the momentary functions to the annual level is also integration over time. Thus the annual photosynthetic production, P, of a tree is

$$P = \int_V \int_{t_1}^{t_2} \rho(x)\, p(x,t)\, dt\, dV \tag{3.20}$$

This integral plays a key role in the modelling of stand development. When combined with Eqs. 3.17–3.19 it yields the annual photosynthetic production as a function of temperature and irradiance within the canopy, enabling approximation of the annual photosynthetic production. The geographical aspect and the effect of the position of the tree in the stand are then automatically introduced into the analysis.

3.2 The Influence of Shoot Architecture on Photosynthesis

Juhan Ross, Pauline Stenberg, Frank Berninger and Pertti Hari

3.2.1 Background

Shoot structure greatly affects light interception and the photosynthesis of a shoot. Consider the simple example presented in Fig. 3.3, showing two shoots with different geometry. In comparison with shoot A, shoot B has longer needles and a larger needle angle, thus resulting in a larger shoot diameter and a smaller density of needles in the shoot. Suppose that for both shoots the surrounding illumination conditions and the photosynthesis light curve of the needle surface elements are the same. Then, in accordance with Fig. 3.3, it is obvious that the needles on shoot B are better illuminated than the needles on shoot A. At the same irradiance then, the photosynthesis rate per unit needle area should logically be higher for shoot B than for shoot A as a result of differences in shoot structure.

The influence of shoot structure on the irradiance distribution and photosynthesis on a Scots pine shoot in a direct radiation field has previously been analysed by Smolander et al. (1987) who found that in a direct radiation field the mean irradiance over the needle surface of a shoot was the major component causing variation in the photosynthetic response of the shoot. In direct radiation the mean irradiance on the needle surface is proportional to the ratio between shoot silhouette area and total needle area (*STAR*) (Oker-

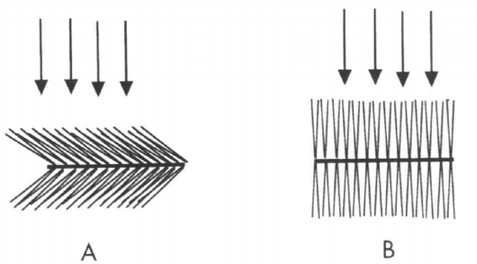

Fig. 3.3. Schematic illustration of two shoots, A and B, with different geometry.

Blom and Smolander 1988). The shoot silhouette area can be determined, e.g., using photography, but not directly from measurements of shoot characteristics.

A Scots pine shoot can be viewed as a cylinder, the dimensions of which are given by the length and width of the shoot axis, needle length and needle angle (Oker-Blom et al. 1983). For an approximate notion of the structure-dependent variation in illumination conditions inside the shoot we propose a new characteristic – the needle living-space (*NLS*), given by the formula

$$NLS = V_S / S_{NS} \qquad (3.21)$$

where V_S is the shoot cylinder volume (cm^3) and S_{NS} (cm^2) is the needle surface area of the shoot. The needle living-space expresses the volume inside the shoot cylinder per unit needle area (ie. the inverse of needle area density). The larger the *NLS* is the smaller the within-shoot shading.

The shoot cylinder volume may be expressed as (cf. Fig. 3.3.)

$$V_S = \pi(d_S/2)^2 l_S = \pi(l_N \sin v_N + d_t/2)^2 l_S \qquad (3.22)$$

where l_S and d_S are the length and diameter of the shoot cylinder, d_t is the twig diameter, l_N is the needle length and v_N is the needle angle. The needle surface area of a shoot equals the mean needle surface area of one needle, $S_N(l_N)$ (here expressed as a function of its length), multiplied by needle density (n_N) and shoot length (l_S),

$$S_{NS} = S_N(l_N)\, n_N\, l_S \qquad (3.23)$$

Formula (3.21) can now approximately be written as

$$NLS \approx \frac{\pi l_N^2 \sin^2 v_N}{S_N(l_N) n_N} \qquad (3.24)$$

(because d_t is small compared to d_s)

From Eq. 3.24 it follows that *NLS* is primarily determined by needle length, needle angle and density of needles per unit length of the shoot axis. All these parameters can be obtained from simple phytometrical measurements. The aim of this study was to experimentally determine the magnitude of the effect of mutual shading of needles on shoot photosynthesis, and to test how successfully this effect can be characterized by the needle living-space.

3.2.2 Experimental Design

Measurements of photosynthesis and shoot architecture were carried out between August 17 and September 6 in 1989 at the Hyytiälä Forest Field Station in Central Finland (61°51´N, 24°17´E, 160 m a.s.l.). The photosynthesis measurements were carried out in the testing phase of the new field measuring system constructed at the Field Station (Hari et al. 1990). Since the measuring system for irradiance was still under construction, a LICOR-sensor above the measuring cuvettes was coupled in the data-logger for measuring irradiance.

One and two year old shoots were collected at the upper part of the crowns of two different trees. Their position in the crown was classified in accordance with the address system developed by Ross et al. (1986). Immediately after cutting, the shoots were placed in a water vessel and kept there until the end of the experiment. The duration of the experiments for different shoots varied from 12 hours to 3 days. Photosynthesis often started to decrease simultaneously with transpiration during sunny days after midday. The probable reason for this decrease is the stomatal reaction, despite the fact that the cut shoot was in the water vessel. When the experiment was continued the next day, the values of shoot photosynthesis in the morning reached those of the previous day. The data when the stomata were closed were excluded from the construction of photosynthetic light curves. The phytometrical measurements of the shoots were carried out after measuring photosynthesis. A modified Tirén's formula was used for determination of the needle surface area (Ross et al. 1986). The architectural characteristics of the shoots are given in Table 3.1.

3.2.3 The Relation Between Shoot Photosynthesis and Needle Living-Space

Seventeen shoots were studied. Shoot photosynthetic light curves, visually fitted to the points measured, are shown as examples in Fig. 3.4. The

Table 3.1. Architectural characteristics of the shoots.

Address	l_s (cm)	d_t (cm)	n_N (cm^{-1})	l_N (cm)	v_N (degr.)	A_N (cm^2)
1	18	1.10	11.5	7.4	30	280
11A	19	0.66	10.7	5.4	30	463
21A	20	0.98	10.8	6.0	50	552
21B	18	0.96	13.9	6.0	30	456
22A	18	1.10	13.7	4.7	70	439
22B	11.5	1.20	13.9	4.0	80	231
31	17.5	0.76	14.3	5.9	25	618
32A	20	0.85	17.0	3.5	45	408
32B	19.1	0.98	13.0	4.3	50	351
42	17.5	0.86	11.1	4.3	45	306
51	10	0.53	22.7	5.3	30	412
61A	13	0.48	18.3	5.3	30	500
61B	13.5	0.46	18.7	4.3	40	288
62	18.8	0.73	20.9	3.7	55	228
772	9.5	0.34	21.5	2.8	60	183
11B	14	0.78	9.8	7.0	30	280
41	12.4	0.73	19.1	5.4	25	443

l_s = Length of the shoot (cm)
d_t = Diameter of the twig (cm)
n_N = Number of needles per cm shoot length (cm^{-1})
l_N = Average length of the needles (cm)
v_N = Average angle of the needles to the shoot (degr.)
A_N = Total needle area of the shoot (cm^2)

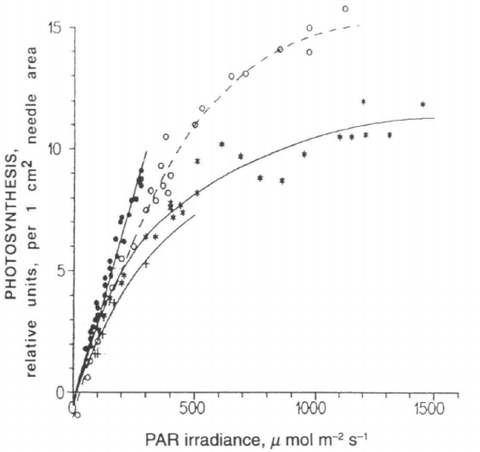

Fig. 3.4. Measured CO_2 exchange rates of some sample shoots as function of irradiance.

scattering of the measurement points characterize the accuracy of the measurement system. The weather conditions prevented complete curves (saturation rates) being obtained for all shoots (Fig. 3.4). From the light curves, the values of shoot photosynthesis at irradiance values of 0, 100, 300, 500 and 1000 μmol $m^{-2}s^{-1}$ were estimated visually. The needle living-space (*NLS*) was calculated in accordance with Eq. (3.21). The mean *STAR*, $\overline{STAR}$, with respect to a spherical shoot orientation, was also calculated for each shoot using Oker-Blom et al's model (1983).

There was a close linear correlation (r=0.916) between $\overline{STAR}$ and *NLS* (Fig. 3.5). The correlation between photosynthesis (P_G) and needle living-space was slightly higher than between P_G and mean *STAR*. Fig. 3.6 shows the linear regressions between shoot photosynthesis and needle living-space (*NLS*) at different irradiance values. The equations obtained were:

$$\begin{aligned} P_G(100) &= 4.30 + 1.40\ NLS & r &= 0.71 \\ P_G(300) &= 6.66 + 3.26\ NLS & r &= 0.85 \\ P_G(500) &= 8.57 + 3.98\ NLS & r &= 0.90 \\ P_G(1000) &= 8.26 + 5.31\ NLS & r &= 0.89 \end{aligned} \qquad (3.25)$$

An attempt was made to approximate the photosynthesis light curves by means of the Michaelis-Menten equation

$$P_N = \frac{a I P_{max}}{a I + P_{max}} - R_g \qquad (3.26)$$

where a is the initial slope, P_{max} is the maximum rate of photosynthesis (lim P_G, $I \rightarrow \infty$) and R_g is the dark respiration (this was assumed to be constant throughout the day). It should be noted that the accuracy of the determination of the parameters P_{max} and a is not high, because of the weather during the measurements. For some shoots, when the CO_2-exchange measurements were carried out during cloudy days, we had data only for the initial part of the curve so that the error in determining P_{max} was potentially large. These shoots were consequently omitted from the analysis when we examined the correlation between the values of the estimated parameters and the needle living-

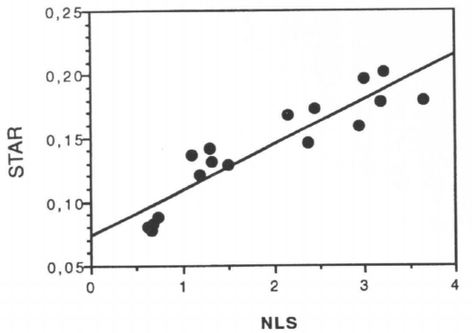

Fig. 3.5. Regression between needle living-space and mean silhouette to total needle area ratio for the sample shoots.

space. The regression analysis showed that there was rather weak correlation (r=0.660) between *a* and *NLS* (Fig. 3.7a), but strong correlation (r=0.822) between P_{max} and *NLS* (Fig. 3.7b). The equations were:

$$a = 0.063 + 0.020\ NLS \qquad r = 0.660$$
$$P_{max} = 11.86 + 6.41\ NLS \qquad r = 0.822 \qquad (3.27)$$

3.2.4 Discussion

Further measurements will be needed to test the usefulness of *NLS* as a measure of shading within a shoot. Although it seems apparent that there would be positive correlation between needle living-space and the light interception efficiency

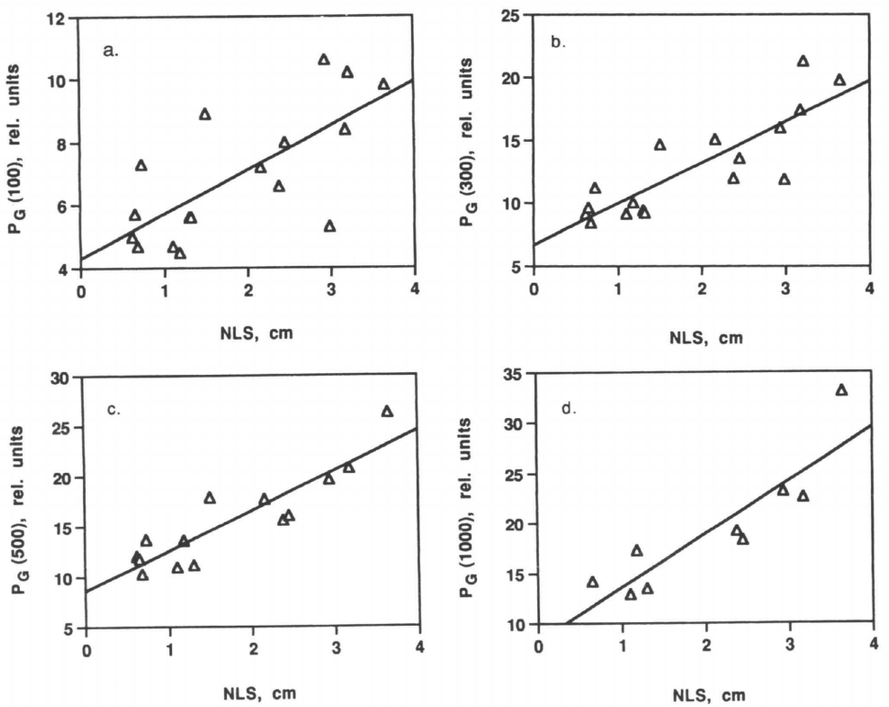

Fig. 3.6. Regression between rate of photosynthesis (P_G) and *NLS* at different irradiance values. (a) *I*=100, (b) *I*=300, (c) *I*=500 and (d) *I*=1000 µmol $m^{-2}s^{-1}$. (Eq. 3.25)

Table 3. 2. Needle living-space, mean silhouette to total needle area ratio and shoot photosynthesis rates at different irradiance values (*PAR*) and the parameters P_{max} and a of the Michaelis-Menten function.

NLS (cm^3 / cm^2)	*STAR* *I*:	Rate of net shoot photosynthesis (relative units) at irradiance 0	100	300	500	1000	P_{max}	*a*
3.65	0.179	–7	2.8	12.8	19.3	26.1	45.7	0.121
1.18	0.121	–3	1.5	7.0	10.6	14.3	25.2	0.057
2.94	0.159	–8.5	2.1	7.5	11.1	14.7	26.6	0.151
1.50	0.128	–5.5	3.4	9.2	12.4	–	23.8	0.138
3.18	0.178	–5	3.4	12.4	15.8	17.6	28.0	0.139
3.22	0.201	–7	3.2	14.3	–	–	–	–
0.73	0.088	–4.5	2.8	6.7	9.2	–	17.2	0.120
1.30	0.142	–3	2.6	6.4	8.2	10.5	15.9	0.080
2.45	0.173	–4	4.0	9.6	12.1	14.3	21.4	0.127
2.16	0.167	–3	4.2	12.1	14.7	–	27.6	0.103
0.65	0.077	–4	1.7	5.6	7.8	10.2	17.1	0.079
0.68	0.083	–3	1.7	5.4	7.3	–	14.7	0.068
1.32	0.131	–3	2.6	6.2	–	–	–	–
2.99	0.197	–2	3.3	9.9	–	–	–	–
1.10	0.136	–2	2.7	7.1	9.0	10.9	15.98	0.089
2.38	0.146	–4.5	2.1	7.5	11.1	14.7	24.8	0.083
0.62	0.080	–3	2.0	6.1	9.1	–	19.1	0.063

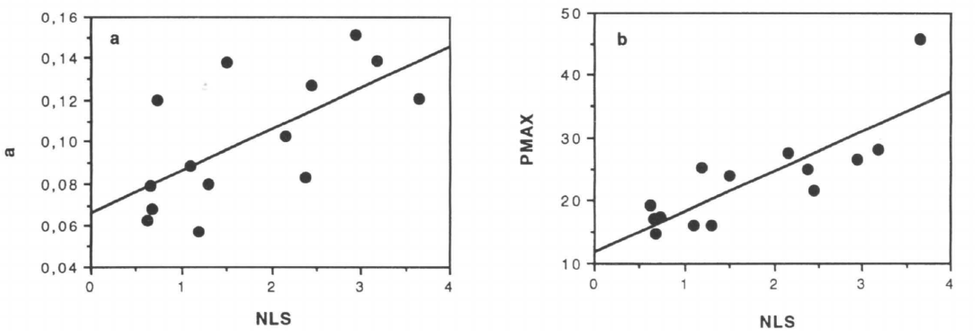

Fig. 3.7. Regression between the *NLS* and parameters ((a) initial slope, and (b) maximum rate of photosynthesis) of the fitted photosynthesis light curves.

of a shoot (cf. Fig. 3.4), there is no a priori reason for the close linear relationship between P_G and *NLS* (Fig. 3.6). In connection with this result the question arises whether the correlation between shoot photosynthesis and needle living-space is real or whether there are some other factors involved. Needle age, for instance, affects the rate of photosynthesis, which is at its maximum for one-year old shoots and decreases with age. However, as can be seen from Table 3.1, the needle living-space is generally larger for two-year old shoots and the correlation between P_G and *NLS* would thus have been still higher had age been considered.

In earlier studies (Oker-Blom et al. 1983, Smolander et al. 1987) the *STAR* of a shoot has been found to be a useful characteristic in expressing the relationship between shoot photosynthesis and

irradiance. The connection between *STAR* and rate of photosynthesis in direct radiation is straightforward because the *STAR* is proportional to the amount of absorbed radiation. In diffuse radiation the same applies if a mean *STAR*, weighted by the directional distribution of irradiance, is used as the characteristic. Since our experiment was conducted in very variable natural illumination conditions it was not possible to separate the photosynthesis data according to sunny and cloudy conditions and calculate the appropriately weighted mean *STAR* for each shoot. A spherically weighted *STAR* was computed instead and used as a complement to *NLS*.

The close correlation between *NLS* and *STAR* (Fig. 3.5) suggests that *NLS* could be a useful measure of light interception and the photosynthetic efficiency of a shoot. However, Smolander et al. (1994) showed that although the needle area density in the shoot cylinder (the inverse value of *NLS*) was one of the major determinants of *STAR* in Scots pine, other factors such as the shoot diameter were important too. In addition (as also seen from Fig. 3.5), the relationship between *STAR* and *NLS* is not a linear one. An advantage of *NLS* over *STAR* is that it is easily obtained from simple phytometrical measurements. A weakness of *NLS* might on the other hand be that, unlike *STAR*, it is independent of the direction of radiation and thus does not account for the possible influence of solar radiation geometry (e.g., direct vs. diffuse radiation) on shoot photosynthesis.

References

Hari, P., Hallman, E., Salminen, R. & Vapaavuori, E. 1981. Evaluation of factors controlling net photosynthetic rate in Scots pine seedlings under field conditions without water stress. Oecol. 48: 186–189.

— , Kaitala, V. & Salminen, R. 1988. The use of intermittent radiation in studying photosynthesis and transpiration. Photosynthetica 22 (2): 236–239.

— , Korpilahti, E., Pohja, T. & Räsänen, P. 1990. A field system for measuring the gas exchange of forest trees. Silva Fennica 24: 21–27.

Kaitala, V., Hari, P., Vapaavuori, E. & Salminen, R. 1982. A dynamic model for photosynthesis. Ann. Bot. 50: 385–396.

Korpilahti, E. 1988. Photosynthetic production of Scots pine in the natural environment. Acta Forestalia Fennica 202. 71 p.

Laisk, A. & Eichelman, H. 1989. Towards understanding oscillations: a mathematical model of the biochemistry of photosynthesis. Phil. Trans. R. Soc. London 323: 369–384.

— & Walker, F. 1986. Control of phosphate turnover as a rate factor and possible cause of oscillations in photosynthesis: a mathematical model. Proc. R. Soc. London B 227: 281–302.

Lohammar, T., Larsson, S., Linder, S. & Falk, S. 1980. Fast-simulation models of gaseous exchange in Scots pine. In: Person T (eds) Structure and function of nothern coniferous forests. Swedish Natural Science Research Council: Stockholm, p. 505–536.

Marshal, B. & Biscoe, P. 1980. A model for C3 leaves describing the dependence of net photosynthesis on irradiance. J. Exp. Bot. 31: 29–39.

Oker-Blom, P., Kellomäki, S. & Smolander, H. 1983. Photosynthesis of Scots pine shoot: The effect of shoot inclination on the photosynthetic response of a shoot subjected to direct radiation. Agric. Meteorol. 29: 191–206.

— & Smolander, H. 1988. The ratio of shoot silhouette area to total needle area in Scots pine. Forest Sci. 34: 894–906.

Pelkonen, P. 1980. The uptake of carbon dioxide in Scots pine during spring. Flora 169: 386–397.

— 1981. Recovery and cessation of CO uptake in Scots pine at the beginning and at the end of the annual photosynthetic period. University of Helsinki, Department of Silviculture, Research notes 30. 95 p.

Ross, J., Kellomäki, S., Oker-Blom, P., Ross, V. & Vilikainen, L. 1986. Architecture of Scots pine crown: phytometrical characteristics of needles and shoots. Silva Fennica 20(2): 91–105.

Smolander, H., Oker-Blom, P., Ross, J., Kellomäki, S. & Lahti, T. 1987. Photosynthesis of a Scots pine shoot: Test of a shoot photosynthesis model in a direct radiation field. Agric. For. Meteorol. 39: 67–80.

— , Stenberg, P. & Linder, S. 1994. Dependence of light interception efficiency of Scots pine shoots on structural parameters. Tree Physiol. 14: 971–980.

Thornley, J. H. M. 1976. Mathematical models in plant physiology. Academic Press: London. 318 p.

4 Theoretical Aspects on Radiation Submodels Used in Forest Growth Models

Tiit Nilson and Pauline Stenberg

4.1 Introduction

Canopy structure or, more specifically, the number and dispersion of leaves is the main determinant of the amount of photosynthetically active radiation (*PAR*, 400–700 nm) absorbed by the canopy. Further, there is a strong link between light interception (absorbed *PAR*), gross photosynthetic production and the growth of a stand. For this reason, practically all process-oriented forest growth models include a canopy radiation submodel to consider the feedback from shading biomass (leaf area) to light interception and photosynthesis (Mäkelä 1990). The general aim of a canopy radiation submodel is to quantitatively describe the functional relationship between canopy structure and photosynthetic radiation regime in a given above-canopy radiation environment.

During recent decades considerable refinement has taken place in the development of canopy radiation models, both at the level of describing canopy structure and in the mathematical treatment of the radiative transfer in plant stands (e.g., Myneni and Ross 1991). This development towards more complex and more realistic canopy radiation models is important particularly since growth models seem to be very sensitive to light interception parameters (Mäkelä 1990). From a growth modelling perspective, however, very complex canopy radiation submodels are not operational in the sense that they become too time-consuming in growth simulations extending over long time periods. It would be convenient if the canopy radiation submodel could be replaced by a simplified relationship (an aggregate equation) of annual potential photosynthetic production and parameters of canopy structure and radiation regime. The requirement for using such a relationship is that it should contain all the relevant variables, ie. incorporate those variables to which the photosynthesis model is most sensitive, and which change during the lifetime of the stand (or during the simulation period).

In order to make simplifications, we need a model with a defined and tested representation of the complexity of the canopy. In this chapter the theoretical basis of models describing the relationships between canopy structure, radiation regime and photosynthesis in coniferous stands is presented.

4.2 Modelling Canopy Structure and Radiation Penetration in Conifers

4.2.1 The Gap Probability

Because *PAR* absorption by green leaves is high, the penetration of *PAR* through the canopy in a given direction is approximated by the fraction of view not blocked by leaves from beneath the canopy (Welles 1990). In canopy radiation models, a statistical approach is commonly used to describe the spatial distribution of leaves in the canopy. The locations of leaves are assumed to be statistically independent random variables generated by a specified probability density function (Mann et al. 1977).

An essential basis for calculating the statistical penetration of radiation is the probability of a gap in different directions $\Omega=(\theta,\phi)$ (θ=zenith angle, ϕ=azimuth) through the canopy, as seen from a specified point X. The penetration of *PAR* can be expressed with help of the indicator function (α), which is a random (Bernoulli) variable, having

the value of 1 when there is a gap between foliage in the specified direction, and 0 otherwise.

The penetration coefficient of direct solar radiation (a_s) to a point X in the canopy is obtained by integrating the indicator function (α) weighted by the normalised radiance distribution $i_S(\Omega)$ over the solid angle (Ω_S) subtending the sun:

$$a_S(X,\Omega) = \iint_{\Omega S} i_S(\Omega)\alpha(X,\Omega)\cos\theta\sin\theta d\theta d\phi \quad (4.1)$$

Analogously, the penetration coefficient of diffuse sky radiation (a_D) is obtained by integrating the indicator function (α) weighted by the normalised distribution of diffuse sky radiance $i_D(\Omega)$ over the upper hemisphere:

$$a_D(X) = \int_0^{2\pi} \int_0^{\pi/2} i_D(\Omega)\alpha(X,\Omega)\cos\theta\sin\theta d\theta d\phi \quad (4.2)$$

The coefficients a_s and a_D correspond to the fractions of direct and diffuse *PAR* transmitted to point (X) in the canopy. Their mean values are obtained by replacing α by its expected value (a), the gap probability in the specified direction.

If leaves are assumed to be independently and randomly distributed in the canopy (e.g., generated by a Poisson process), the gap probability in a specified direction is given by:

$$a = E[\alpha] = \exp(-Gul), \quad (4.3)$$

where l is the length of path of the solar beam within the canopy, u is the mean leaf area density along this path, and G is the "mean projection of unit foliage area" (Ross and Nilson 1965). G was originally defined as the ratio of projected to one-sided (planar) leaf area; however, because the one-sided area of a needle is not a well-defined concept, we define G as the ratio of projected to all-sided leaf area. In accordance with this, the leaf area density (u) is also defined on an all-sided area basis (Stenberg et al. 1994).

Equation 4.3 is the basis of practically all statistical light penetration models. In non-homogeneous vegetation, such as coniferous forest stands, however, it cannot be used in this form but requires some modification.

4.2.2 *Models Used to Describe Coniferous Stand Structure*

Grouping in a coniferous stand typically occurs at many different hierarchical levels (Norman and Jarvis 1975, Oker-Blom 1986, Nilson 1992). Grouped distribution refers to a spatial pattern where the positions of elements are positively correlated, ie., the probability that an element is situated near another one is larger than for a purely random (Poisson) pattern. In conifers, several grouping levels may be distinguished. Needles are clumped into shoots, which are nonrandomly positioned in branches and whorls of the individual tree crowns. In addition, the spatial pattern of trees (tree crowns) is often grouped. The effect of grouping on light penetration can be described hierarchically dividing the stand into subcomponents representing the most important grouping levels (e.g., Oker-Blom et al. 1991). Below we shall describe submodels used to describe coniferous stand structure, with special reference to Scots pine.

Stand models may be given either in the form of tree locations and tree size parameter vectors (tree height, crown length and diameter, trunk diameter at breast height and at the height of the lowest living whorl, etc.) specified for each tree in a certain forest compartment (Hari et al. 1985), or given analytically as the distribution functions of tree locations and size (Nilson 1977). The pattern of tree location may be given as measured, simulated by a computer (Pukkala 1988, Gusakov and Fradkin 1990) or by some theoretical distribution function (Nilson 1977), e.g., by the widely used Poisson distribution or by some stochastic process (Tomppo 1986). According to the Poisson distribution the probability $P_i(S)$ of i trees occurring in a plot of area S (m^2) is

$$P_i(S) = (\lambda S)^i \exp(-\lambda S) / i!\ ,\ i = 0, 1, 2 \quad (4.4)$$

where λ is the stand density (trees per m^2).

Small deviations from the Poisson tree distribution pattern towards regularity or grouping may be approximated by introducing a correction factor (Nilson 1992). For example, the probability of no trees in a plot of area S may be calculated as:

$$P_o(S) = \exp(-\lambda c S) \quad (4.5)$$

where $c = \ln(GI)/(GI-1)$, GI being Fisher's grouping index – the ratio between the variance and the mean value of the stem number occurring in a plot of area S.

In a *tree crown model* the crown shape and dimensions should first be given. The crown forms most commonly used to describe Scots pines are a truncated ellipsoid of rotation and a cone. Oker-Blom et al. (1986) suggested a Scots pine crown model describing the crown as a cone in the upper part (approximately a half of the total crown length), a cylinder in the middle and an intersected sphere at the bottom of the crown. In some cases, e.g., when trees are grown densely in rows, rotationally non-symmetrical crown shape models may be needed.

Scots pine *whorls* may be modelled as crown sections cut by horizontal planes corresponding to the tree height increment of the corresponding year. A further subdivision of the whorls into branches is possible, but if the distribution of branches within the whorl is sufficiently uniform, it is appropriate to describe whorl and crown structure directly in terms of the spatial and angular distribution of leaves or shoots in the crown. For larger trees it may be necessary to define an empty (non-foliated) region around the stem (Koppel and Oja 1984).

The uniform, beta, normal, and Weibull distributions are commonly used to describe the spatial distribution of leaves in a crown. Although a non-uniform distribution of leaf area can be used to incorporate some grouping effect, continuous distributions cannot be used to describe very small-scale variation in leaf area density as is caused by the clumping of needles on shoots. A way to overcome this problem is to choose the shoot as the basic element, and define the density function of shoots instead of leaves (needles). For example, Stenberg et al. (1993) used the beta distribution to describe both the vertical distribution of shoots in the crown and the horizontal distribution of shoots in a whorl. In this approach, however, a model of shoot structure is needed.

The Scots pine *shoot* can be viewed as a cylinder, the dimensions of which are given by shoot length, needle length and needle angle (Oker-Blom et al. 1983). When viewed from a particular direction the shoot cylinder has a certain transmittance (gap fraction), defined as the ratio of gap area (non-shaded area) in the shoot cylinder projection area to total cylinder projection area (Oker-Blom and Smolander 1988). The shading of a shoot in a particular direction is determined by its effective projection area or "silhouette area" in that direction, and the "silhouette leaf area to total leaf area ratio" (*STAR*) expresses the ratio of the effective projection area of the shoot to its total needle surface area (Carter and Smith 1985, Oker-Blom and Smolander 1988). *STAR* is conceptually analogous to the G-function (Eq. 4.3), the only difference being that they are defined for different foliage elements (leaves and shoots). The *STAR* of a shoot depends on shoot geometry (particularly needle angle and density) and varies with the angle between the shoot axis (the twig) and the direction of projection (radiation). *STAR* is smaller than the G-function for individual leaves because of the mutual shading by needles on the same shoot.

For describing the angular distribution of shoots the same distributions as used for planar leaves (e.g., Ross 1981) may be used. The most widely used leaf angle distribution is the spherical distribution, defined such that the leaf has no preferred orientation in space. The G-function (Eq. 4.3), here defined as the ratio of projected to total (all-sided) leaf area, then has the value G=0.25, independently of the direction of radiation (see Lang 1991). For spherically oriented shoots, the mean ratio of projected shoot area to total needle area is denoted $\overline{STAR}$ (Oker-Blom and Smolander 1988). It is smaller than 0.25; for Scots pine shoots around 0.15.

In Stenberg et al.'s material (1993), comprising measurements of shoot azimuth and zenith angle in 25 young Scots pine crowns, the angular distribution of shoots was not spherical and the mean shoot angle (to the vertical) increased with depth in the canopy. Despite this fact, however, the spherical distribution may serve as a reasonable approximation when exact measurements are not available.

4.2.3 *Light Penetration in a Grouped Stand*

Based on the models outlined above, we give equations for the penetration of radiation in a stand where: (1) the spatial pattern of trees is defined by a Poisson distribution, (2) trees are

divided into size classes and the crown structure of trees in the same class is similar, (3) crowns are rotationally symmetrical, and (4) the within-crown shading is independent of the between-crown shading.

Assuming that the within-crown and between-crown shading are independent, the mean penetration of radiation to a point (x,y,z) within a tree crown can be given as a product of two gap probabilities, one corresponding to gaps through the neighbouring crowns (a_1) and the other to gaps within the tree crown considered (a_2), ie.:

$$a(x,y,z;\theta,\phi) = a_1(x,y,z;\theta,\phi)\, a_2(x,y,z;\theta,\phi) \qquad (4.6)$$

where (θ, ϕ) (θ=zenith angle, ϕ=azimuth) denotes the direction of radiation.

The probability of a gap within the crown is given by:

$$a_2 = \exp(-G(\theta,\phi)u\,l(x,y,z;\theta,\phi)) \qquad (4.7)$$

(see Eq. 4.3) where l is the length of path of the solar beam in direction (θ,ϕ) to point (x,y,z) within the crown, u is the mean leaf area density in the crown along this path. (Note that if a uniform leaf area distribution within the crown is assumed, u is constant.) To calculate the length of path (l), the crown shape and dimensions are needed.

The ratio of projected to total leaf area (G) depends on the leaf orientation. It normally varies with the direction of radiation, the only exception being the spherical leaf orientation, in which case G=0.25 (when defined on an all-sided leaf area basis). Grouping of needles into shoots can be incorporated in the model (Eq. 4.7) by replacing G by the mean *STAR*, which depends on the shoot orientation and shoot structure. Because of shading by needles in the same shoot, *STAR* is smaller than G, implying an increased gap probability. However, when the shoot is used as the basic element, the gap probability varies within and between shoots. Thus, if the point (x,y,z) considered lies within a shoot, a_2 should be multiplied by an additional factor (a_3), corresponding to the probability of a gap within the shoot.

If the forest stand is described by the locations of all trees, the probability of a gap for each tree intersected by the direction of view (radiation) may be calculated separately by Eq. (4.7), and the overall gap probability (a_1) is obtained as the product of individual gap probabilities. In a Poisson stand with trees divided into N size classes of identical trees, the following analytical formula may also be used for the probability of a gap through neighboring crowns (a_1) (Nilson 1992):

$$a_1 = \exp(-\sum_{i=1}^{N} \lambda_i S_i(z,\theta)(1 - a_{2i}(z,\theta))) \qquad (4.8)$$

In Eq. (4.8), λ_i denotes the stand density (number of trees per m^2) in size class i, S_i is the projection area of the tree crown envelope on a horizontal plane at the height z when projected in direction θ, and $a_{2i}(z,\theta)$ is the probability of a gap in a single tree crown in that direction, averaged over the whole crown projection region at the height z.

Note that according to our assumptions, a_1 is independent of the horizontal coordinates (x,y) and the azimuth (ϕ), and the gap probability (a_2) within a crown (Eq. 4.7) depends only on the relative position of the point (x,y,z) in the crown of a given size class. The gap probability (a) varies with the direction of radiation; however, due to the small angular size of the solar disc, the mean transmitted fraction of direct solar radiation is obtained from Eq. (4.6), with (θ, ϕ) denoting the direction of the sun's midpoint.

4.3 Temporal and Spatial Variation of Radiation in a Stand

The total irradiance Q at a point on a horizontal plane within the canopy can be expressed as

$$Q = S_o'\, a_S + D_o\, a_D + Q_o\, a_{sc} \qquad (4.9)$$

where S_o' and D_o are the direct and diffuse solar irradiance (on a horizontal plane above the canopy), $Q_o = S_o' + D_o$ is the total incident irradiance, a_s is the penetration coefficient of direct solar radiation (Eq. 4.1), a_D is that of diffuse radiation (Eq. 4.2), and a_{sc} is the relative irradiance caused by downward scattered *PAR*.

Several approximate formulae have been derived for the scattered component of irradiance (e.g., Ross 1981). However, as conifer needles have a high absorption coefficient in the *PAR* region, the contribution there to total radiation by the scattered component is minor. Moreover, because even under oversimplified assumptions the calculation of a_{sc} leads to very complex equations, this component is usually ignored in calculations of photosynthesis.

4.3.1 Spatial Variation

In our model, the penetration coefficients a_s and a_D are stochastic variables with expected values which can be interpreted as mean transmitted fractions of direct and diffuse radiation at statistically equivalent points, i.e., at points where the gap probabilities are equal (e.g., two points at the same relative position in trees of the same size class). The value of Q obtained by replacing the penetration coefficients with their expected values may thus be interpreted as a mean irradiance transmitted to a given relative position in trees of the same size class.

The spatial variation of irradiance over a horizontal plane in the canopy may be separated as resulting from two components: (1) differences in the amount of shading leaf area at different locations in the canopy, and (2) a "stochastic" component which depends on the occurrence of a gap in the sun's direction. The first component creates gradients of mean irradiance in the canopy while the second component creates areas of shade, sunflecks and penumbras. When considering the irradiance on the surface of a leaf, a third component of variation results from different leaf orientations.

The irradiance at a given point in the canopy is the sum of the direct, diffuse and scattered components of radiation (Eq. 4.9). The statistical behaviour (scale of variation) of diffuse radiation is quite different from that of direct radiation because it is formed as an integral over the solid angle of the hemisphere, which exceeds the solid angle of the sun by a factor of almost 10^5. Because the degree of statistical dependence (covariance) between the occurrence of a gap in different directions decreases rapidly with angular distance between these directions, the diffuse irradiance may be considered as an average of nearly independent "random" variables. Therefore, it has a distribution tending to the normal distribution (Ross 1981), with a small variance (Gutschick 1984).

The direct irradiance at any given point on the horizontal plane depends on whether there is a gap between foliage in the sun's direction. If parallel solar beam geometry was assumed, the direct irradiance over a horizontal plane would be characterised by a two-valued distribution representing sunflecks and shaded areas respectively. However, the sun has an angular diameter of approximately 0.5° (0.0094 radians), which implies that a leaf or needle situated further than ca. 10 times its width away cannot obscure the whole solar disc. The actual non-parallel solar beam geometry creates areas of penumbra, where the sun is neither fully visible nor totally obscured (Miller and Norman 1971). Thus, the distribution of direct radiation on the horizontal plane is characteristically U-shaped. The frequency with which penumbras occur thus depends primarily on canopy height and size of leaves. Consequently, the usually deep crown and small dimensions of needles characteristic of conifers, are very efficient in creating penumbra (Stenberg 1995).

4.3.2 Temporal Variation

The incident radiation field is determined by geographical location (latitude) and atmospheric conditions. Temporal variation in irradiance at a specific point in the canopy is caused by changes in incoming radiation (changing solar angle, cloud movement) and by foliage movement.

A convenient but also quite rough approximation of the incident radiation time distribution is considering only clear sky and overcast situations and weighting them according to average sunshine duration. The latter may be taken from the data of the nearest actinometrical or meteorological station. Corresponding irradiance values as functions of solar elevation may either be obtained from empirical actinometrical data or from some analytical expressions given in the literature (e.g., Weiss and Norman 1985).

For a clear sky situation, the temporal variability of the diffuse component $D_o a_D$ in Eq. (4.7) is relatively small and may be assumed to be approximately constant within a short time period (e.g., an hour). Assuming that the incident direct radiation also has a constant value during the period considered, the time distribution of total irra-

diance at a point within the canopy, $f_t(Q)$, is entirely determined by the time distribution of the direct solar radiation penetration coefficient, $g_t(a_s)$,

$$f_t(Q) = g_t((Q - D_o\, a_D)/\, S_o') \quad (4.10)$$

Alternatively, in an overcast situation, the total irradiance at the point of interest may be approximated as:

$$Q = D_o a_D \quad (4.11)$$

In a case where the incident diffuse radiation D_o cannot be assumed to be constant we have to consider its time distribution, $f_t(D_o)$, the time distribution of total irradiance in an overcast situation being:

$$f_t(Q) = f_t(D_o a_D) \quad (4.12)$$

During a short clear sky period the temporal distribution of a_s at a fixed point is qualitatively similar to the spatial distribution of a_s over statistically equivalent points at a given moment during the period considered, both having a U-shaped density function.

4.4 Estimating Canopy Photosynthesis

Assuming that the rate of photosynthesis is a function of irradiance only, and that the temporal variation in irradiance is slow compared to the response time of photosynthesis, canopy photosynthesis can formally be expressed as an integral over both time and canopy space of the instantaneous photosynthetic rate at points on the leaf surface area (cf. Eq. 3.20).The integral over space (leaf area) may be approximated as a weighted sum of the rates at representative points in the canopy and the integral over time may then be approximated as a weighted sum of momentary rates at representative sky conditions.

Calculation of canopy photosynthesis thus involves integration over time and space (leaf area). We will discuss some methods by which the mean photosynthesis during a time period (integration over time) or the mean photosynthesis of a group of photosynthetic units (integration over leaf area) can be estimated from certain characteristics of the irradiance distributions.

For a given incident radiation field, a canopy radiation model provides estimates of the mean transmitted fractions of the direct and diffuse components of radiation, $S_o' a_S$ and $D_o a_D$, to any specified point on the horizontal plane. When calculating the instantaneous rate of photosynthesis of a leaf, there are two important aspects to be considered: (1) the direct irradiance on a leaf varies with leaf orientation, and (2) use of the mean irradiance leads to an overestimate because of the concavity of the photosynthetic radiation response curve. In addition, if the model is formulated using the shoot as the basic element, the reduction in mean irradiance caused by the shoot itself (within-shoot shading) must be considered (Oker-Blom 1986).

For diffuse radiation use of the mean irradiance is usually not considered to be a serious problem, because the variation of diffuse radiation between statistically equivalent points is small compared to the variation of direct radiation. Neither is the diffuse irradiance on a leaf sensitive to the leaf orientation.

The direct solar irradiance on a leaf is given by $S_o \cos(\omega) a_S$, where S_o denotes the irradiance of direct solar radiation on a plane perpendicular to the sun, and ω denotes the angle between the leaf normal and the sun. The mean direct irradiance is obtained by replacing a_S with its mean value. For direct solar radiation, however, the mean irradiance seldom represents a good estimate of the actual momentary irradiance at a given point. If we ignore the penumbra, the gap probability (mean transmittance) would still be sufficient to describe the penetration of direct solar radiation. In that case (ie., when parallel solar beam geometry is assumed) the direct solar irradiance transmitted has only two possible values and their probabilities are uniquely determined by the gap probability. However, irradiance distributions in conifers are much influenced by penumbra. For example, Stenberg (1995) showed that the shading from a shoot is completely penumbral at a distance of 1 m from the target point. The penumbral irradiance at a specified point in the canopy can be estimated by simulation techniques, but these techniques are too laborious for routine use and some faster algorithms should be found.

4.4.1 Beta Distribution Approximation

A possible way towards faster algorithms seems to be the approximation of irradiance distributions by some theoretical distribution functions. During clear skies, typical irradiance distributions in conifers have a particular U-shaped form,so that the beta distribution seems to be most suitable for fitting these distributions. Pfreundt (1988) has demonstrated the effectiveness of using the beta distibution approximation for this purpose.

Let us assume that the density function $h(a_S)$ of the direct solar radiation penetration coefficient, a_S, may be described by the beta distribution:

$$h(a_S) = \frac{\Gamma(p+q)}{\Gamma(p)\Gamma(q)} a_S^{p-1}(1-a_S)^{q-1},\ 0 < a_S < 1 \quad (4.13)$$

The problem is reduced to the determination of the two parameters of the beta distribution, p and q. One condition for this can easily be found – the mean value of this distribution, $p/(p + q)$, must be equal to the gap probability at point (x,y,z) in the solar direction (θ, ϕ),

$$p/(p + q) = a(x,y,z;\ \theta,\phi) \quad (4.14)$$

To determine both of the parameters of the beta distribution, another relation such as for the variance must be found. Unfortunately, there is no simple way to calculate the variance of the direct solar radiation penetration coefficient. It is mainly determined by shoot number and geometry and particularly by the distances of the shading shoots from the point of interest.

Pfreundt (1988) has applied a parametrization technique for determining the unkown beta function parameter q. He found that if there is only one layer of shoots causing shading, then there is a fairly proportional relation between the parameter q and the shading shoot layer density. The slope of the respective line is determined by the distance to the shading layer, and he found another relation consisting of two linear parts to determine the slope. The parameter p was determined from the condition that the mean value of the distribution equals the probability of a gap through the shading layer. If there is more than one layer of shading shoots and each layer causes a beta distributed random penetration coefficient, the resulting penetration coefficient is also beta distributed.

Rather simple equations connect the mean value and the variance of the multilayer penetration coefficient with those of individual layers. In order to find the variance of the direct radiation penetration coefficient, a_S, in addition to gap probabilities for all layers causing shading, the distances of shading layers should thus be estimated for all points of interest. The distances between whorls within a crown can easily be determined. More difficulties arise in determining distances to whorl layers of neighbouring trees if tree locations are not given explicitly. However, analytical methods enable us to estimate these distances too. Since the nearest whorls evidently cause most of the variance of the penetration coefficient, it is important to be able to describe the within-crown shading and shading caused by the nearest neighbours more accurately.

The beta distribution may be used to describe both the spatial and the temporal distribution of a_s. However, the interpretation of parameters p and q is somewhat different when the temporal distribution is considered. For instance, a great part of the temporal variation of irradiance at a given point during clear skies is not related to canopy structure but results of foliage movement.

4.4.2 Estimates Based on Moments of the Irradiance Distribution

The next logical simplification is using only moments of irradiance distribution functions to calculate photosynthesis (e.g., Hari et al. 1984, Lappi and Smolander 1984, Smolander and Lappi 1985). With this approach, it is possible to consider the irradiance time distribution moments, as well as the spatial distribution moments. For instance, by using a quadratic function such as the second-order Taylor expansion to approximate the photosynthetic light response curve, one can produce several approximate algorithms for calculating photosynthesis from the mean and variance of the irradiance. The weaknesses of this method are that photosynthetic response curves cannot always be approximated well by the second-order Taylor series and that "inconvenient" U-shaped irradiance distributions make using only the first two moments of the distribution insufficient. However, calculating higher irradiance distribution moments from theoretical concepts is a rather diffi-

cult task (Anisimov and Menzhulin 1983).

In the above method we integrate an approximate response function over the correct irradiance distribution. An alternative method is to integrate the true response function over an approximate irradiance distribution (e.g., the beta distribution discussed earlier). If the distribution of irradiance does not have a simple theoretical shape on which to base the approximation one may use the two-point distribution (cf. Smolander and Lappi 1985) for which the irradiance equals the mean irradiance plus or minus the standard deviation, with equal probability.

4.4.3 The Use of Aggregate Equations

As mentioned earlier, it would be convenient if the radiation submodel could be replaced by an aggregate equation between photosynthetic production and some properties of canopy structure and incoming radiation. Such an equation should contain all relevant variables needed to get a satisfactory approximation, particularly those which change during the life-time of a stand. The variables which should be included can be identified, e.g., by performing a sensitivity analysis on more complex canopy-radiation models.

Oker-Blom et al. (1989) studied the relationship between annual potential photosynthetic production and intercepted radiation (*PAR*) in modelled stands of different structure. When the interception of a stand was increased by (a) increasing the number of trees or (b) increasing the crown size, the ratio of photosynthetic production to intercepted radiation remained fairly similar, ie., at a fixed amount of intercepted *PAR*, variation in crown size and shape (height-width ratio) and stand density had only a small impact on the photosynthetic production.

A reason why there might be a close relationship between (gross) photosynthetic production and light interception may be explained as follows. If we have a fixed total interception rate, the total area of sunlit needles is to a large extent predetermined and changes in tree geometry, excepting perhaps shoot angle distribution, cause only a vertical redistribution of the same sunlit needle area and have little effect on the total photosynthesis of the canopy. However, this redistribution may considerably influence the photosynthetic productivity of the trees of different size classes. It is therefore important to be able to estimate the total interception rate and the amounts of radiation intercepted by the trees of different size classes. This can be done quite effectively by using theoretical formulas similar to Eq. (4.8) (Hari et al. 1985, Nilson 1992).

Based on the model described by Oker-Blom et al. (1989), Mäkelä (1990) derived some simplified equations between the annual photosynthetic production and stand characteristics. She found that in a horizontally homogeneous stand the potential photosynthetic production could be closely approximated by a negative-exponential function of the leaf area index. In a grouped stand composed of Poisson distributed individual trees the same equation was adequate when the leaf area index was replaced by an "effective leaf area index" which was a function of stocking density, crown leaf area index, and crown shape.

At a fixed leaf area index, the photosynthetic production was always smaller in a grouped stand than in a homogeneous stand. The difference was found to be particularly sensitive to the relative crown coverage, which largely determines *PAR* interception. The result supports the hypothesis that the amount of intercepted *PAR* is the main determinant of canopy photosynthesis. Thus in developing the function describing the degree of photosynthetic interaction (cf. Chapter 6) in a given stand, attention should be paid to those stand characteristics with a strong influence on radiation interception. In addition, however, the role of penumbra and shoot structure on local rates of photosynthesis, especially deeper down in the canopy, should be elaborated (Stenberg 1995, 1996).

Geographical aspects (the effect of latitude) should also be taken into account. The amount and angular distribution of incoming irradiance affect the relationship between photosynthesis, leaf area and irradiance in different ways. First, due to the concavity of the photosynthesis light curve, an increase in total incoming radiation leads to a proportionately smaller increase in photosynthetic production. Accordingly, Oker-Blom et al. (1989) found that the simulated ratio of photosynthetic production to intercepted *PAR* was higher at more northerly latitudes, with a larger proportion of lower irradiance in the incoming radiation. For the same reason, the increase in annual photosynthetic production at lower (more southerly) latitudes is proportionately smaller than the increase in the total incoming radiation. Relative light interception per unit of *LAI* is also smaller because the increase in total radiation is accompanied by a shift towards higher inclinations in its angular distribution (Stenberg 1996).

4.5 Discussion

Radiation submodels used in forest growth models are in general quite simplified considering the level of knowledge on radiative transfer in plant canopies (e.g., Myneni and Ross 1991). The reason asserted for this is that very complex models of light interception and photosynthesis are not operational in long-term simulations. However, results obtained using rather complex models suggest that since they could fairly easily be aggregated into simple equations containing only a few variables (e.g., Mäkelä 1990), the complexity of models does not necessarily restrict their use.

In the version of the forest growth model used in this study (Chapter 6), the supply of light (PAR) at a given geographical location determines the potential photosynthetic production, and the decrease in photosynthesis is modelled as a function of downward cumulative leaf area. Relative photosynthesis or "the degree of photosynthetic interaction" (cf. Hari et al. 1985) is defined as the ratio of the photosynthetic production at a given level in the canopy to the maximum potential photosynthetic production obtained from an unshaded leaf surface at the top of the canopy.

Making use of the estimation methods coupled with the theoretical formulas presented above, one can perform a reasonably realistic sensitivity analysis of the dependence of the annual photosynthetic production of a forest on any structural parameter considered. This would make it possible to introduce some new structural parameters into the "degree of photosynthetic interaction" (Hari et al. 1985), defined up to now only in terms of the downward cumulative leaf area index. Among the new parameters might well be the downward cumulative needle area of the tree considered, the crown shape parameter of the tree, e.g. the crown projection area at a solar elevation characteristic of the geographical location, a parameter for the tree pattern, etc. Further computer simulations must be performed to confirm this conjecture. In deriving simplified equations for estimating canopy photosynthesis, however, it should be kept in mind that "the simplified models can be as good as the original, complex models but they cannot be any better" (Mäkelä 1990). It is important, therefore, to simultaneously develop and test theoretical models describing the relationship of canopy structure, radiation and photosynthesis.

References

Anisimov, O.A. & Menzhulin, G.V. 1983. On the statistical laws of radiation transfer within inhomogeneous vegetation. (in Russian). Meteorol. i Hydrol. 7: 61–66 .

Carter, G.A. & Smith, W.K. 1985. Influence of shoot structure on light interception and photosynthesis in conifers. Plant Physiol. 79: 1038–1043.

Chen, J.M., Black, T.A. & Adams, R.S. 1991. Evaluation of hemispherical photography for determining plant area index and geometry of a forest stand. Agric. For. Meteorol. 56: 129–143.

Gusakov, S.V. & Fradkin, A.I. 1990. Computer modelling of spatial structure of forest communities. (in Russian). Minsk, Nauka i Tekhnika. 112 p.

Gutschick, V.P. 1984. Statistical penetration of diffuse light into vegetative canopies: Effect on photosynthetic rate and utility for canopy measurement. Agr. Meteorol. 30: 327–341.

Hari, P., Nilson, T., Salminen R., Kaipiainen L., Korpilahti, E. & Ross, J. 1984. Nonlinear dependence of photosynthetic rate on irradiance and its consequences for estimates of the amount of saccharides formed. Photosynthetica 18: 28–33.

— , Kaipiainen, L., Korpilahti, E., Mäkelä, A., Nilson, T., Oker-Blom, P., Ross, J. & Salminen, S. 1985. Structure, radiation and photosynthetic production in coniferous stands. University of Helsinki, Department of Silviculture, Research Notes 54. 233 p.

Koppel, A. & Oja, T. 1984. Regime of diffuse solar radiation in an individual Norway spruce (Picea abies (L.) Karst.) crown. Photosynthetica 18: 529–535.

Lang, A.R.G. 1991. Application of some of Cauchy's theorems to estimation of surface areas of leaves, needles and branches of plants, and light transmittance. Agric. For. Meteorol. 55: 191–212.

Lappi, J. & Smolander, H. 1984. Integration of the hyperbolic radiation-response function of photosynthesis. Photosynthetica 18: 402–410.

Mäkelä, A. 1990. Adaptation of light interception computations to stand growth models. Silva Carelica 15: 221–239.

Mann, J.E., Curry, G.L., Hartfield, D.J. & Demichele, D.W. 1977. A general law for direct sunlight penetration. Math. Bioscien. 34: 63–78.

Miller, E.E. & Norman, J.M. 1971. A sunfleck theory for plant canopies. I. Lengths of sunlit segments along a transect. Agron. J. 63: 735–738.

Myneni, R. & Ross, J. (eds.) 1991. Photon-vegetation interactions: Applications in remote sensing and plant ecology. Springer-Verlag. 565 p.

Nilson, T. 1977. A theory of radiation penetration into non-homogeneous plant canopies. In: The penetration of solar radiation into plant canopies. (in Russian). Inst. Phys. Astron., Estonian Acad. Sci., Tartu. p. 5–70.

— 1992. Radiative transfer in nonhomogeneous plant canopies. In: Stanhill, G. (ed.), Advances in Bioclimatology 1, p. 59–88. Springer-Verlag.

Norman, J.M. & Jarvis, P.G. 1975. Photosynthesis in sitka spruce (Picea sitchensis (Bong.) Carr.). V. Radiation penetration theory and a test case. J. Appl. Ecol. 12: 839–878.

Oker-Blom, P. 1986. Photosynthetic radiation regime and canopy structure in modelled forest stands. Acta Forestalia Fennica 197: 1–44.

— , Kellomäki, S. & Smolander, H. 1983. Photosynthesis of a Scots pine shoot: The effect of shoot inclination on the photosynthetic response of a shoot subjected to direct radiation. Agric. For. Meteorol. 29: 191–206.

— , Kotisaari, A., Kellomäki, S., Ross, J. & Smolander, H. 1986. Crown projection area of young Pinus sylvestris: a model and its test. Scand. J. For. Res. 1: 67–74.

— & Smolander, H. 1988. The ratio of shoot silhouette area to total needle area in Scots pine. Forest Science 34: 894–906.

— , Pukkala, T. & Kuuluvainen, T. 1989. Relationship between radiation interception and photosynthesis in forest canopies: Effect of stand structure and latitude. Ecological Modelling 49: 73–87.

— , Lappi, J. & Smolander, H. 1991. Radiation regime and photosynthesis in coniferous stands. In: R. Myneni and J. Ross (eds.), Photon-Vegetation Interactions: Applications in remote sensing and plant ecology. Springer-Verlag. p. 469–499.

— , Kaufmann, M.R. & Ryan, M.G. 1991. Performance of a canopy light interception model for conifer shoots, trees and stands. Tree Physiology 9: 227–243.

Pfreundt, J. 1988. Modellierung der räumlichen Verteilung von Strahlung, Photosynthesekapazität und Produktion in einem Fichtenbestand und ihrer Beziehung zur Bestandesstruktur. Univ. Göttingen, Berichte des Forschungszentrums Waldökosysteme/ Waldsterben, Reihe A, Bd.39. 163 p.

Pukkala, T. 1988. Effect of spatial distribution of trees on the volume increment of a young Scots pine stand. Silva Fennica 22: 1–17.

Ross, J. 1981. The radiation regime and architecture of plant stands. Dr. W. Junk Publishers, The Hague. 391 p.

Ross, J. & Nilson, T. 1965. Penetration of direct solar radiation in agricultural crops. (in Russian). In: Problems of radiation regime of plant canopies. Inst. Phys. Astron., Estonian Acad. Sci., Tartu. p. 25–64.

Smolander, H. & Lappi J. 1985. Integration of a nonlinear function in a changing environment: estimating photosynthesis using mean and variance of radiation. Agric. For. Meteorol. 34: 83–91.

Stenberg, P. 1995. Penumbra in within-shoot and between-shoot shading in conifers and its significance for photosynthesis. Ecological Modelling 77: 215–231.

— 1996. Simulations of the effect of shoot structure and orientation on vertical gradients in intercepted light by conifers. Tree Physiology 16: 99–108.

— , Smolander, H. & Kellomäki, S. 1993. Description of crown structure for light interception models: Angular and spatial distribution of shoots in young Scots pine. Studia Forestalia Suecica.191: 43–50.

— , Kuuluvainen, T., Kellomäki, S., Grace, J.C., Jokela, E.J. & Gholz, H.L. 1994. Crown structure, light interception and productivity of pine trees and stands. In: Gholz, H.L., McMurtrie, R. & Linder, S. (eds.), A comparative analysis of pine forest productivity. Ecological Bulletins (Copenhagen) 43: 20–34.

Tomppo, E. 1986. Models and methods for analysing spatial patterns of trees. Comm. Inst. For. Fenn. 138.

Weiss, A. & Norman, J.M. 1985. Partitioning solar radiation into direct and diffuse, visible and near-infrared components. Agric. For. Meteorol. 34: 205–213.

Welles, J.M. 1990. Some indirect methods of estimating canopy structure. Remote Sensing Rev. 5: 31–43.

5 Geographical Variation in the Regularities of Woody Structure and Water Transport

Eero Nikinmaa, Leo Kaipiainen, Markku Mäkinen, Juhan Ross and Tanja Sasonova

5.1 Introduction

The processes that bring about material exchange between the structure of a plant and its surroundings are relatively well known, as for example the photosynthesis chapter of this volume indicates. However, much less is known of the ways materials are used in growth and morphological and anatomical development. There is still incertainty about how substrata supply and plant growth substances affect the cambial activity and cell enlargement (e.g. Ford 1981, Aloni 1987, 1991, Savidge 1991). From the point of view of analysing tree growth these questions are crucial since they determine both the ways in which the materials are consumed and how new materials will be taken up in the future.

Early process-based models of tree growth simply ascribed growth to resource intake, so that a constant proportion of the usable pool of resources was utilised for growth of the individual compartment of a tree (e.g. foliage, branches, stem, roots) (e.g. Hari et al. 1982, McMutrie and Wolf 1983, Mäkelä and Hari 1986). The problem with this approach is that it missed the functional role of structure. Improvement was made when the implications of architectural and structural patterns were considered in carbohydrate allocation. For example, Hari et al. (1985), Valentine (1985), Mäkelä (1986), Ludlow et al. (1990), Nikinmaa (1990) and Nikinmaa and Hari (1990) derived carbon allocation from the pipe model theory (cf. Shinozaki et al. 1964a). The more general principle of functional balance (e.g. Brouwer 1962) was adapted by many of those models. This assumes that different compartments of trees are connected functionally and there should be regularities in the relative quantities which are determined by their functioning such as water transport in wood.

While the use of allometric relationships in growth modelling is tempting when the control of growth is still rather weakly understood, it has problems. Generalizations require extensive empirical data from stands with a known history. Alternatively, the allometric relationships can be related to their functional features and derive the variation in the relationships from the variation in the environment affecting the functions (e.g. Berninger et al. 1995). In the particular case of the pipe model this could mean that the transpiration by needles and water transport in wood are explicitly described by their dimensional relationships. We know that the latter is not exactly the case. Neither is the functional role of wood in water transport clear. It is thus necessary to study the dimensional relationships that can be associated with structure and functions over a wide range of very different conditions.

The function of wood has been attributed to both water transport and mechanical support for a long time. Along the lines of Leonardo da Vinci (according to Zimmermann 1983), Jaccard (1913, cited by Assmann 1970), Huber (1928, according to Zimmermann 1983) and Shinozaki et al. (1964 a, b) have related the woody cross-sectional area to water conductivity or foliage biomass. Pressler introduced the theory of stem formation in accordance with the "foliage capacity" of the upper parts of the tree in 1865 (cited by Assmann 1970).

The mechanical stem form theory was advanced in late 19th century by Schwedener and Metzger (1874 and 1893 respectively, according to Ylinen 1952). The stem was considered "a cantilever beam of uniform resistance against the bending force of wind". It implied that stem diameters raised to the third power would increase propor-

tionally with the increasing distance from the central point of application of the wind force. Ylinen (1952) developed the mechanical stem form theory further, showing that if the parameters describing the wind-resisting crown area and the elasticity modulus of trees are known, then it is possible to construct realistic relative diameter / relative height curves for trees with different relative crown length.

Huber (1928) indicated that, contrary to the pipe model theory, there is no constant ratio between foliage mass and the water-supplying wood cross-section within a tree, but that the ratio decreases towards the top of the tree. Following the ideas of Huber, Zimmermann (1983), Ewers and Zimmermann (1984) and Tyree et al. (1987) among others have analysed the hydraulic architecture of trees. From their work it is apparent that the difference in hydraulic conductivity within a tree between the smallest twigs and the main stem may be large.

Many workers have found a linear relationship between the foliage area or foliage biomass and stem sapwood cross-sectional area at stand level (see review by Waring et al. 1982, Kaufman and Troendle 1981, Long et al. 1981, Kaipiainen and Hari 1985, Hari et al. 1986). However Albrektson (1984), Long and Smith (1988), Keane and Weetman (1987), Espinosa Bancalari et al.'s (1987) results suggest that there is variation in this ratio depending on the average ring width, the size of cross-sectional area of stem or the growth rate of trees, all of which are often intercorrelated. Whitehead (1978) reported that the relationship was linear within stands of Scots pine and independent of tree spacing, but varied between different sites.

Long et al. (1981) analysed bole structure from both the mechanical and the pipe model point of view. They found that both theories could be applied but that in the stem segments below the crown the heartwood formation must be included in the physiological water-conducting theory to fulfil the mechanical support requirements.

The dimensional connections between woody structure and the quantity of foliage in tree crowns are frequently attributed to their functions, mainly water transport. In this chapter, we examine how these regularities vary between very different geographic locations, by trying to connect dimensional relationships between different parts of the tree to the surrounding environmental conditions. We pay most attention to those dimensions that could be related to water transport. The first part of this chapter considers aspects influencing water transport in wood at different levels of aggregation. Empirical results of the geographic variation of the structural regularities and their dynamics in young Scots pine stands follow and the chapter closes with a discussion of the significance of these observations for predicting Scots pine growth in different climates.

5.2 Water Transport in Scots Pine

5.2.1 The Different Levels of Phenomena Affecting Water transport through Wood

A forest is a complex system in which several levels of both temporal and spatial hierarchy can be identified. The proper treatment of the different levels of hierarchy and particularly the transitions from one level to another is a key question in the analysis of forest functions. Each level has its own characteristic structural and functional features and regularities.

At the most detailed level, water transport through wood is affected both by its properties and the processes that affect transpiration. At tree level the water transport pathway and the growth and senescence processes that determine the relative quantities of different tissues need to be considered. Finally the total quantities of transpiring biomass and its spatial distribution are important features at stand level when the water flow through forest ecosystems is studied.

The following chapters examine these different levels of water transport. The main idea is first to outline dimensions that could be related to the water transport of wood and second to suggest possible trends in structural regularities between foliage and wood in different geographical regions. First a brief literature review of the Scots pine wood properties and their implications on water transport is undertaken. This is followed by empirical results on the water transport pathways in Scots pine. Finally stand level water transport and transpiration is discussed.

5.2.2 Water Transport in Scots Pine Xylem

5.2.2.1 The Xylem Structure of Scots Pine

Xylem in Scots pine, as in the other conifers, consists primarily of longitudinal tracheids. The proportion of the ray volume of the total volume is only about 5 to 6 % (Kärkkäinen 1985).

Siau (1984) reports that the tracheid lengths of normal sapwood is 3500 µm and the lumen diameter is between 20 to 30 µm. Fengel (1969) examined the average diameters of tracheids in early and latewood and reported values of 25.3 µm and 23.5 µm respectively along the tangential axis and 30.2 µm and 20.8 µm along the radial axis. Vysotskaya et al. (1985) also report big variation along the radial axis but very little along the tangential axis. Sanio (1872) showed that the diameter of tracheids increased when moving from younger to older tree rings and similarly within the same tree ring when moving from the upper stem parts downwards. The pattern can also be observed in tracheid length (e.g. Helander 1933, Bailey 1958, Dinwoodie 1961). In Helander's material the length of tracheids varied between 1 and 4 mm depending on the point of observation. The size of the branch tracheids has generally been found to be shorter than that of the stem ones (see review by Dinwoodie (1961)).

Tracheids are connected through numerous pairs of bordered pits, mainly situated in the radial walls at the both ends of the cells (Kärkkäinen 1985). The "overlapping" area between tracheids is larger in longer tracheids and so the number of connecting pits is bigger (Carlquist 1988). The average effective diameter of these pits varies between 0.02 and 4.0 µm (Siau 1984). They are greatest in the earlywood and smallest in the latewood. Scots pine has a torus in the pit which is capable of moving against the pit walls, closing the pit completely if excessive pressure differences exist between adjacent tracheids. Normally, the size of the torus is about a third to a half of the diameter of the pit chamber (Siau 1984). Pit size is most likely related to the tracheid size since they are both determined at the phase of the cell extension and depend on the fibril density of the primary cell wall (Tyree and Sperry 1989).

Tracheid cell walls consist of middle lamellae between cells and primary and secondary walls. The secondary wall consists of different layers which can be distinguished from the microfibril pattern. The cell wall thickness of the middle section varies between 1 to 5 µm and this is mainly responsible for the difference between the early and latewood. There is only a very narrow band of latewood in the tree rings within the living crown (Larson 1969) but as one moves downward along the stem the proportion of latewood from the cross-section increases (Larson 1969, Denne 1978, Hari, pers. com.).

5.2.2.2 Water Conduction in Tracheids

The rise of water from roots to leaves is generally explained by cohesion theory, introduced independently by Askenasy 1895 and Dickson and Joly 1894 (cited by Gregory 1977). According to this theory, water forms continuous columns from leaves to the tips of the roots. Transpiration from the leaves creates negative pressures within the water-transporting woody parts of the plant, which drives water upward towards the transpiring leaves.

Transpiration thus creates a pressure gradient within the xylem, which has a certain resistance to flow opposing water movement through it. This resistance depends on the xylem structure. The pressure gradient and flow resistance together determine how much water moves through a cross-sectional area in a given time unit.

One tracheid can be assumed to resemble a cylindrical pipe. Also, water flow velocity in xylem is small (e.g. Zimmermann 1983). Under these conditions, the Hagen-Poisseule equation is a good approximation of general equations of the flow mechanics and can be used to estimate the flow resistance in xylem as follows:

$$Q = -\frac{\pi r^4 \, dP}{8 \delta \, dx} \qquad (5.1)$$

where Q is the water flow velocity (m^3/s), r is the radius of a tracheid (m), δ is the dynamic viscosity of water (about 0.001 Nsm^{-2}), dP is the pressure difference between the ends of the cell (Pa) and dx is the length of the cell (m).

Equation (5.1) shows that the tracheid diameter is a critical factor affecting water flow. For example, within one tree ring the large tracheid cavities

in the early wood should dominate the water transport in that ring. However, very wide vessels are not always the most efficient for water transport since they are more vulnerable to embolism than narrow ones. The reasons for this are not well known, but it has been suggested that it might have something to do with the volume surface area ratio (Carlquist 1988, Tyree and Sperry 1989).

Water flow through the whole tree is obtained by adding the flows over all tracheids. However, use of Eq. (5.1) involves assumptions that may not be realistic. First, tracheids seldom resemble a cylinder but are closer to an ellipse or even a rectangle in cross-section. In these cases a correction term can be derived for Eq. (5.1). Second, the pressure within wood is considered constant in a radial direction. The most critical weakness of this approach is that it does not consider the resistance caused by pits joining tracheids together nor that of frictional forces caused by the cell walls (Carlquist 1988). It has been observed that the resistance calculated from Eq. (5.1) and that measured differ somewhat depending on the species in question. Pothier et al. (1989) measured resistances which were more than twice the values calculated with Eq. (5.1) for Jack pine. Haskins and Ford (1990) suggested that for these reasons one should also consider relationships other than the Hagen Poisseule equation to describe the water flow through tracheids.

Tracheid length is an important factor affecting the water transport capacity of wood because the intertracheidal pits have a strong influence on water flow (Carlquist 1988). These pits also prevent cavitation from moving from one cell to another, which greatly increases the integrity of the conifer xylem against unfavorable environmental conditions such as drought, or even more importantly, winter freezing (Zimmermann 1983).

Efficient water transport thus exerts contrasting requirements on the structural features of tracheids. The tracheid diameter and length should be large to guarantee efficient water transport but increased size increases the probability of cavitation and the proportion of transport structure that cavitations influence. Niklas (1986) suggested that in the early evolution of land plants, the diameters and lengths of conducting cells may have increased to some limit defined by the probability of cavitation and the growth of bigger plants was possible only after cells started growing in the cross-sectional direction.

The water conductance through a woody section is affected by the tracheid size distribution and by the trends in the earlywood / latewood ratios. Judging from the tracheid size distribution in the earlywood and as Pothier et al. observed (1989), the water conductance should be lower the more distal the part in question is. If, however, one studies conductivity at the dimensional level the different proportion of latewood along the transport path can affect the results (see Chapter 5.2.2.1). Considering the opposite trends one might expect variation in the relationship between cross-sectional area of wood and the foliage mass or area. However, there seem to be regularities in the quantities of water-transporting structure when measured at corresponding points in the crown within a stand or between similar size stands in the same region (Hari et al. 1985). Crown base seems to be a practical reference height since it changes with the tree growth, maintaining its relative position in the stem structure.

5.2.3 Water Pathways in the Tree

5.2.3.1 Background

Water pathways in trees from the fine roots up to the needles can be considered as a balanced system of water transport where all elements (roots, stem, branches, needles) display the ability to conduct the same amount of water. Even though all organs may have different conductivity due to differing anatomical properties, the total water flow through different wood sections is conditioned biologically and should have fairly strict implications for the total quantities of such tissue.

It is important to know which part of wood conducts water and how this is related to the architecture of the tree in considering the quantitative relationship between wood and foliage. The aim of this chapter is to analyse the relationships between the architecture of a tree and the water movement at different points in its xylem. The main objectives are first to see whether water flow has a regular pattern in roots, stem and branches and whether that can be linked to the position of both uptaking and transpiring organs and second if the conversion of conducting wood into non-conducting tissue is connected to changes in the architecture, especially to the crown base recession.

5.2.3.2 Materials and Methods

A dying technique was used to study the water pathways in xylem. Four sets of sample trees, selected subjectively from the sides of the experimental stands described in more detail by Kasimirov et al. (1977), were treated with dye solution. They were poor *Calluna* type stands situated 50 km north of Petrozavodsk (62°13' N 34°10' E).

Water Transport Pathways in Branches, Stem and Roots

Holes were drilled through the centre of the stems, branches and roots of nine 30–80 year-old trees of the dominant canopy layer. The holes were immediately filled with acid fuchsine dye solution. Four days later the trees were felled and cross-sectional discs from which the transport path was analysed were cut.

A similar method was applied to study the water path in the roots and branches of four 60 to 80 year-old sample trees selected from the same area on the same criteria as above. Dye solution was applied at the base of a branch and in the root xylem at a distance of 0.8–1.3 m from the root collar.

Relations Between the Amount of Water-Transporting Tissue and Crown and Branch Architecture

A third set of four experimental trees of about 30 years old was subjectively selected to obtain additional information about the cross-sectional area of conductive xylem. The roots of these trees were dug out and cut at the point where they were one centimeter thick, after which they were quickly immersed in water. The roots were cut under water and when the end of the root had been kept in water for 30 minutes, the water was immediately replaced by the dye solution.

The fourth set of experimental trees was from depressed and dominant canopy layers (22–44 years old). The proportion of the conducting xylem in the stem was detemined. For these purposes the root system was cut at about 20–50 centimetres from the root collar whereupon the stem was immediately dropped into a nearby lake. About 15–20 centimetres were sawn from the lower part of the stems under water. The cut ends were kept under water for one hour. Thereupon they were immediately dropped into dye solution.

An analogous method was used to investigate branch xylem. A sawn-off branch was immediately dropped into a container of water where it was cut in the middle of the first annual elongation of the branch. When the transpiration stream had been re-established the cut end of the branch was placed in dye solution. A total of 20 branches between 3 to 22 years were sawn off six trees between 30 to 80 years which had been subjectively selected from the same area as the others.

Cross-sectional discs of roots, stems and branches were cut both from the sample trees and the sample branches 1–3 days after the dying started, so that dye had had adequate time to flow through the wood. The number of annual rings, both water-conducting and non-conducting, were counted. The number of living whorls of branches was calculated in all stems and branches.

All the measurements were carried out during rainy or cloudy weather in August after an extensive period of rainy days, so that the trees were amply supplied with water and the evaporative demand of the air was low.

5.2.3.3 Results and Discussion

Water Transport Pathways in Branches Stem and Roots

Some examples of the pattern of water movement in roots, stems and branches are demonstrated in Fig. 5.1. When the dye was injected close to the base of the roots it usually ran straight along the root axis (Fig. 5.1a, 2–4). As the solution was injected at a larger distance from the collar where the roots were 1 cm in diameter the dye pattern at the cross section of the root at the root collar was often quite irregular (Fig. 5.1a, 1). This might be associated with the influence of water uptake

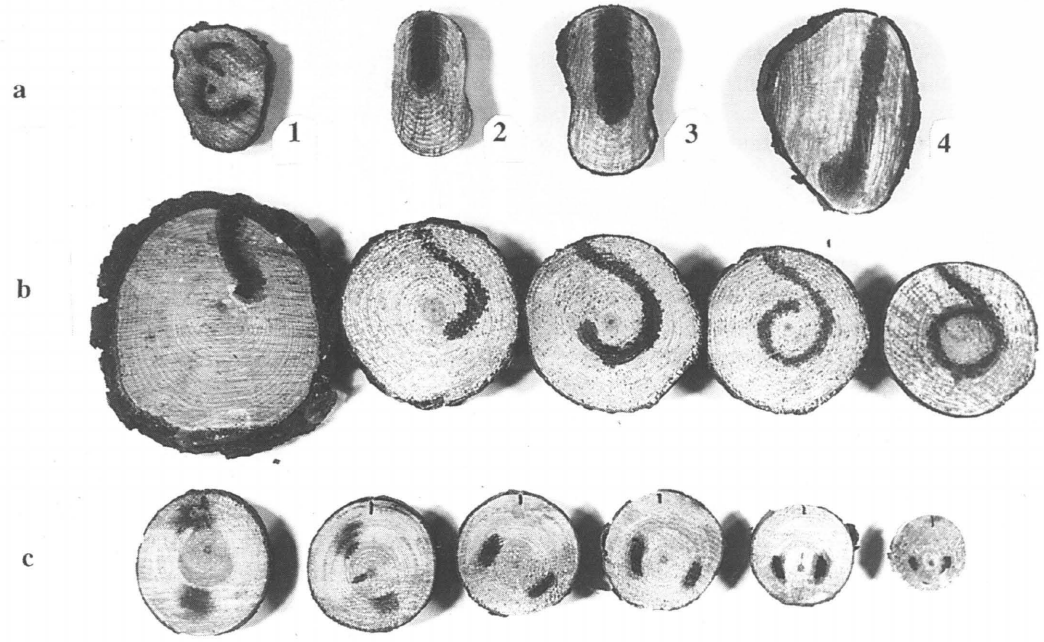

Fig. 5.1. Water pathway in xylem: a) at root collar when dye was injected to smaller than 1 cm diameter root (1) and when dye was injected to large roots (2–4), b) in the stem at different heights from the base upwards and c) in a branch from the base towards the tip. The dye was injected to xylem at the base of the stem and the branch.

from the lateral root suckers which are oriented in soil without any regular pattern. All annual layers were capable of conducting water in the roots studied.

The movement of water in stems is spiral (see Fig. 5.1b), the pattern twisting clockwise as it moves upwards. However, the pitch of the spiral varies significantly between trees, apparently relating to the annual height growth of the trees. Water made a complete turn around the stem over a distance of 3 metres in a tree with a 35 cm average annual height growth (Fig. 5.1b), and a tree with a 16 cm annual height growth has a spiral pitch of 140 cm. All pines under study had eight to nine whorls between a complete turn in water path which would suggest a relationship between the water pathways and the branch arrangement in the crown.

The spiral pattern of water pathways in the stem xylem is well known (Vite and Rudinsky 1959, Zimmermann and Brown 1971). It is usually explained by the properties of the xylem structure and by the pattern of location of pores in the tracheid walls. Vite and Rudinsky (1959) emphasized that spiral water movement is more effective than a directly vertical one, providing more effective water distribution to all parts of the crown.

The dye, injected at the base of a branch vertically, i.e. parallel to the stem axis, usually made a 90° turn by the beginning of the needle-bearing part of the branch and moved further parallel to the branch axis (Fig. 5.1c). The solute movement was consistent with the horizontal orientation of the sub-branches within branches.

Connections Between the Amount of Water-Transporting Tissue and Crown and Branch Architecture

In earlier work it has been observed that the number of annual rings making up the heartwood depends on the age of a tree and its ecological

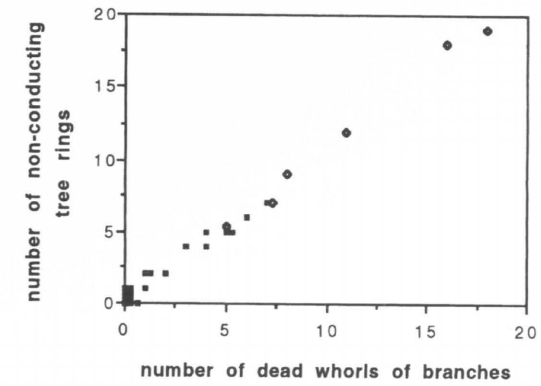

Fig. 5.2. The relationship between the number of annual tree rings not conducting water, and the number of dead whorls. The black boxes stand for branches and stars stand for trees.

growth conditions (Chavchavadze 1979). In this work the numbers of whorls no longer supporting foliage and of non-water-conducting tree rings were counted from 6 trees and 20 branches. The results show a close relationship between the number of non-water-conducting layers and death whorls (Fig.5.2).

The above results can also be tested experimentally. When the branches are cut off from lower whorls one may expect the number of water-conducting rings to be equal to the number of whorls left. Lower branches were removed from an 11-year-old tree four months prior to a dye injection; the four topmost whorls were left. The dye was found in the four annual rings (Fig. 5.3). In this kind of experiment one has to take care that the branches are not cut shortly before a colour injection. Water shortage in the stem and a certain degree of water transpiration from fresh cuts may bring about rise of dye solute in tree rings without a whorl on top.

All results were obtained for trees growing in various conditions in the same stand and for branches at different positions in the crown. The regularities observed in this work would therefore suggest that they actually describe the association between architecture and water transport in Scots pine. However, further work is required to verify the generality of these observations.

These results would also suggest that the movement of water from one tree ring to another is quite limited in Scots pine. A tree ring and the whorl it terminates at are formed simultaneously. If the lateral flow of water from one tree ring to another is small within the stem, then the flow may cease when the last branches to which the tree ring directly extends (ie. the uppermost whorl of that year when the tree ring was formed) die.

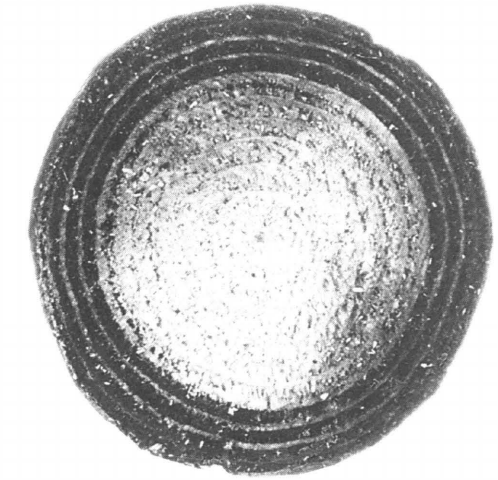

Fig. 5.3. The relationship between the number of the water-conducting annual layers and the number of living whorls in trees with 4 living whorls.

Horizontal rays are a potential radial water transport channel between tree rings through the quite impermeable latewood. In *Pinus sylvestris* particularly there seems to be quite a high proportion of ray tracheids with an open pit structure which would facilitate considerable radial and tangential permeability (Siau 1984). However, it seems that the radial water flow, at least for young trees, does not play a significant role in tree rings no longer connected directly to the living crown. Long et al. (1981) suggested that heartwood formation and the pipe model considerations together produce mechanically stable structures. The above observation could be an indication of this.

The results of the research illustrate interdependent relations between the structural characteristics of a tree and the properties of the water movement process in its pathway system. It seems, at least in relatively young Scots pine trees, that the whole area of the stem in the living crown or the

branches above the whorl of the lowest living subbranches seem to be capable of conducting water. Where there are partially dead whorls the diameter of the active xylem ought to be measured between them.

The same regularities in branches would imply that as the trees grow older the average age of branches increases and the proportion of non-conducting tree rings in branches increases. In this case, it cannot be assumed the whole cross-sectional area below the crown base of the stem would be entirely water-conducting. However, these results would also suggest that where dimensional comparisons between trees in different geographical locations are made, the crown base is the most appropriate measuring height, at least for young trees.

5.2.4 Stand Level Water Transport and Transpiration

5.2.4.1 Introduction

Water flow through trees is controlled by the atmospheric properties that drive the transpiration processes and refill the soil, the water storage capacity of the soil and the water transport and transpiration properties of the trees. Different processes affect transpiration on different spatial and temporal scales. For example, the weather is extremely variable in the Scots pine growing area but the climate at each location seems to be quite stable, the variation in the annual mean temperature being only few degrees but the difference between maximum and minimum temperature during the day sometimes exceeding 20°C. In these conditions one might expect a flexible response from stomata to variable environmental conditions, but more conservative relationships between water-conducting and water-transpiring tissue as a response to smaller variation in annual averages. It may be hypothesized that in such conditions the driving forces of water flow and the actual observed growing season transpiration at stand level should yield quite constant values from year to year although short-term variations may be considerable.

To test this hypotheses we analyse the growing season totals of the spatially and temporally strongly variable water flow through the stem and the components driving it through the woody structure, ie. the water potential difference and the flow resistance that varies as a function of the water content in the xylem. As a step further, we analyze how the stand level transpiration varies in different conditions. Finally, the implications of these results for the acclimatization of trees in prevailing conditions, especially on their structural growth, are discussed.

5.2.4.2 Materials and Methods

A heat pulse method was used to study the water flow through stems. As described by Kaipiainen et al. (1981) it could also be applied to determining the water concentration of the stem. This is based on the empirical regression between the time of maximal temperature difference after a heat pulse and the temperature conductivity for wood of different water content determined by Kaipiainen et al. (1981) for Scots pine.

The mass flow rate of water in stems and water potentials in roots and shoots were monitored in three pine stands from 1977 to 1979 using the heat pulse method. The water potentials were measured using Scholander´s bomb. The stands (62°13´N, 34°10´E) were growing 50 km north of the city of Petrozavodsk. The soil of the stands was sandy, but the water table level varied from stand to stand at average levels of 0.6 m, 1.2 m and over 3 m, which generated a clear difference in fertility between the sites. The stands are described in detail by Kasimirov et al. (1977).

Monitoring series consisted of daily measurements of maximum and minimum values of the water flow rate from stem, branches and the water potentials of shoots and roots. In addition, 40 daily patterns of hourly water flow and water potential were determined from the same points. The total number of water flow rate measurements was about 3500 and that of water potentials about 2800.

The stands were growing in a rather humid northern climate. During the fairly normal summers 77–79 the rains were able to compensate for the water loss caused by transpiration. The water concentration in the soil remained rather high. The minimum water potential observed in the soil was –0.05 MPa.

5.2.4.3 The Results and Discussion

Water Mass Flow

The mass flow rate varies considerably during the course of a day. It has a clear maximum before noon and a minimum at sunrise. The maximum observed flow velocity of water was 15.6 cm/h and the mass flow rate 9.1 g/(cm^{2}h). These values are low compared to those reported by Hinkley et al. (1978).

Changes in water storage smooth the variation in the mass flow rates caused by the environmental variation, suggesting that the mean value measured at the base of the stem reflects the annual average conditions of the site.

Annual mean mass flow rate varied only a little over the three years in the various stands thus supporting the hypothesis of the work above (see Table 5.1). The mean mass flow rate can be converted into the annual amount of transpired water per cross-sectional area of sapwood by multiplying the mean rate by the number of days in the vegetation period May–September ie. 150 days. The mean annual amount of transpiration in the research stands was 101 tnm^{-2} (sapwood).

Table 5.1 Annual mean mass flow rates, U, water concentration in xylem, Wa, amount of transpired water, Q, and ratio of amount of transpiration and amount of rainfall during vegetation period, T_r.

Year	U g/cm^{2}h	Wa %	Q mm	T_r %
Stand 1 (water table 0.6 m)				
1977	3.3	112.8	163.3	42
1978	3.2	119.2	139.5	40
1979	3.4	109.8	165.9	62
mean	3.3	111.4	156.2	
Stand 2 (water table 1.2 m)				
1977	3.1	115.6	184.3	47
1978	2.9	114.8	151.3	43
1979	3.2	106.6	193.6	43
mean	3.1	112.3	176.4	
Stand 3 (water table 3.0 m)				
1977	3.3	114.6	137.4	35
1978	2.9	120.6	109.0	31
1979	3.3	108.6	134.6	51
mean	3.2	114.6	127.0	

The amount of transpiration calculated from the measurements from single trees is 30–60 % of the amount of precipitation during the vegetation period. Since direct measurements of stand transpiration require instrumentation which was not available, the estimate could not be checked against measured data from the same stand. However, the magnitude seems to fit with the present idea of the role of transpiration in the water balance on poor, sandy soils. It is evident that the high values for water velocity reported by Hinkley et al. (1978) would result in unreasonably high estimates of transpiration in Karelian conditions.

Water Potential

Transpiration decreases water pressure in twig xylem, generating a pressure difference between roots and twigs. This pressure difference is the driving force of water flow in the woody structures of a tree. The water potential, Ψ, measured by the Scholander bomb, is very close to the hydraulic pressure in the wood. The water potential of shoots, Ψ_s, varies diurnally and during the growing season, reflecting the pattern of transpiration and depletion of soil water. Water potential has a clear minimum, Ψ_s^{min}, in the early afternoon and a maximum, Ψ_s^{max}, at sunrise. The lowest shoot water potential observed was –1.5 MPa, and the maximum shoot water potential varied from –0.3 to –0.67 Mpa. The variation was clearly smaller in roots. The minimum root water potential during the daytime, Ψ_r^{min}, was from –0.22 to –0.45 Mpa. The maximum values at night, Ψ_r^{max}, were stable, varying between –0.2 and –0.26 Mpa. The woody structures level out the variation driven by the daily variation in the water pressure deficit of the air, resulting in more stable situation in the roots which is also reflected in the flow rates as mentioned earlier.

The tree structure should be able to withstand a certain, commonly observed, range of variation in transpiration. The mean values are more stable, indicating the general water transport level at which trees operate in a certain region. The variation in the water potentials between years is extremely small when compared with the variation over one day. Thus the mean pressure difference

Table 5.2 The annual mean maximum and minimum values of water potential in the three experimental stands 1977–1979. *S* stands for shoots and *r* for roots.

Year	ψ_S^{min} MPa	ψ_S^{max} MPa	ψ_r^{min} MPa	ψ_r^{max} MPa
1977	–1.01	–0.44	–0.32	–0.22
1978	–0.97	–0.43	–0.31	–0.22
1979	–1.01	–0.44	–0.32	–0.23

between shoots and roots is fairly constant, evidently a reason for the stable mean annual mass flow (see Table 5.2).

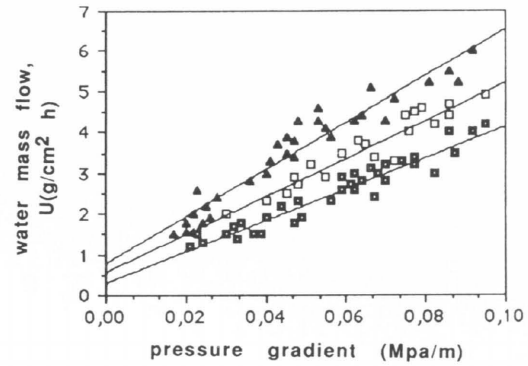

Fig. 5.4. The water mass flow rate as a function of stem water potential gradient at three different wood water concentrations (triangles 125–115 %, open boxes 115–105 % and filled boxes 105–95 %). The slope of the regression lines is the water conductivity of wood.

Flow Resistance

Pressure difference is not the only factor determining the mass flow rate. Water flow occurs in very small tracheids about 0.03 mm in diameter. The water flows from tracheid to tracheid through numerous pits 0.002 mm in size. These small transport pores hinder water movement. This effect is introduced into the analysis as water flow resistance, *R*. The analogy of Ohm´s law allows the determination of water flow resistance using the water pressure gradient and the mass flow rate. The dimension of stem water flow resistance is $MPasm^{-2}$ for a given tree. The specific resistance ie. the resistance of a piece of wood per unit length allows comparison between different trees. This normalized resistance has a dimension of $MPasm^{-3}$.

The resistance depends on the water concentration of the stem (e.g. Sellin 1991). Fig. 5.4 shows the water mass flow rate as a function of driving force (water potential gradient within measured stem segments) at three different wood moisture levels. As can be seen, the slope of the regression lines (ie. the stem water conductivity) changes as a function of stem water content. There is a slight hint of non-linearity with wet wood as the pressure gradient increases but it needs to be studied in more detail before any conclusions can be drawn.

The effect of the stem water content on the water flow resistance is evident from this work. Stem water concentration is low during periods of sunny weather in midsummer and high during prolonged rainy periods in autumn. The annual range of the variation of water content was from 85 % to 140 % (water mass / dry wood mass) and the greatest daily range was 15 %. This also generates temporal variation in the stem water flow resistance. The minimum observed specific resistance was 0.48 10^4 $MPasm^{-3}$ and the maximum 0.84 10^4 $MPasm^{-3}$.

Since the observed annual mean values of stem water content are quite stable (Table 5.1) the mean of the stem water flow resistance is also stable on these results. This stability, when related to the stability of water pressure difference between shoots and roots, explains the observed stable values of the mean of the annual mass flow rate per unit of sapwood cross-sectional area (henceforth denoted by AMFC).

5.2.4.4 Stand Level Water Transpiration

The transpiration at stand level also depends on the total amount of transpiring foliage apart from the factors described previously. The annual constancy of transpiration per sapwood area means that a) the year to year conditions are similar and both the transpiring foliage mass relative to wood cross-sectional area and the type of response of

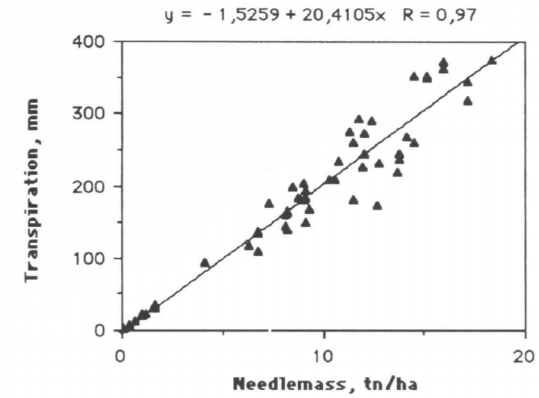

Fig. 5.5. The stand level water transpiration as a function of stand fresh needle weight.

foliage to the environment would be relatively constant or b) the conditions vary but the foliage regulates transpiration through stomatal action and the total foliage mass varies such that regular water flow through wood follows.

Khilmi (1957) observed from the data presented by Ivanov et al. (1951) and Moltshanov (1952) that a unit mass of needles transpired approximately equal amounts of water in a course of a year. The mean amount of transpiration per ton of needles in the experimental stands was 391 ton. This research line was continued by Rudakov (1979), who also found that the annual transpiration per unit mass of needles did not depend on stand age, soil fertility or geographical area.

We merged our observations with earlier findings in the literature to see whether the same trend also holds in this wider comparison. There are available in the literature 49 measurements and estimates of annual amounts of transpiration and the needle mass from Scots pine stands in the area of the former Soviet Union (see references above). The methodology applied to estimate these values varies somewhat. Including our own, there are 58 estimations in all. The data represents a wide geographical variation in the former Soviet Union, from North Karelia to the southern Don region, from Western Russia to the East in Kazakhstan. The age of the stands varies from 6 to 150 years. The regression between fresh needle mass and annual amount of transpiration is rather tight as can be seen in Fig. 5.5.

According to the above regression one ton of needles, fresh weight, transpires 20.4 tons of water. The fresh weights can be converted to dry weights in the experimental situation by using a correction coefficient with a value of 0.48, derived by Kasimirov et al. (1977). Thus one ton of needles, dry weight, transpires 42.0 tons of water in a year. This value seems to be independent of the properties of the site.

Some caution needs to be applied to the results since there are several methodological problems involved in the research on annual and stand level water transpiration. The measurements are also tedious to carry out. The above results may suffer from the methodological differences in the measurements since most of the data is collected from the literature. However, since it is unlikely that all the workers have made similar systematic errors, we can have some confidence in the general trend observed.

The above result would suggest that at our site the relationship between the transpiring foliage and sapwood area would indeed be relatively constant and that the stomatal response to diurnally variable but stable weather conditions on the growing season scale produces constant linkage between the total amount of foliage and annual transpiration. The total foliage mass is naturally related to growth and senescence processes and is thus related to the stand production process as well.

The result is more surprising on a geographically variable scale since the climate changes affect both the potential evapotranspiration and the water availability. The potential evapotranspiration in the southernmost range of Scots pine in Russia is almost 1.5 times that of the northenrmost conditions (calculated by Thornwaite method, Berninger et al. 1995). The observation implies changes in the annual transpiration per unit mass of foliage and probably changes in the total amount of transpiring foliage. However, such constancy in transpiration per unit mass of needles tends to suggest that the foliage mass wood cross-sectional area relationship might not vary too much geographically.

Different levels of water availability and demand can trigger reduction in needle mass, raising of the lower limit of the crown base, increase and redistribution of fine roots to deep soil layers etc. The constant needle-specific transpiration can

be understood as an outcome of acclimatization and adaptation of the tree structure to the conditions on the site. This phenomenon is evidently very important when developing an analysis of the dynamics of pine stands in its large growing area.

5.3 Relationship between Sapwood Area and Foliage Mass in Scots Pine

5.3.1 Introduction

The pipe model theory states that there are regular ratios between the water-conducting wood cross-sectional areas at different points along the transport path and the foliage quantity supplied by the wood. From the previous chapters it has become clear that woody properties vary according to the position within the tree and possibly also according to the growing conditions. For various reasons measurements done at the height of the crown base should give the most stable results.

The stand-level measurements of transpiration on the other hand suggested that no major changes in the foliage mass / sapwood area relationship should take place. This seemingly contrasting observation to the variations in woody properties leads us to study the geographical variations in the relationship between sapwood area and foliage mass and total area. The main hypothesis was that stand level observations of transpiration, should yield quite constant ratios between the foliage mass or area and the wood cross-sectional area within stands measured at the crown base of each tree over the geographical range were Scots pine grows.

5.3.2 Materials and Methods

5.3.2.1 Locations and Types of Measurements

The measurements were carried out between 1982 and 1989 in Muddusniemi, in Finnish Lapland (69°N, 27°E), Hyytiälä, Southern Finland (62°N, 24°E), Petrozavodsk, Russian Karelia (62°N, 34°E), Voronez, South Russia (52°N, 40°E) and Irkutsk, Siberia (53°N, 103°E).

The measurements were made in a hierarchical manner, consisting of: 1) measurements of the geometrical characteristics of needles to determine possible changes in their specific leaf area, 2) measurements of the relationship between total needle dry mass and cross-sectional area of wood in branches below the lowest living whorl of sub-branches to establish the relationship between branch cross-sectional area and foliage mass, 3) measurements of cross-sectional areas of wood in the stem below the living whorls and cumulative cross-sectional areas of branches of the whorls to relate branchwood area to stemwood area, 4) total cross-sectional area of water-conducting roots and the cross-sectional area of stem below the living crown to relate transport roots to stemwood and 5) total fine root biomass and the cross-sectional area of transport roots.

5.3.2.2 The Experimental Stands

The experimental sites were selected from stands that had recently closed canopy with a maximum height of about 10 m. The sites were chosen so that they were on poor to medium fertile sites in the local conditions. A description of the main stand characteristics is presented in Table 5.3 and the size distribution of the trees is presented in Fig. 5.6.

The biggest differences between the sites were in age and height of the stands. The Muddusniemi and Petrozavodsk stands were smaller and more open, which is reflected in the low average height of the crown base. The crowns of the trees were quite narrow in Muddusniemi. Most stands were even-aged but in the Petrozavodsk stand there were clear indications of more varied age structure (see Fig. 5.6). All stands were in the phase of recent canopy closure or were just about to reach it. There was a clear change in growing conditions of the stands from north to south, which is reflected in the average age of the stands (measured at the stump height ie. about 10 cm). This shows in the time it has taken for the stands to reach more or less the same size.

The Voronez and Hyytiälä stands were planted pine stands whereas the rest were naturally seeded (Petrozavodsk) or naturally regenerated. Both in the Muddusniemi and Voronez stands there are

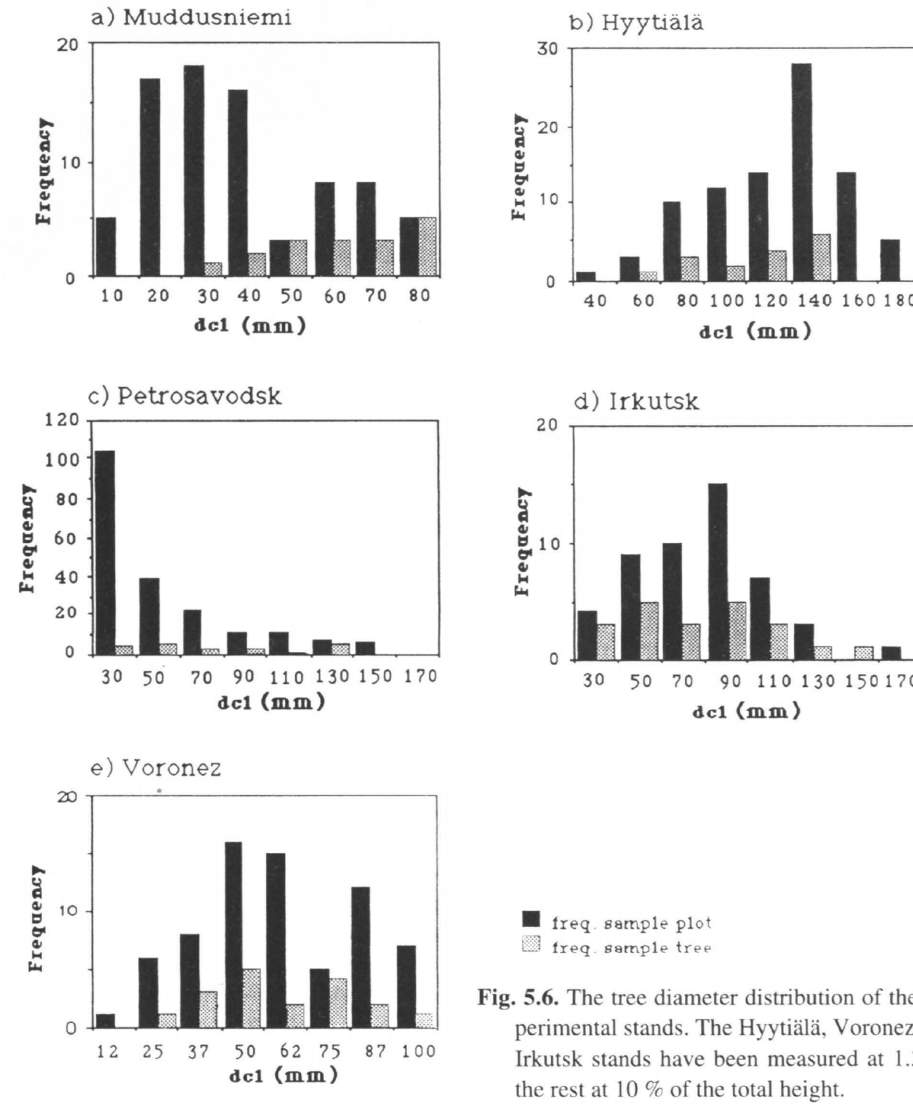

Fig. 5.6. The tree diameter distribution of the experimental stands. The Hyytiälä, Voronez and Irkutsk stands have been measured at 1.3 m, the rest at 10 % of the total height.

some signs of double-peaked size distribution which one quite often sees in the canopy closure phase (Ford 1975).

5.3.2.3 The Measurements

Sample Trees

About 20 sample trees were subjectively selected from each stand except at Hyytiälä where random sampling was used. The selection criteria for sample trees were that the trees should appear healthy, with one main stem only and their size distribution should be such that all the size classes present in the stand would be equally represented in the measurements. Because of the selection method the characteristics of the Petrozavodsk stand are not exactly the same as the average values calculated from experimental trees (Fig. 5.6).

Table 5.3 The main characteristics of the experimental stands.

Location	Age, a	Height, m		$D_{1.3}$,cm		Hcr, m		Dcb, cm	
	$\bar{x}$	$\bar{x}$	s	$\bar{x}$	s	$\bar{x}$	s	$\bar{x}$	s
Voronez	16	7.5	1.9	7.6	3.1	4.3	0.6	5.6	2.3
Irkutsk	24	6.7	1.3	7.2	3.0	2.6	0.4	6.3	2.6
Petrozavodsk	28	3.5	2.0	4.6	3.4	1.3	0.6	3.8	4.0
Hyytiälä*	22	9.4	1.6	11.6	1.6	5.2	0.6	7.3	2.1
Muddusniemi	43	3.2	1.3	4.3	2.1	1.1	0.4	3.6	2.0

Location	Density n/ha	Bacb m^2/ha	Size of l. clim. sp, m^2	N of trees
Voronez	6320	15.6	125	79
Irkutsk	4900	15.3	100	49
Petrozavodsk	5830	6.6	343	200
Hyytiälä	2900	12.1	300	87
Muddusniemi	5333	5.4	150	80

$\bar{x}$ = average, s = standard deviation, $D_{1.3}$ = diameter at breast height, Hcr = height of the crown base, Dcb = diameter at the crown base, Bacb = stand basal area at the crown base, Size of l. clim. sp = Size of light climate sample plot

*The Hyytiälä values were calculated from the sample trees with exception of diameter at breast height.

Needle Measurements

To determinate the relationship between the geometric properties at needle and shoot level, a sample of shoots representing different parts of the crown were collected from the Muddusniemi, Petrozavodsk, Hyytiälä and Voronez stands. All shoots were described according to classification system of Ross et al. (1986). The following needle and shoot characteristics were measured: needle length (l_N, in mm), needle width (b_1, in mm), needle thickness (b_2, in mm), dry needle weight (m_N, in mg), shoot length (l_S, in cm) and number of needles per 1 cm of shoot, (n_N, in 1/cm).

The needle characteristics of every shoot were determined as a mean of 20 to 50 sample needles. Tiréns (1926) formula was used for calculating needle area, S_N:

$$S_N = \frac{\pi}{2} l_N \left(\frac{b_i}{2} + b_2 \right) + b_1 l_N \qquad (5.2)$$

The mean area of a single needle is utilized in determining the needle area of a shoot, S_{NS}

$$S_{NS} = l_S n_N S_N \qquad (5.3)$$

Branch Measurements

A sample of 15 to 20 branches was subjectively selected from the branches of the sample trees with the exception of Hyytiälä, so that the whole size distribution was equally represented and comprised the sample branches from different positions in canopy.

In Hyytiälä 16 sample trees were randomly selected from the stand to determine the ratio between the branch cross-sectional area and the stem cross-sectional area. From another set of 14 randomly selected trees from dominant and co-dominant canopy layers, 30 % of branches were selected systematically from the second uppermost whorl downwards for analyses of branch area and needle mass relationship.

Cross-sectional area measurements were made so that, based on the dying experiments, the entire cross-section could be expected to consist of only water-transporting sapwood. The diameters of all branches were measured below the lowest living whorl of sub-branches in two perpendicular directions and the diameter of the stem was measured in two perpendicular directions below the lowest living whorl of branches from all the sample trees.

Trunk Measurements

The trunk diameters below all living whorls were measured from all sample trees in Voronez and Hyytiälä, from three trees in Muddusniemi and Petrozavodsk and six trees from Irkutsk. All the diameter measurements were done below the bark and a whorl was a judged alive if more than half of the initial number of branches in the whorl were still alive. All the diameter measurements were carried out with accuracy calipers (accuracy 0.1 mm). For diameters greater than 5 cm standard calipers used in forest measurements were utilized (accuracy 1 mm).

Coarse Root Measurements

The coarse roots (>2 mm) were dug out when possible from the sample trees from Petrozavodsk and Voronez. The diameters of the main roots were measured at the point where their diameter seemed to attain a constant value, ie. where the basal swelling was no longer noticeable. Generally, this occurred between one and two metres from the stem. In Voronez, a clear bole root could be distinguished in most of the trees. The diameter measurements of these roots were difficult to carry out using the method described since there was not always a clear point at which the tapering of the roots stopped. The measurements of the bole roots were thus marked separately. The roots of 16 trees altogether from Petrozavodsk were analysed using this method. The corresponding number for Voronez was 13.

Fineroot Measurements

The amount of fine roots attached to the excavated coarse roots was estimated in Petrozavodsk, where soil was fine sand. The coarse roots were carefully dug out of the soil and all roots smaller than 2 mm in diameter were detached. The sample was dried and weighed, after which the samples were ignited and the dry weight was estimated as the difference in weight before and after combustion.

Special Sample Plot

Apart from the sample plots mentioned, a sample of 15 branches was selected from Ahvenanmaa, Finland (60°N, 20°E) from a sample plot fulfilling the same criteria as the others. The same measurements were made on these branches.

All the measurements were made early in August after the needle growth had ceased but before the shedding of the old needles, ie., at the

Table 5.4 General properties of the experimental trees by location

Location		Muddusniemi	Hyytiälä	Petrozavodsk	Irkutsk	Voronez
N of trees		17	16	16	23	16
Dcb, cm	$\bar{x}$	4.92	7.2	5.91	5.22	4.89
	s	2.12	2.1	3.24	2.85	1.75
Height,	$\bar{x}$	4.17	11.6	–	6.40	7.63
tot.	s	1.21	1.6	–	1.87	1.03
Hcb, m	$\bar{x}$	2.72	5.2	–	3.80	4.09
	s	0.94	0.6	–	1.51	0.92
Br/Wh*	$\bar{x}$	3.2	4.7	3.6	5.3	5.9
Living* whorls	$\bar{x}$	20.3	8.6	16.3	8.80	7.7
Age, y	$\bar{x}$	38.4	22.0	–	22.5	16.0
	s	6.11	0.0	–	1.68	0.0

Dcb = diameter below living crown, Hcb = height of the living crown, Br/Wh = number of branches per whorl, $\bar{x}$ = average, s = standard deviation
* the number of sample trees from which branches and whorls were counted per location varied between 3 and 21.

time of the maximal needle biomass with exception of Hyytiälä, where the branches were analysed at the end of October after the old foliage had fallen completely.

The characteristics of the experimental trees are shown in the Table 5.4. They were slightly different, depending on location. At Muddusniemi trees were generally older but smaller, having more branch whorls but also a shorter living crown than the more southerly trees, especially those of Voronez. A big difference in the stem form was also observed. This is reflected in a much larger ratio between diameter below crown/tree height in Muddusniemi than in Voronez. There was also a north to south decrease in the average number of living whorls per tree and an increase in the average number of living branches per whorl.

The size distribution of the sample trees was similar in each stand with the exception of Hyytiälä, where the sample trees were slightly bigger. This meant that the systematic sample consisted of a more or less equal number of trees from different size classes but representing the population sampled with a different weight (see Fig. 5.6).

5.3.3 The Results

5.3.3.1 Geographic Variation in Needle Dimensions and Specific Needle Area

It would seem that the unshaded but not shaded needles are bigger in the more favourable growing conditions of Hyytiälä and Voronez than in Muddusniemi and Petrozavodsk. However, it would seem that the width of shaded needles actually increases in more northernly stands.

There is a linear regression between needle width and needle thickness. It is practically the same in Petrozavodsk, Hyytiälä and Voronez. The needles in Muddusniemi are however different, being 1–2 mm wider than the others at the same thickness.

The regression of needle thickness on needle length also seems to be the same for unshaded needles in Petrozavodsk, Hyytiälä and Voronez but lower for the shaded needles. The shaded needles at Petrozavodsk and Voronez are about 0.2 mm thinner than the unshaded ones. The regression is very different at Muddusniemi. The needle thickness increases three times more rapidly as a function of needle length than in the other locations and since they are wider at the same thickness they increase even more in width. This might indicate adaptation to the extreme climate in the far north. On the other hand, the illumination conditions seem to have considerable influence on needle dimensions. The biggest difference between the unshaded and shaded needles

Table 5.5 Mean needle characteristics at the various experimental stands (n = 300–600/ location)

Location	Unshaded needles b_1	b_2	l	Shaded needles b_1	b_2	l
Muddusniemi	1.57	0.76	34	0.90	0.32	17
Petrozavodsk	1.55	0.77	44	0.70	0.40	10
Hyytiälä	1.90	0.90	73	0.80	0.42	30
Voronez	1.70	0.80	76	0.62	0.32	20

b_1= width, b_2= thickness, l= length (all the values are given in mm).

Table 5.6 The parameters of the linear regression between needle width and needle thickness for experimental stands

Location	Gradient	Intercept	R-squared
Muddusniemi	0.35	1.70	0.94
Petrozavodsk	0.23	2.33	0.94
Hyytiälä	0.15	2.15	0.97
Voronez	0.12	2.25	0.98

Table 5.7 The values of the parameters in linear regression of needle thickness on needle length for each experimental stand.

Location	Gradient	Intercept	R-squared
Muddusniemi	0.13	0.0260	0.94
Petrozavodsk			
(unshaded needles)	0.46	0.0070	0.84
(shaded needles)	0.36	0.0043	0.92
Hyytiälä			
(unshaded needles)	0.45	0.0069	0.72
Voronez			
(unshaded needles)	0.20	0.0078	0.98
(shaded needles)	0.28	0.0032	0.94

Table 5.8 Values of the coefficients A_1 and A_2 in the simplified Tire'n's formula (Eq. 5.4) and the needle area (*NA*) of different sized needles (20 and 50 mm long) in the experimental stands.

Location	A_1	A_2	*NA* l_N=20mm	*NA* l_N=50mm
Muddusniemi	0.03	0.120	0.5	3.0
Petrozavodsk				
(unshaded)	2.22	0.040	0.6	2.1
(shaded)	1.65	0.025	0.45	1.4
Hyytiälä	2.17	0.038	0.55	2.0
Voronez				
(unshaded)	0.90	0.045	0.35	1.65
(shaded)	1.35	0.018	0.35	0.96

Table 5.9 Needle area (*NA*) as a function of dry needle weight (*W*) in Voronez and Muddusniemi, $NA = aW^b$. Values are in mm and mg.

Location	a	b	R-square	Needle area when W=5	W=20	W=50
Voronez	36.96	0.617	0.951	99.8	234.7	413.0
Muddus-niemi	21.70	0.737	0.983	71.0	197.4	387.8

was in Voronez, where the total stand level needle biomass was also the highest.

The regressions between the dimensions of a needle enable the determination of needle area using only needle length and Tiréns formula (5.2) becomes:

$$S_N = A_1 l_N + A_2 l_N^2 \qquad (5.4)$$

where coefficients A_1 and A_2 depend on the regression coeficients between needle length and thickness and width. This simplified method is more convenient than the original Tirén formula.

There is variation in the regressions of needle width or thickness on needle length between locations and also between the layers in the canopy. Thus the coefficients in Eq. (5.4) also have specific values for each location.

A needle of the same length has a very different area depending on geographical location and position in the canopy. For, example an unshaded needle of 5 cm length of in Muddusniemi has about 1.8 times the area of a corresponding needle in Voronez. The area of an unshaded needle is about 1.5 times higher than a shaded needle of equal length. However, in Voronez, the area of small unshaded and shaded needles is the same.

Dimensional relationships of needles change between sample plots. The needles in Muddusniemi were generally both thicker and wider than similar needles in Voronez and have higher surface area per unit length. Table 5.9 presents the relationship between the total leaf area and dry weight of a needle for Voronez and Muddusniemi. An exponential model was fitted in both locations. The specific leaf area decreased as the leaf mass increased, as expected. Needles of the same weight seemed to have a systematically higher surface area in Voronez than in Muddusniemi. The relative difference decreased however as the size of the needles increased. The largest recorded in Voronez was just above 50 mg and in Muddusniemi around 45 mg.

5.3.3.2 Foliage and Wood Cross-Sectional Area Ratios

The regression between the needle biomass and the branch cross-sectional area below the lowest living whorl of sub-branches was linear in all the experimental stands (see Fig. 5.7 a–f). However, the slope of the regression was different between stands. The parameter values for different stands are shown in Table 5.10 The intercept varied between sites, but was not statistically significant.

The Hyytiälä values were not directly comparable with the others since they represented the annual minimum foliage mass whereas the rest were measured at the occurrence of the maximum needle mass. Also a different sampling design was used in Hyytiälä.

The regression between total branch cross-sectional area in the living crown and the stem cross-sectional area at the base of the living crown were strongly correlated within a stand (see Table 5.11 and Fig. 5.8). The regression was generally linear although some curvilinearity could be observed, especially in the Voronez stand. Both in Hyytiälä and Irkutsk most of the points measured were remarkably close to a straight line with exception of

Table 5.10 The regression Eqs. of dry needle mass (g) as a function of branch cross-sectional area (mm^2) below the lowest living whorl of sub-branches.

Location	Intercept	Slope	Std.error	Conf.lim. 5% risk	R-squared	RMSE
Voronez	–1.93	0.751	0.045	0.66–0.84	0.939	13.65
Irkutsk	–1.46	0.622	0.03	0.56–0.68	0.964	8.42
Ahvenanmaa	–2.96	0.693	0.05	0.59–0.80	0.959	8.60
Hyytiälä	–1.84	0.566	0.022	0.52–0.61	0.901	15.12
Petrozavodsk	–1.19	0.452	0.007	0.44–0.47	0.995	5.19
Muddusniemi	1.78	0.435	0.019	0.40–0.47	0.966	9.34

Table 5.11 The regression Eqs. for the total branch cross-sectional area (mm^2) in the living crown as a function of stem cross-sectional area (mm^2) below the living crown.

Location	Intercept	Slope	Conf. lim. 5% risk	R-square	C.V.
Voronez	–723.5	1.57	1.30–1.84	0.92	24.6
Irkutsk	–431.3	1.16	1.03–1.29	0.94	28.6
*	–280.3	1.05	1.00–1.10	0.99	12.0
Petrozavodsk	91.5	1.02	0.88–1.16	0.94	23.4
Hyytiälä	–761.6	1.28	1.08–1.48	0.93	16.1
*	–581.8	1.20	1.09–1.31	0.98	8.6
Muddusniemi	–299.1	1.019	0.91–1.13	0.96	18.6

* One outlier has been left out

one "outlier" which clearly had a higher branch cross-sectional area total in comparison to the stem cross-sectional area below the living crown. The parameters of the regression lines with and without the "outlier" are presented for these locations in Table 5.11. The tree from which the outlying observation was made in Hyytiälä had a different appearance from the rest of the stand with a clearly bigger crown with many thick branches than the other trees and a lower pruning limit.

There were obvious changes in the regression coefficients between the sites (see Table 5.11). The Voronez values were different from those of Muddusniemi and Petrozavodsk. The Irkutsk values were of the same magnitude as Petrozavodsk and Muddusniemi if the outlier value was not considered. Similarly, if the outlier had been left out in Hyytiälä, the values would have come closer to Muddusniemi, Petrozavodsk and Irkutsk than Voronez. The residuals of the regressions, especially in Irkutsk, were no longer homoscedastic if the outliers were included in the analysis.

The same cross-sectional area at the crown base in the Voronez stand could support about three times the needle biomass of the Lapland stand and according to the results of the previous chapter the difference was even bigger on leaf area bases. Both the differences in the regression between the needle mass and the branch cross-sectional area and that between the total branch cross-sectional area and the stem cross-sectional area contributed to the difference by approximately the same amount.

5.3.3.3 The Root Ratios

We asked whether there were similar regularities between fine roots and wood as between foliage and wood structure. The sandy soil of the Petrozavodsk stand facilitated the removal of fine roots from the soil. In addition the cross-sectional area of the coarse roots both from Petrozavodsk and Voronez was measured in the manner described earlier.

There was a significant linear regression be-

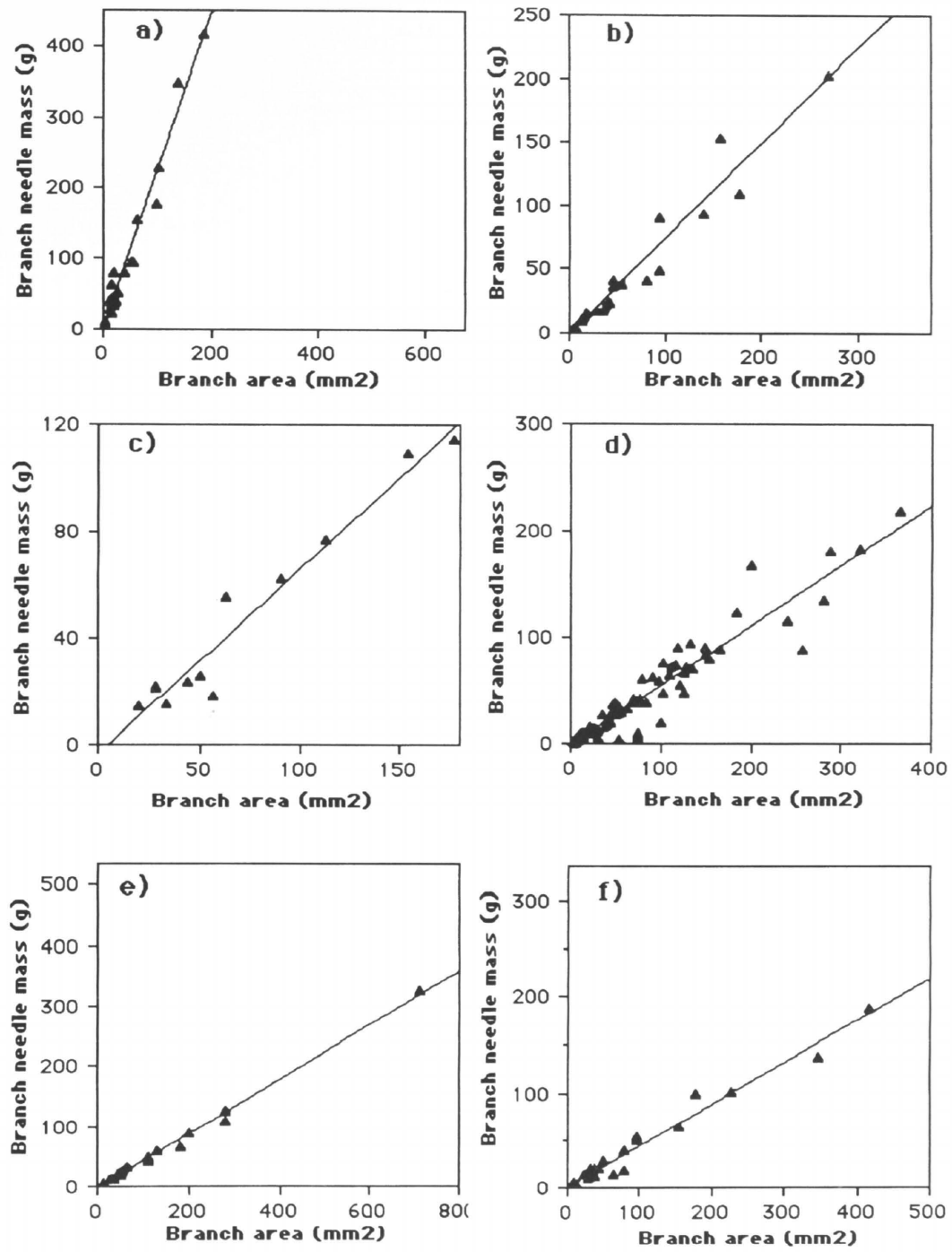

Fig. 5.7. Branch needle mass as a function of branch cross-sectional area below the lowest living whorl of sub-branches in a) Voronez, b) Irkutsk, c) Ahvenanmaa, d) Hyytiälä and e) Muddusniemi. The relative scale between y and x axes is the same in each graph.

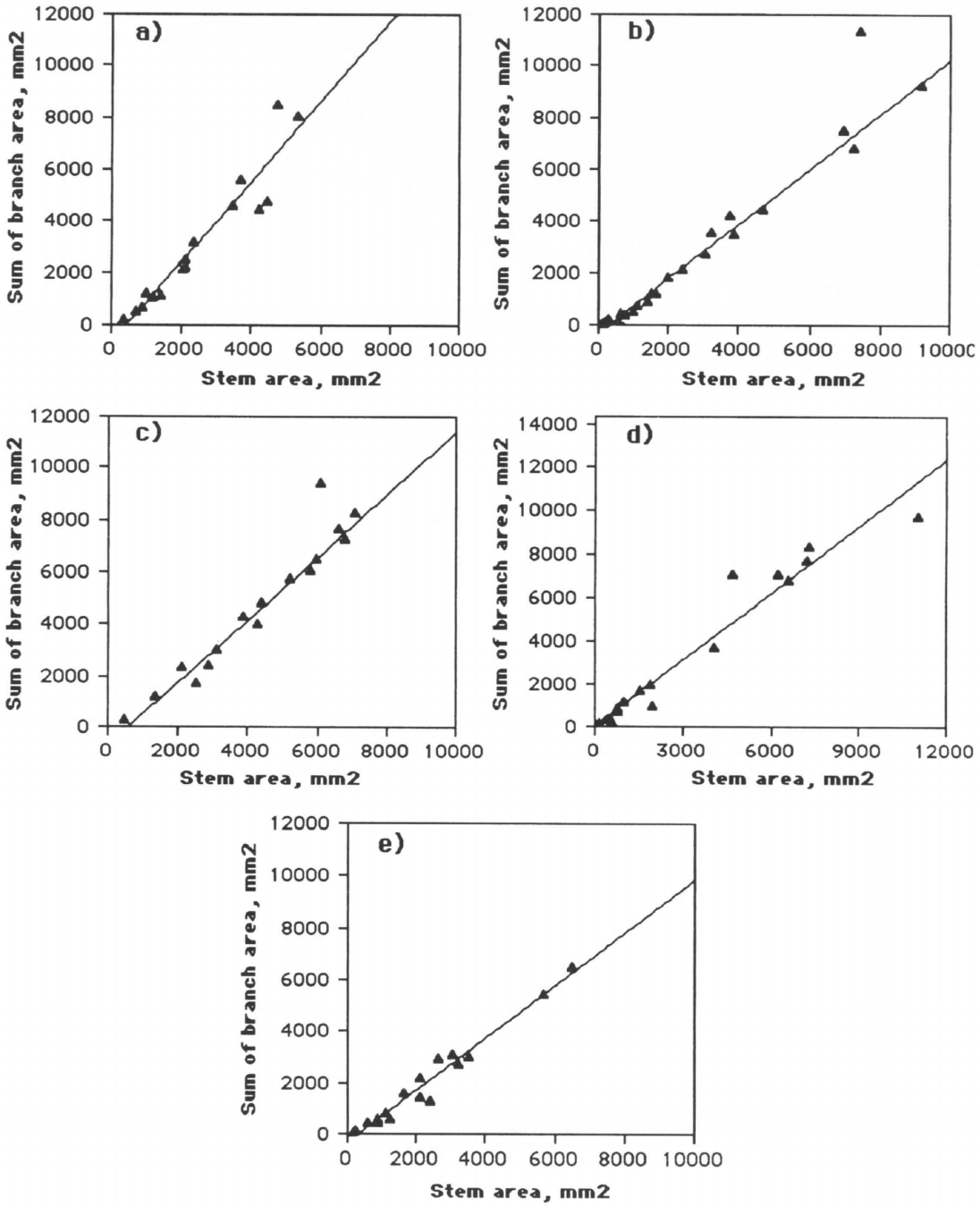

Fig. 5.8. Total tree branch cross-sectional area below the lowest living whorl of sub-branches as a function of stem cross-sectional area below the living crown in a)Voronez b) Irkutsk c) Hyytiälä d) Petrozavodsk and e) Muddusniemi. The relative scale between y and x axes is the same in each graph.

tween the fine-root mass and the transport root cross-section (see Fig. 5.9). There was more variation in this relationship than generally obtained for the needle mass / branch area relationship but that might reflect the difficulty involved in the exact determination of the fine-root mass per coarse root. The ratio between the needle mass and fine-root mass for early August derived from the regression Eqs. was about 10:1, ie. there was about ten times more standing foliage mass than fine-root mass.

There was a linear regression between the sum of cross-sectional area of transport roots and the stem cross-sectional area below the living crown both in Petrozavodsk and Voronez (see Fig. 5.10 a and b). The gradient in the simple linear model explaining the total transport root cross-sectional area as a function of stem cross-sectional area below the living crown was slightly steeper in Voronez than in Petrozavodsk. The differences were less than between stem and branches (see Table 5.12). The differences between sites were not significant because of wide variation.

The variation in the coarse root cross-sectional area / stem cross-sectional area function was markedly higher in Voronez than in Petrozavodsk. We asked whether the existence of a bole root could be the reason for the wider variation (Fig. 5.11 a and b) As can be seen, stem area below the living crown did not explain the variation in the

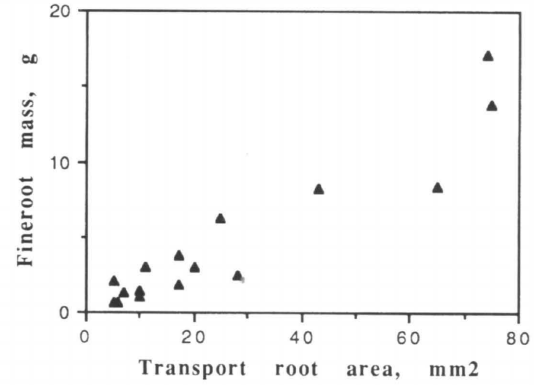

Fig. 5.9. The mass of fine roots as a function of transport root cross-sectional area.

Table 5.12 The regression Eqs. of a) fine-root mass as a function of transport root cross-sectional area and b) transport root cross-sectional area as a function of stem cross-sectional area below the living crown.

Location	Intercept	Gradient	R^2
a) Fine roots			
Petrozavodsk	–0.182	0.187	0.89
b)Transport roots			
Voronez	42.89	0.42	0.58
*	–98,62	0.34	0.74
Petrozavodsk	–47.38	0.223	0.95

* Only the lateral roots were considered; see text for explanation.

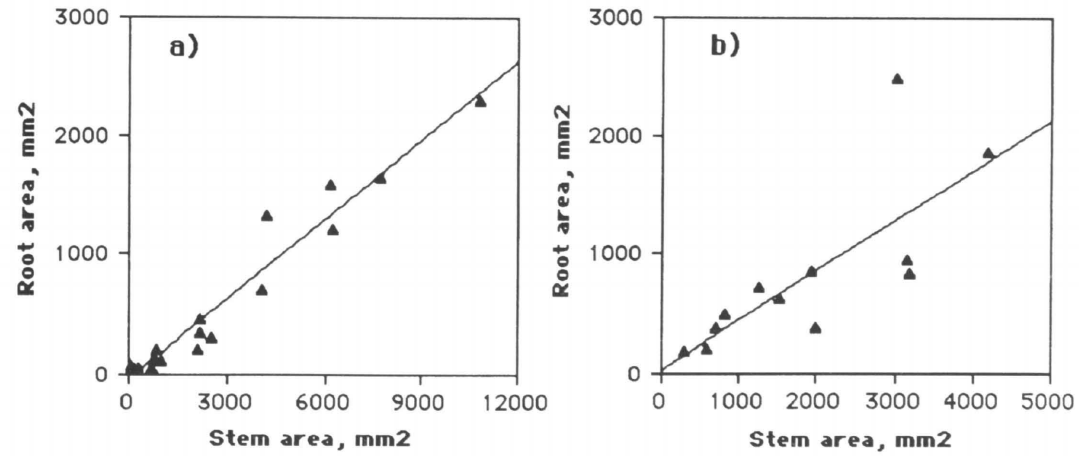

Fig. 5.10. The total of the cross-sectional area of transport roots as a function of stem cross-sectional area below the lowest living whorl of branches in a) Petrozavodsk and b) Voronez.

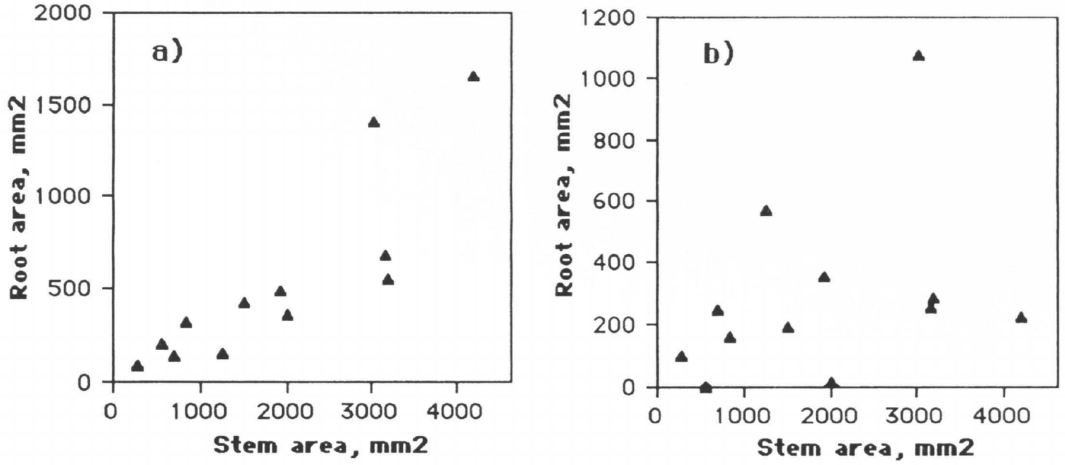

Fig. 5.11. The sum of a) lateral root cross-sectional area and b) the bole root cross-sectional area as a function of a stem cross-sectional area below the lowest living whorl in Voronez.

total bole root diameters. On the other hand, as can be seen from Table 5.12, much of the variation in the lateral transport root cross-sectional area could be explained by the stem cross-sectional area.

5.3.3.4 Within-Crown Variation in Branch Area / Stem Area Ratio

We anticipated trends in the branchwood cross-sectional area / stemwood cross-sectional area relationship within a living crown due to trends in tracheid size distribution (Chapter 5.2). Fig. 5.12 a–c presents the relative differences in branch / stem cross-sectional area ratio of each whorl from the treewise average as a function of the whorl number from Hyytiälä, Irkutsk and Voronez where stem cross-sectional areas were measured below each whorl. The branch cross-sectional area was the sum of cross-sectional areas of the branches of a whorl and the stem cross-sectional area was calculated as the difference between the area measurements above and below each whorl of branches.

There was no general trend in the relationship observed within the crown. There was an increase followed by decrease in Voronez moving from the top of the tree downwards. However, same trend was not present in Irkutsk or Hyytiälä.

5.4 The Relationship between the Foliage Increase and Tree Ring Growth within the Crowns of Scots Pine

5.4.1 Introduction

The pipe-model approach can be used to derive the carbohydrate allocation between the woody parts of a tree in branches, stem and roots as well as foliage (Hari et al. 1985, Valentine 1985, Mäkelä 1986, Ludlow et al. 1990, Nikinmaa 1990, Mäkelä 1990). The use of the pipe model for such purposes implies that the observed ratios remain unchanged from one moment to another. Much attention has been paid to examining the foliage area or biomass as a function of sapwood cross-sectional area (Waring et al. 1982, Kaufman and Troendle 1981, Hari et al. 1986, Albrektson 1984, Long and Smith 1988). However, less attention has been paid to clarifying the dynamics of how the ratio between needle biomass and sapwood area is maintained. Earlier observations of the quite constant annual water transport through the stem, constant transpiration per unit mass of foliage and the constant relationship between foliage mass and sapwood cross-sectional area from the Petrozavodsk stand would support the hypothesis that the relationship would remain fairly stable from year to year.

According to the pipe model theory, the cross-

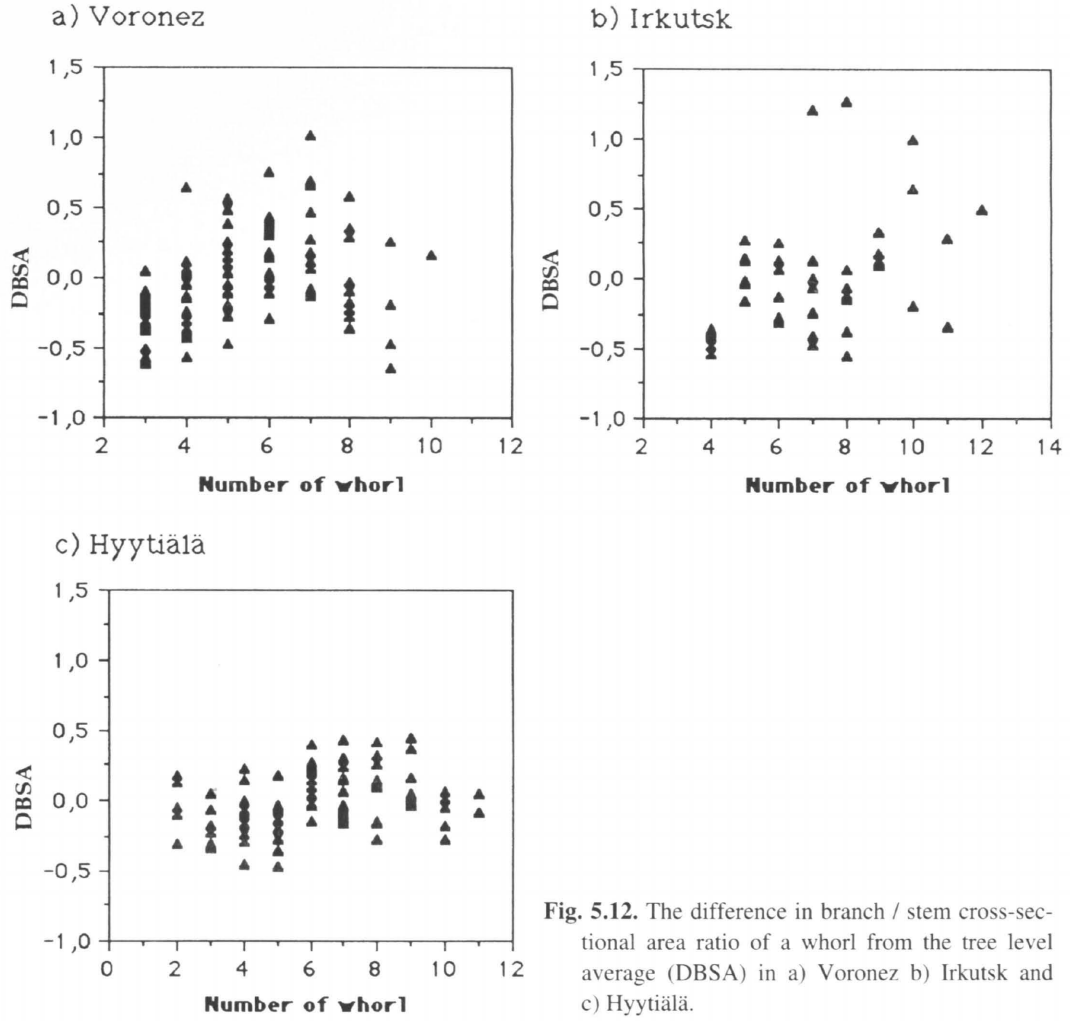

Fig. 5.12. The difference in branch / stem cross-sectional area ratio of a whorl from the tree level average (DBSA) in a) Voronez b) Irkutsk and c) Hyytiälä.

sectional area of the newest growth ring at any height should be proportional to the cumulative change in the needle biomass above the point of measurement plus the formation of the non-functional heartwood at that height. If it is assumed that no heartwood formation takes place within the living crown (Chapter 5.2), then the cross-sectional area of the newest growth ring would be proportional to the cumulative change in needle biomass above that height within the living crown.

5.4.2 Materials and Methods

The dynamics of the sapwood area / needle biomass ratio were studied from one tree from Voronez and one tree from Hyytiälä. The Hyytiälä tree was 4.8 m tall and had a diameter below the living crown of 2.83 cm. The lowest living whorl was at 2.6 m. The corresponding values for the Voronez tree were height 6.57 m, diameter below the crown 5.31 cm, and the height of the lowest living whorl 1.9 m. The Hyytiälä tree had 10 living whorls of branches and the Voronez tree had nine.

The stem diameters below each whorl of branches were measured in two perpendicular directions

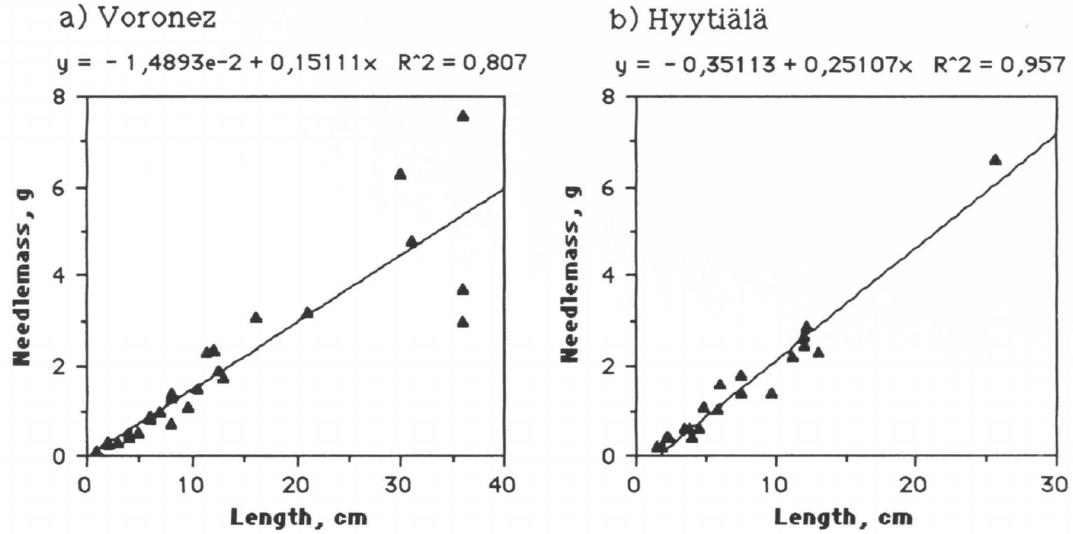

Fig. 5.13. The regression between the shoot length and needle mass in a) Voronez and b) Hyytiälä.

below the bark from both of the trees. The width of the outermost tree ring was also measured, resulting in four tree ring width measurements per height. The same measurements were carried out on each of the branches below the lowest living whorl of sub-branches.

The lengths of the newest shoots were measured in each branch from both trees. A sub-sample of 20 shoots in Hyytiälä and 28 shoots in Voronez was selected from the shoot population to determine the regression between the needle biomass and the shoot length. Every fifth branch was systematically selected from the top of the tree downwards in Hyytiälä. The newest shoot of the main axis of the branch and that of the sub-branch situated closest to the central point of the living crown of the branch were selected for biomass analyses. The sample shoots in Voronez were selected subjectively, trying to represent the entire shoot size and position distribution equally in the sample.

The lengths of the branch internodes just below the oldest needle-bearing internodes were measured to estimate the amount of needle biomass which died the previous autumn. It was assumed that the ratio between internode length and needle biomass was the same as in the newest shoots. The measurements were made at the stage of greatest needle mass in August. There were four living needle-age classes at the time of the measurement. There were altogether 200 new shoots and 139 internodes just below the needle-bearing part of the trees in Hyytiälä, the corresponding numbers for Voronez being 514 and 278.

5.4.3 Results

The regressions between the shoot length and the needle mass is shown in Fig. 5.13 a and b. It is not quite linear in Voronez and the variation in the regression increases with the size of the shoots. However, for the purpose of this work it was felt that linear regression between shoot length and needle mass could be used. The regression lines for Voronez and Hyytiälä were very similar, excluding the two outlying shoots in Voronez.The changes of tree ring area above and below each whorl and the needle mass change at the same whorl are shown in the Fig. 5.14 a and b. There is much variation between different values, as could be expected with such an inaccurate method of estimating the needle mass change. However, the relationship between needle mass change and tree ring width change seemed to be linear within the living crown for both the Hyytiälä and Voronez tree (see also Table 5.13). Of course, more points would be needed to be able to draw any

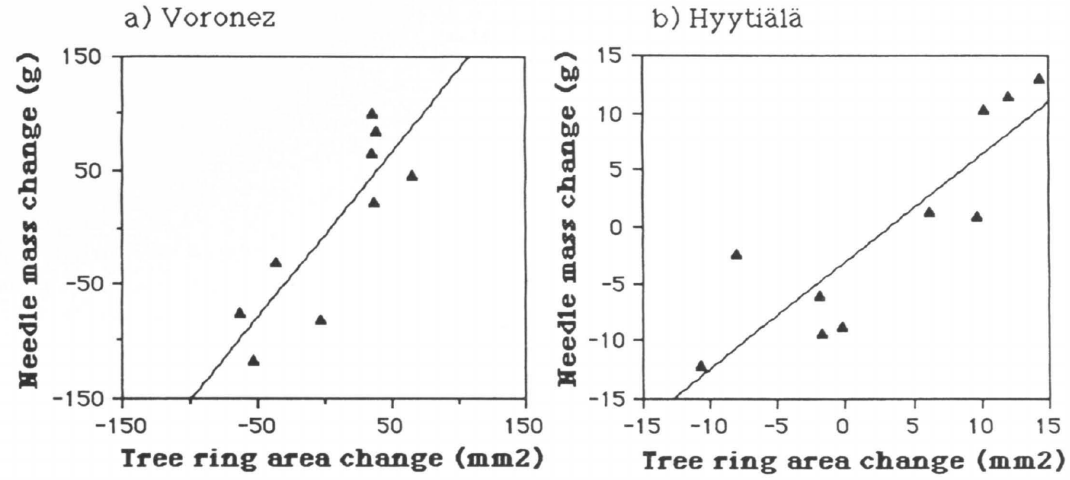

Fig. 5.14. The change of the tree ring area above and below the whorl of branches as a function of needle mass change in the same whorl a) in Voronez b) in Hyytiälä.

Table 5.13 The coefficients of the regression lines for needle mass change as a function of tree ring area change.

Location	Intercept	Parameter estimate	R^2
Hyytiälä	–2.97?	0.923	0.756
Voronez	–7.173	1.427	0.683

conclusions. However, the ratio between the needle mass change per unit cross-sectional area change in Voronez and Hyytiälä was comparable to the results of Chapter 5.3. The absolute value of the slope however was about double to that of the needle mass cross-sectional area relationship.

5.5 Final Remarks

Constant annual transpiration per unit mass of foliage, only small variations in annual water transport through the unit area of sapwood and the tight relationship between sapwood cross-sectional area and total foliage biomass that were observed in Petrozavodsk fit together well. On the other hand, the constant transpiration per unit foliage mass that was independent of climate and increasing foliage biomass or area per unit sapwood area from north to south seem contradictory.

In the north-south gradient the growing conditions improve with milder climate but simultaneously the availability of water becomes a more important growth-influencing factor. Zimmermann (1983) suggested that the hydraulic architecture of trees is such as to guarantee the functioning of the central part of the water pathway which also represents the longest lasting "investment" in structure. If unfavorable conditions should occur, the breaking of water columns is restricted to the most distal parts possible. The results of this study indicated that in the southern conditions of Voronez there was both more foliage per unit branch cross-sectional area and more branch cross-sectional area in comparison to stem cross-sectional area than more in the north. Berninger et al. (1995) simultaneously analysed variation in potential evapotranspiration and the changes in branch and stem-sapwood area relations, partially from the same data as presented here, and observed a close relationship between the two. As they pointed out, such changes imply either pressure changes along the transport pathway from branches to stem or changes in the water conductivity of wood.

Increasing evapotranspiration favours structures that differentiate between proximal and distal parts of the water transport pathway. On the other hand,

Tyree and Sperry (1989) suggested that structures that can avoid or reverse winter embolism become more important further to the north. This could mean that there should not be large differences in the structure along the transport path since it is equally subjected to low temperatures at all points. The quantitative variation in the relative cross-sectional areas between stem and branches show a big difference in the more evaporative conditions but hardly anything in the moist northern climate. This could reflect structural acclimatization or adaptation to different hydraulic demands.

The growth rate of trees increased along the north-south gradient, correlating with the trends observed in the needle mass and cross-sectional area ratios. This kind of correlation has also been observed in other studies (e.g. Albrektson 1984, Long and Smith 1988). However, the growth rate differences within northern stands (Muddusniemi, Petrozavodsk or Hyytiälä) did not affect the branch area (or foliage mass) / stemwood area ratio. In the southerly Voronez stand there was a slight tendency to increasing foliage mass per sapwood area as the tree size grew. The latter observation coincides with the findings of Kuuluvainen et al. (1988) that high biomass was associated with branchiness and long crowns. On the other hand, as Berninger et al. (1995) pointed out, the growth rate effect was clearly inferior to the differences explained by the climatic variables.

It seems reasonable that the xylem structure which plays a major role in keeping the functional parameters stable from year to year is not the same in very different climatic conditions and that there should be differences in woody structure which cannot be explained solely by the different growth rate. Tyree and Sperry (1989) have suggested that the plants are operating near the brink of catastrophic xylem dysfunction due to water stress and that the number of leaves, their stomatal regulation and the quantity and physiology of the xylem need to be in balance.

The water-conducting capacity of wood depends heavily on the lumen diameter and the length of the tracheids (see Chapter 5.2). Generally, the wood density in Scots pines is inversely proportional to the growth rate (Kärkkäinen and Uusvaara 1982, Kärkkäinen 1985). Vysotskaya et al. (1985) measured the tracheid size distribution of trees growing in dry and moist conditions and found that the tracheid size increases with the width of the annual rings in dry growing sites but in moister conditions such was not the case. Pothier et al. (1989) report that the permeability increased as a function of site quality and stand age in Jack pine stands. At young ages the permeability was correlated with the tracheid lumen diameter.

Unfortunately no data on woody micro structure was collected from the stands studied here. Dinwoodie (1961) reports the work done by Echors (1958), who studied the tracheid length trends in different geographic races of Scots pine. He found a decreasing trend from south to north, but did not consider the internal variation of trees in tracheid length (see Chapter 5.2) which may be partially responsible for his results (Dinwoodie 1961). However, as the tracheid length and diameter are normally connected (Carlquist 1988), these results suggest that stemwood is more conductive in more southerly conditions.

The needle mass and the sapwood cross-sectional areas in branches, stem, coarse roots and the quantity of fine roots were all linearly related. The water flow measurements and the connections between the flow pathway and tree architecture (see Chapter 5.2) are consistent with the observed regularities in cross-sectional areas. The results support the idea that the growth of foliage and associated structures in branches, stem and fine roots are closely related (e.g. Larson 1969) and that there is a quantitative connection between the cross-sectional areas measured at different heights along the transport path within a tree (e.g. Shinozaki 1964a). However, as the results indicate, the corresponding cross-sectional area varies greatly along the transport path so that the stem sapwood area is about four times the cross-sectional area of transport roots. As pointed out this implies changes either in the water conductivity within the xylem or the pressure gradient driving the flow. However, in conifers the proportion of practically non-conductive latewood also varies along the the stem and between tree parts and can have an effect on the relationships observed.

The constancy of the dimensions of the transport path and the standing biomasses at both ends of it imply that the change in one component is associated with a proportional change in another. Since the change of one component consists of

growth and senescence, both should be considered in the analyses of the observed dynamic regularities.

Rather a gross method of investigating the dynamics of structural growth between various components was used here. The results yielded a linear dependency between the needle mass change and the tree ring growth. The difference in the dynamic ratios between Hyytiälä and Voronez were of a similar magnitude to the static values but the slopes were about double. This would mean that there would be more needles per unit cross-section of wood as the proportion of the annual growth from the total wood cross-sectional area increases. This seemed to be the case in the fast-growing southerly Voronez stand, as the regression between the branch area, which also reflects the total crown foliage, and the stem cross-sectional area below the crown was slightly exponential, ie. bigger trees with faster growth had more needles per cross-section than smaller trees.

The pipe model theory was first put forward as a morphological model of tree structure (e.g. Shinozaki et al. 1964a, b). The results of this work indicate that it can be a very fruitful approach in analysing tree structure. However, as already pointed out by Huber (1928), the results also indicated that the ratio between woody cross-sectional area and the foliage biomass varies at different positions along the transport path and between locations. The transpiration per unit amount of foliage, however, seemed to remain constant over a wide geographical range. Together these results imply considerable changes in the fine structure of wood and in the way the resources are allocated among the different parts of trees: Smaller share of the resources to stem allows higher foliage growth. The estimated foliage biomass of the Voronez stand was over 18 tn/ha (Chapter 4) which is clearly higher than previously observed in Finland (Mälkönen 1974, Ilonen 1981). On the other hand if the results are correct, then the same cross-sectional area of sapwood in Voronez would conduct about three times more water than in Muddusniemi in a growing season. The changes in growth and function reflect also variation in radiation interception and radiation use efficiency and they need to be considered in accounting for the acclimatization of trees to different conditions.

The input-output reactions and growth processes operate at different hierarchial levels which makes the analysis of structure and functions difficult. While the actual mechanisms of growth processes especially are still poorly known, an approach in which aggregated environmental variables are related to structural properties can bring new insight to the question.

The approach using the pipe model as an approximation between the foliage and woody growth, has indicated the great importance that the formation of structure has on the use of acquired resources (Hari et al. 1985, Mäkelä 1986, Valentine 1985, see also Chapters 6 and 7). The woody structure is however a result of the past history of the stand, which imposes limits on the stand functions. Therefore, all work that can bring us new information on the structure / function interaction gives us improved means of estimating the tree and stand growth in different conditions.

The present results concerning the variation of regularities in tree structure need still to be confirmed. The studies by Berninger and Nikinmaa (1995) and Berninger et. al. (1995) with a larger data set partially using the same results as in this study support our observations. On the other hand a larger dataset collected from southern Finland demonstrated that there was not a similar range of variation as observed here (Ärölä and Nikinmaa, unpublished results). However, if structural variation is a more general trend it opens up a new opportunity to introduce geographical aspects into growth models utilizing pipe model theory.

References

Albrektson, A. 1984. Sapwood basal area and needle mass of Scots pine (Pinus sylvestris L.) trees in central Sweden. Forestry 57(1): 35–43.

Aloni, R. 1987. Differentiation of vascular tissues. Ann. Rev. Plant Physiol. 38: 179–204.

— 1991. Wood formation in decidious hardwood trees. In: Raghavendra, A. (ed.). Physology of trees. John Wiley & sons, New York. p. 175–197.

Assmann, E. 1970. The principles of forest yield study. Pergamon Press, Oxford, 506 p.

Bailey, I.W. 1958. The structure of tracheids in relation to the movement of liquids, suspensions and undissolved gases. In: Thimann, K. ed., The physiology

of forest trees. Ronald Press, New York. p. 71–82.
Berninger, F. & Nikinmaa, E. (1995). Foliage area–sapwood area relationships of Scots Pine (Pinus sylvestris) trees in different climates. Can. J. For. Res. 24: 2263–2268.
Berninger, F., Mencuccini, M., Nikinmaa, E., Grace, J. & Hari, P. (1995). Evaporative demand determines branchiness of Scots pine. Oecologia 102: 164–168.
Brouwer, R. 1962. Distribution of dry matter in the plant. Netherlands Journal of Agricultural Sciences 10: 361–376.
Carlquist, S. 1988. Comparative wood anatomy: Systematic, ecological and evolutionary aspects of dicotyledon wood. Springer Verlag, Berlin-Heidelberg, 436 p.
Chavchavadze, E.S. 1979. Drevesina hvoinih. L. Nauka 192.
Dinwoodie, J.M. 1961. Tracheid and fibre length in timber: A review of the literature. Forestry 34(2): 125–144.
Denne, M.P. 1979. Wood structure and production within the trunk and branches of Picea sitchensis in relation to canopy formation. Can. J. For. Res. 9: 406–427.
Espinosa Bancalari, M.A., Perry, D.A & Marshall, J.D. 1987. Leaf area–sapwood area relationship in adjacent young Douglas fir stands with different early growth rates. Can. J. For. Res 17: 174–180.
Ewers, F.W. & Zimmermann, M.H. 1984. The hydraulic architecture of balsam fir (Abies balsamea). Physiol. Plant. 60: 453–458.
Fengel, D. 1969. The ultrastructure of cellulose from wood. Part I: Wood as the basic material for the isolation of cellulose. Wood Sci. Technol. 3(3): 203–217.
Ford, E.D. 1975. Competition and stand structure in some even-aged plant monocultures. J. Ecol. 63: 311–333.
— 1981. Can we model xylem production by conifers. In: Linder, S. eds., Understanding and predicting tree growth. Studia Forestalia Suecica, Stockholm. p. 19–29.
Gregory, S.C. 1977. A simple technique for measuring the permeability of coniferous wood and its application to the study of water conduction in living trees. Eur. J. For. Path. 7: 321–328.
Hari, P., Heikinheimo, P., Mäkelä, A., Kaipiainen, L., Korpilahti, E. & Samela, J. 1986. Trees as a water transport system. Silva Fennica 20: 205–210.
— , Kaipiainen, L., Korpilahti, E., Mäkelä, A., Nilson, T., Oker-Blom, P., Ross, J. & Salminen, R. 1985. Structure, radiation and photosynthetic production in coniferous stands. Helsinki, 233 p.
— , Kellomäki, S., Mäkelä, A., Ilonen, P., Kanninen, M., Korpilahti, E. & Nygren, M. 1982. Metsikön varhaiskehityksen dynamiikka. Summary: Dynamics of early development of tree stand. Acta Forestalia Fennica 177. 39 p.
Haskins, J.L. & Ford, E.D. 1990. Flow through conifer xylem: Modeling in the gap between spatial scales. In: Dixon, R.K., Meldahl, R.S., Ruark, G.A. & Warren, W.G. (eds.), Process modeling of forest growth responses to environmental stress. Timber Press, Portland, Oregon. p. 58–63.
Helander, A.B. 1933. Kuusen ja männyn vesisolujen pituusvaihtelut. Summary: Variations in tracheid length of pine and spruce. Puutekniikan tutkimuksen kannatusyhdistyksen julk. 14. 75 p.
Hinkley, T.M., Lassoie, J.P., Running, S.W. 1978. Temporal and spatial variations in the water status of forest trees. Forest Science, monogr. 20. 72 p.
Huber, B. 1928. Weitere quantitative Untersuchungen über das Wasserleitungssystem der Pflanzen. Jahrb. Wiss. Bot. 67: 877–959.
Ilonen, P. 1981. The development of dry matter production of young Scots Pine (Pinus sylvestris) stands. M.Sc.-thesis. University of Helsinki. Department of Silviculture. 54 p.
Ivanov, L., Silina, A., Shmur, B. & Tselniker, J. 1951. Ob opredelenii transpiratsionogo rashoda drevostoem lesa. Bot. J. 36(1): 5–20.
Kaipiainen, L., Sazonowa, T. & Tihov, P. 1981. Transpiratsionje potoki v xyleme sosni i dynamica potribljenia vlagi. Lesovedenije 2: 27–34.
— & Hari, P. 1985. Consistencies in the structure of Scots pine. In: Tigersted, P., Puttonen, P. & Koski, V. (eds.), Crop Physiology of Forest Trees. Helsinki University Press, Helsinki. p. 32–37.
Kärkkäinen, M. 1985. Puutiede (wood science, in Finnish). Sallisen kustannus, Sotkamo, 415 p.
— & Uusvaara, O. 1982. Nuorten mäntyjen laatuun vaikuttavia tekijöitä. Summary: Factors affecting the quality of young pines. Folia Forestalia 515. 28 p.
Kasimirov, N.N., Volkov, A., Sjabtshenko, S., Ivantshikov, A. & Morosova, R. 1977. Obmen veshestv i energii v sosnovyh lesah jevoropeiskogo severa. NAUKA, Leningrad, 304 p.
Kaufman, M. & Troendle, C. 1981. The relationship of leaf area and foliage biomass to sapwood conducting area in four subalpine forest tree species. For. Sci 27: 477–482.
Keane, M.G., & Weetman, G.F. 1987. Leaf area–sapwood cross-sectional area relationships in repressed stands of lodgepole pine. Can. J. For. Res. 17: 205–209.
Khilmi, G.F. 1957. Teoretitcseskaja biofisica lesa. Moscow. 245 p.
Kuuluvainen, T., Kanninen, M. & Salmi, J.P. 1988. Tree architecture in young Scots pine: Properties, spatial distribution and relationships of components of tree architecture. Silva Fennica 22: 147–161.
Larson, P. R. 1969. Wood formation and the concept of wood quality. Yale University, School of Forestry Bulletin 74. New Haven. 54 p.
Long, J.N. & Smith, F.W. 1988. Leaf area–sapwood area relations of lodgepole pine as influenced by stand density and site index. 18: 247–250.
— , Smith, F.W. & Scott, D.R.M. 1981. The role of Douglas-fir stem sapwood and heartwood in the mechanical and physiological support of crowns and development of stem form. Can. J. For. Res 11: 459–464.
Ludlow, A. R., Randle, T. J. & Grace, J. C. 1990. Developing a process-based growth model for sitka spruce. In: Dixon, R. K., Meldahl, G. A., Ruark, G. A. & Warren, W. G. (eds.). Process modeling of forest growth responses to environmental stress. Timber Press, Portland, Oregon. p. 249–262.
Mäkelä, A. 1986. Implications of the pipe model theory on dry matter partitioning and height growth of trees. J.Theor. Biol. 123: 103–120.
— 1990. Structural-functional relationships in whole tree growth: resource allocation. In: Dixon, R.K., Meldahl, R.S., Ruark, G.A. and Warren, W.G. (eds). Process Modeling of Forest Growth Responses to Environmental Stress. Timber Press, Portland, Oregon. p. 81–95.
— & Hari, P. 1986. Stand growth model based on carbon uptake and allocation in individual trees. Ecol. Modelling 33: 205–229.
Mälkönen, E. 1974. Annual primary production and nutrient cycle in some Scots Pine stands. Comm. Inst. For. Fenn. 84(5). 87 p.
McMutrie, R. & Wolf, L. 1983. Above- and below-ground growth of forest stands: a carbon budget model. Annals of Botany 52: 437–448.
Moltshanov, A. 1952. Gidrologitseskaja rol sosnovih lesov na pestsanih potsvah. Isdatelstvo ANSSR, Moskova, 487 p.
Nikinmaa, E. 1990. Application of cost-benefit principle on stand growth: A carbon budget model approach. Silva Carelica 15: 155–166.
— & Hari, P. 1990. A simplified carbon partitioning model for Scots pine to address the effects of altered needle longevity and nutrient uptake on stand development. In: Dixon, R.K., Meldahl, R.S., Ruark, G.A. & Warren, W.G. eds., Process modeling of Forest Growth Responses to Environmental Stress. Timber Press, Portland, Oregon. p. 263–270.
Niklas, K.J. 1986. Computer simulations of branching patterns and their implications on the evolution of plants. Lectures of mathematics in the life sciencies 18: 1–50.
Pothier, D., Margolis, H.A., Poliquin, J. & Waring, R.H. 1989. Relation between the permeability and the anatomy of jack pine sapwood with stand development. Can. J. For. Res. 19: 1564–1570.
Rudakov, V. 1979. O nesavisimosti sootnoshenija mesdu velitsinami transpiratsii i massi hvoi u sosni obiknovennoi ot pogodnih uslovi. Isvestija geografitseskogo obshestva 3(2).
Ross, J., Kellomäki, S., Oker-Blom, P. Ross, V. & Vilikainen, L. 1986. Architecture of Scots pine crown: phytometric characteristics of needles and shoots. Silva Fennica 20(2). 91–105.
Sanio, K. 1872. Über die Grösse der Holzzellen bei der gemainen Kiefer (Pinus sylvestris). Jahrb. Wiss. Bot. 8: 401–420.
Savidge, R.A. 1991. Seasonal cambial activity in Larix lariciana saplings in relation to endogenous indol-3-ylacetic asid, sucrose and coniferin. Forest Science 37(3): 953–958.
Sellin, A. 1991. Hydraulic conductivity of xylem depending on water saturation level in norway spruce (*Picea abies* (L.) Karst). J. Plant Physiol. 138: 466–469.
Shinozaki, K., Yoda, K., Hozuni, K. & Kira, T. 1964 a. A quantitative analysis of plant form – The pipe model theory I Basic analysis. Jap. J. Ecol. 14: 97–105.
— , Yoda, K., Hozumi, K. & Kira, T. 1964 b. A quantitative analysis of plant form – the Pipe Model Theory. II. Further evidence of the theory and its application in forest ecology. Jap. J. Ecol. 14: 133–139.
Siau, J.F. 1984. Transport processes in wood. Springer-Verlag, Berlin-Heidelberg, 211 p.
Tirén, L. 1926. Om barrytans storlek hos tallbestånd. Med. Stat. Skogsfors. Anstalt. 23: 295–336.

Tyree, M.T., Flanagan, L.B., & Adamson, N. 1987. Response of trees to drought. In: Hutchinson, T.C. & Meema, K.M. (eds.). NATO ASI Series, Vol G16. Effects of atmospheric pollutants on forests, wetlands and agricultural ecosystems. Springer-Verlag, Berlin–Heidelberg. p. 201–216.

— & Sperry, J.S. 1989. Vulnerability of xylem to cavitation and embolism. Annu. Rev. Plant Phys. Mol. Bio. 40: 19–38.

Valentine, H.T. 1985. Tree-growth models: derivations employing pipe model theory. J. Theor. Biol. 117: 579–584.

Vite, J.P. & Rudinsky, J.A. 1959. The water conducting system in conifers and their importance to the distribution of trunk injected chemicals. Contrib. Boyce Tompson Inst. 206: 27–38.

Vysotskaya, L.G., Shaskin, A.V. & Vaganov, E.A. 1985. Analyses of the size distribution of tracheids in the annual rings of pines growing under various moisture conditions. (Translation from Ekologiya 1: 35–42, January–February). Planum Publishing Corporation.

Waring, R., Schroeder, R. & Ohren, R. 1982. Application of the pipe model theory to predict canopy leaf area. Can. J. For. Res. 12: 556–560.

Whitehead, D. 1978. The estimation of foliage area from sapwood basal area in Scots pine. Forestry 51: 137–149.

Ylinen, A. 1952. Über die Mechanische Schaftformtheorie der Bäume. Silva Fennica 76: 1–50.

Zimmermann, M.H. 1983. Xylem structure and the ascent of sap. Springer Verlag, Berlin, Heidelberg, 193 p.

— & Brown, C.L. 1971. Trees: structure and function. Springer Verlag, Berlin-Heidelberg, 336 p.

6 Stand Model

Eero Nikinmaa and Pertti Hari

6.1 General

The results in previous chapters have shown that there are geographic variations both in the functions and structure of scots pine. However, they cannot be used directly to predict the growth and development of the trees of this species in different climatic conditions. As outlined in the introduction, the environment, material exchange processes, internal metabolic processes and the structure of trees are interconnected, producing the long-term growth and development of the tree. The spatial and temporal time scale of these different aspects of tree growth can be very different, so that special analyses of the whole system is needed. Such an analysis should be detailed enough to include the species specific characteristics but general enough to allow regional modifications to be made without having to alter the fundamental characteristics of the system.

A natural starting point to analyse the growth of a whole plant are its mass and energy balances. We chose carbon budget since carbon is the main element in organic material (about 50 % of scots pine dry weight (Linder and Axelsson 1982)). On the other hand carbon is an indirect measure of fixed energy and also of its use (Chapin III 1989). The selection of carbon as the main substance for the mass balance was facilitated by the considerable knowledge of the processes of carbon fixation and the behaviour of light in the canopy among our research group (Chapters *2–4*, Nilsson 1977, Ross 1981, Hari et al. 1985, Hari et al. 1986a, Oker-Blom 1986, Oker-Blom et al. 1991).

Apart from carbon, the water and nutrient flows are important determinants of growth. Each of these flows is governed by processes that take place on very different time scales. For example, photosynthesis responds to very rapid changes in the photon flux density but simultaneously there seems to be a strong seasonal component involved (see Chapters 2, 3 and 4). The instantaneous reactions affect transpiration which is the driving force for water transport and uptake. However, it seems that beyond this rapid variation there are regularities between the structure of trees and the water flows through the system over extended periods of time, which can reflect much more aggregate acclimatization to prevailing conditions (see Chapter 5).

Rather than trying to model all the rapid processes that lead to growth in detail, we focused our modelling attempts in more detail to describe the acclimatization of trees to the prevailing environment through changes in their structure. We assumed that the functions of different structures depend on their environment. On the other hand, we assumed that the local environment would consist of some external component that could be given as a driving variable or parameter and of an internal interaction component that depends on the growth and development of the stand. It would then be changes in the parameter values of the external environment and the description of the internal interaction that would eventually bring about the variable growth in different regions.

The kind of model structure can naturally be realized in several ways. In our approach, we assumed that growth would be distributed so that the nutrient and carbon balances would hold simultaneously, ie. carbon and nutrient intake would correspond to consumption. To simplify the treatment of resource distribution, carbon and nutrient balances were related by assuming a constant ratio between carbon and nutrients in the tissue. The effects of water on growth were assumed by taking the regular connections between different parts of tree in agreement with the pipe model approach as given.

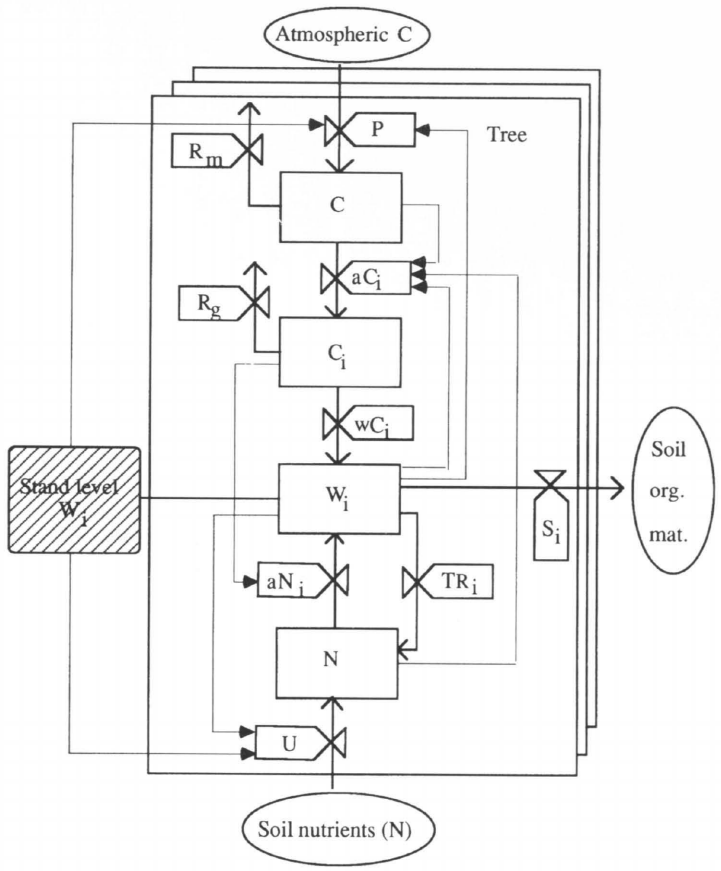

Fig. 6.1. Schematic representation of the model with its main interactions. C stands for the carbon pool of the plant, C_i is the carbon in biomass compartment i, W_i is the dry matter of the biomass compartment i, N the nutrient pool of the plant, P the carbon uptake, U the nutrient uptake, a the allocation, w the conversion efficiency of carbon into structure, R_m the maintenance respiration, R_g the growth respiration, TR_i is the nutrient retranslocation from biomass compartment i and S_i is the senescence of biomass compartment i.

The material exchange between the plant and its environment was calculated at the annual level. The values for the annual quantities of materials exchanged through unit mass of exchange surface were derived from both empirical studies (e.g. Mälkönen 1974, Korpilahti 1988) and separate sub-models to derive those which could be used (e.g. Hari et al. 1991, see also Chapter 2). The effect of organ position within the plant community on its functions as the light climate varies was also based on empirical studies (Kellomäki et.al. 1979). A schematic presentation of the model is given in Fig. 6.1.

The model has been constructed basically in three steps. In the first version, the structure of a stand and the carbon uptake of a tree in a stand was modelled (Hari et al. 1982, Mäkelä and Hari 1986). The carbohydrate distribution for the formation of the tree was then improved in several model versions (Hari et al. 1985, Mäkelä 1986, Mäkelä 1988, Hari et al. 1989, Mäkelä 1990, Nikinmaa and Hari 1990, Nikinmaa 1990). Finally, the nitrogen budget and uptake is described more explicitly in the present version together with some modifications on the distribution of growth.

Originally the stand model was developed for

sandy soil conditions in Central Finland and Karelia, since our main experimental sites were in this region. We make the first attempt to expand the model to cover the whole scots pine growing area by introducing the dependence of the parameter values describing the functions and structure on geographical location.

6.2 Stand Structure

At least as important a question as the temporal scale of the model is that of its spatial resolution. The scaling from one hierarchy level to another is one of the major problems in analysis of ecosystem structures and function (e.g. Hari 1980, de Wit 1982b, Schmidt et al. 1989, Sprugel et al. 1991). As a rule of thumb, all the main interactions affecting the system should be included, but there should be minimal interaction between the system and those aspects which are used as driving variables in the model (de Wit (1982a)).

Our objective was to analyse growth and development of Scots pine at the stand level in different regions. The main interactions between individuals in plant populations such as tree stands are caused by the resource depletion which various plants or plant parts create as they grow. Thus one would need to model the population as the sites of resource acquisition and their effect on resource availability to be able to describe the population dynamics (e.g. Hari et al. 1982, Ford and Sorrensen 1992). The tree was selected as the basic unit of the stand model.

The simplest alternative is to derive mean tree values from stand level calculations using allometric rules (Mohren 1987). Huston et al. (1988), on the other hand, suggested that models operating at the level of individuals would be more realistic since they can include both genetic and environmental variation between individuals. They also maintain that organisms are primarily affected by the local interactions with other organisms. The first option is insufficient to describe the dynamics of tree size distribution in the stand, which is interesting from the management point of view, while the latter results in a complicated solution. The concept of size classes provides a solution that can describe the essential of size distribution dynamics without resulting in very complicated model structures.

It was assumed that there is no horizontal variation between trees in their growing conditions in the size class approach. In other words, the spatial interactions are reduced to one dimension. The position of a tree within a stand would then be determined solely by the vertical position of its crown in the canopy. It is also assumed that the soil conditions are homogeneous.

Let us assume that the stand is formed by several size classes. Let Y_i denote the dry mass of plant compartment i and let subscripts *n, b, s, c, r* stand for needles, branches, stem, coarse roots and fine roots. Let N_l denote the number of trees per unit stand area in the l^{th} size class and X_i^l the dry mass of the plant compartment i of the tree in the size class l. The stand level and tree level are related as follows:

$$Y_i = \sum_l N_l X_i^l \qquad (6.1)$$

where $i = n, b, s, c, r$.

To describe the vertical position of the tree crowns one has also to model the height and the height of the crown base of each tree and the needle distribution between these points. It was assumed that the shape of the needle biomass height distribution does not change during stand development. This distribution was described by the following Eq. (Kellomäki et al. 1980):

$$\chi_m^l = C\left(\frac{h^l - z}{h^l - l_{cb}^l}\right)^p \left(\frac{z - l_{cb}^l}{h^l - l_{cb}^l}\right)^q \qquad (6.2)$$

where $\chi_m^l(z)$ is the needle biomass of a tree of size class l in a unit layer at height z (kg DM $m^{-1}tree^{-1}$), h (m) is the height of the tree, l (m) is the pruning limit height, p and q are parameters. Parameter C is a scaling factor to guarantee that the integral of Eq. (6.2) between h and l_{cb} equals the needle mass of the tree (X_n) (Hari et al. 1982). The height growth and pruning limit height change are described later on.

6.3 Carbon Balance of the Stand

We wanted to study the long-term interaction between ambient resource availability and stand growth and development. For those reasons the

analyses were focused at the annual level. As mentioned in the introduction this decision forced us to make certain assumptions about the functioning of forests. First, the model assumes that the carbon uptake by unit needle mass and the nutrient uptake by unit fine root mass depend mainly on the environment. We also assumed that the stand effects on the environment of a single exchange organ and the size of the effect can be estimated from the total number of exchanging organs in the stand at the beginning of each year. The annual material exchange could then be calculated from the ambient conditions and the biomasses of the exchanging organs and their position within the stand. In this approach the major systematic changes to material exchange per exchange site at annual level would be caused by changing relative position due to stand growth. On the other hand, the stand growth would be determined by the material uptake of individual trees represented by the size classes and how these resources are distributed among the different organs of the plant. In what follows we shall treat each of these components of these interactions in detail and derive a dynamic model of stand growth.

The mass of each plant compartment changes through growth and senescence. Let G_i denote the annual growth and S_i the annual senescence of plant compartment i. The masses of successive years of each size class are related as follows (in kg):

$$X_i^l(k+1) = X_i^l(k) + G_i^l(k) - S_i^l(k) \tag{6.3}$$

where $i = n, b, s, c, r$.

The dynamic carbon balance of a stand can now be expressed as follows:

$$Y_i^l(k+1) = \sum_l (N_l(k) + \Delta N_l)(X_i^l(k) + G_i^l(k) - S_i^l(k)) \tag{6.4}$$

where ΔN_l is the change in the number of stems per unit stand area during year k.

In what follows the changes taking place at tree level are treated first. This is followed by the treatment of the changes in the number of stems. For the sake of clarity, the size class index is omitted from Eqs. when only tree level changes are treated.

Let P denote the annual photosynthetic production of a tree (kg C tree^{-1}), R the annual maintenance respiration of already existing parts (kg C tree^{-1}), a_i the allocation coefficients of photosynthetic production to different plant compartments and w_i the conversion efficiency of carbon to structure (kg DM (kg C)$^{-1}$). We can now express new growth as:

$$G_i(k) = a_i(k)\omega_i(k)(P(k) - R(k)) \tag{6.5}$$

where $i = n,b,s,c,r$

Requiring the conservation of mass and assuming that there is no storage of carbohydrates at annual bases (ie. $\sum a_i(k) = 1$) we get:

$$\sum_i G_i/\omega_i = P(k) - R(k) \tag{6.6}$$

In other words, it is also assumed that carbon which is not used for respiration is used for growth at annual bases.

In the next section the different components of growth are treated separately. First, the modelling of carbon inputs and outputs is described followed by the description of how the carbon is distributed between various organs. This section includes simple formulations for nutrient and water balance. After growth, the modelling of senescence is described and finally an outline of how the geographical aspects should be treated is discussed.

6.4 Photosynthetic Production

6.4.1 The Photosynthetic Production of a Tree

The leaf and shoot level results of Chapter 3 should be converted to tree level in order to be able to utilize them in the construction of the stand model. The linkage between photosynthetic rate and the photosynthetic production of a tree per year is obtained by integrating the spatially and temporally variable photosynthetic rate over crown volume, V, and growing period

$$P(k) = \int_v \chi(x) \int_{t_k}^{t_{k+1}} p(x,t)\, dt\, dv \tag{6.7}$$

where $\chi^{(x)}$ is the three-dimensional needle area distribution of a tree (m^2/m^3) and $p(x,t)$ the photosynthetic production in the point x within the canopy (v) at time t.

In this chapter we calculate annual photosynthetic production of a tree as a function of its foliage height distribution, potential annual production of a Scots pine needle without shading effect and the total shading effect which the trees of the stand exert on the foliage of the tree in question. This simplification is possible because irradiance explains a high proportion of the momentary variation in the photosynthetic rate within a stand (Chapter 3). For the treatment of the shading effect in photosynthesis, we introduce a concept termed interaction.

6.4.2 Measure of Interaction

Eq. (6.7) for the annual photosynthetic production by a tree can be reformulated as follows:

$$P(k) = \int_{t_k}^{t_{k+1}} p(x_0,t)\, dt \int_V \chi(x) \frac{\int_{t_k}^{t_{k+1}} p(x,t)\, dt}{\int_{t_k}^{t_{k+1}} p(x_0,t)\, dt} dV \tag{6.8}$$

where x_o is a point located at the top of the canopy.

The first integral in this Eq. corresponds to the annual photosynthetic production in unshaded conditions per unit area of leaves. Let us denote this by P_0 (kg C m^{-2}). The ratio of the two integrals is a measure of the change in photosynthetic production caused by interactive shading. For this reason, let us define the degree of interaction, t, as follows :

$$\tau(x) = \frac{\int_{t_k}^{t_{k+1}} p(x,t)\, dt}{\int_{t_k}^{t_{k+1}} p(x_0,t)\, dt} \tag{6.9}$$

The instantaneous rates of photosynthesis at different heights within the canopy are largely determined by irradiance, I. It is then assumed that other environmental factors mainly affect the unshaded photosynthetic rate (see Chapter 3) and not the shape of the photosynthesis light response curve. This simplification allows us to further develop Eq. (6.9):

$$\tau(x) = \frac{\int_{t_k}^{t_{k+1}} \frac{I(x,t)}{I(x,t)+\alpha}\, dt}{\int_{t_k}^{t_{k+1}} \frac{I(x_0,t)}{I(x_0,t)+\alpha}\, dt} \tag{6.10}$$

This integral only includes integration of irradiance over time.

6.4.3 Homogeneity Assumption

In a horizontally homogeneous canopy, the degree of interaction depends only on the shading leaf area above the point under consideration. Let $\chi^l(z)$ denote the needle area in unit depth layer of tree size class l at the height z. The homogeneity assumption permits us to simplify the treatment of interactions. The shading leaf area, $LAI(z)$ above height z per unit ground area is now:

$$LAI(z) = \sum_l N_l \int_z^{h_{max}} \chi^l(z)\, dz \tag{6.11}$$

The relationship between the shading leaf area index LAI and the degree of interaction can be determined empirically, as in Fig. 6.2 (Kellomäki et al. 1979). Let h_{max} and l_{min} denote the maximum and minimum heights in the canopy and $\tau^*(z)$ the empirically defined degree of interaction as a function of canopy height (see Fig. 6.2).

$$P^l(k) = P_0 \int_{l_{min}}^{h_{max}} \chi^l(z)\tau^*(z)\, dz \tag{6.12}$$

This expression enables the photosynthetic production of the trees to be modelled as a function of interaction between them which is derived from stand structure. This plays a fundamental role in generating the differences in the development of the various size classes.

Hari et al. (1982) provide the interaction curve at biomass bases. Their formulation has been simplified by Sievänen (pers. comm.) in the following form:

$$\tau_m^*(z) = \frac{1.}{1.+0.026\, B(z)^{0.58}} \tag{6.13}$$

where $\tau_m^*(z)$ is the interaction determined on needle mass bases at height z and $B(z)$ is the foliage biomass of the stand per unit area in the layer (h_{max},z) (kg DM m^{-2}).

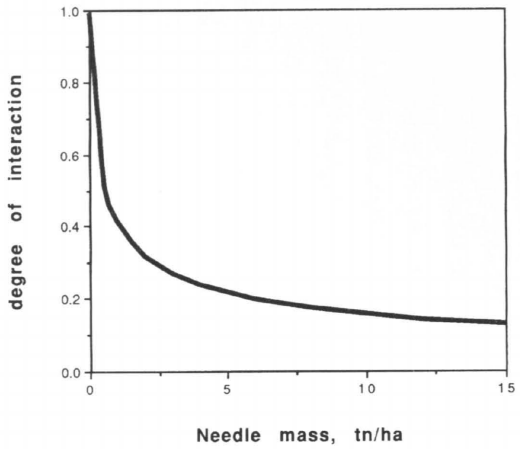

Fig. 6.2. The regression of degree of interaction on shading leaf area according to Eq. (6.13)

The latter is calculated similarly to $LAI(z)$:

$$B(z) = \sum_l N_l \int_z^{h_{max}} \chi_m^l(z)\, dz \qquad (6.14)$$

where $c_m{}^l(z)$ is the needlemass height distribution of size class l tree, giving the photosynthetic production of a tree in size class l:

$$P^l(k) = P_0 \int_{l_{min}}^{h_{max}} \chi_m^l(z)\, \tau_m^*(z)\, dz \qquad (6.15)$$

where P_0 is the photosynthetic production in unshaded conditions per unit mass of needles (kg C (kg DM)$^{-1}$).

In this paper no attempt is made to integrate the annual photosynthetic production per unit mass of needles, P_0, from the momentary photosynthetic rates. For example the approach of Korpilahti (1988) and Hari et al. (1991) could be used. We use P_0 as a driving variable from the photosynthetic field measurements and Korpilahti's (1988) climatic data. The photosynthetic production model closely resembles the structure formulated by Hari et al. (1982). The issues introduced in chapter 4 were not considered in this version of the model. However, their implications for the results are discussed later in this work.

6.5 Respiration

There are two main types of process releasing carbon dioxide in trees, ie. the maintenance of living organisms and transformation of carbohydrates into structure. The first component of carbon dioxide release is often called maintenance respiration and the second growth respiration. Growth respiration is derived from the theoretical calculations based on the structure and composition of different chemical compounds and how much energy is required to build them up (Penning de Vries et al. 1974). If the chemical composition of various plant organs is known, it is possible to calculate the conversion efficiency of carbon into structure (w_i) and also to calculate the annual growth respiration parameters (r_{gi}) (kg C kg DM^{-1}). The growth respiration for the whole tree, R_g (kg C tree^{-1}) can be calculated by using the proportional amounts of different tissues and their growth respiration rates (e.g. Mohren 1987):

$$R_g = \sum_i r_{gi} G_i \qquad (6.16)$$

where i = n, b, s, c, r.

The maintenance respiration of a tree, R_m (kg C tree^{-1}), is also tissue type specific and is mainly determined by the protein turnover rate in the tissue (Penning de Vries 1975). If the protein content of different organs is known, then it is possible to approximate their average maintenance respiration rates (see e.g. Mohren 1987). This results in a form approximating growth respiration. The maintenance respiration of the existing structure of a tree can be calculated as follows:

$$R_{mi} = \sum_i r_{mi} X_i \qquad (6.17)$$

where i = n, b, s, c, r.

One uses the total mass of plant compartments (X_i) instead of new growth (G_i) to calculate the annual maintenance respiration.

The specific maintenance respiration rate is determined by the rates of metabolic processes. Since the biochemical reactions usually depend exponentially on temperature, the maintenance respiration rate can be assumed to have similar

dependence on temperature. It is assumed that 10 degrees increase in the temperature doubles the respiration rate (Penning de Vries 1975). Annual respiration rates are obtained by integrating the temperature effect over the year:

$$r_{mi} = r_{mi}^* \frac{\int_{t_k}^{t_{k+1}} 2^{(T(t)-TB)/10^\circ C}\, dt}{t_{k+1} - t_k} \qquad (6.18)$$

where i refers to the symbols n, b, s, c and r and r_{mi}^* is the respiration rate at the base temperature chosen (kg C kg DM^{-1} h^{-1}), TB is the base temperature (°C), $T(t)$ is the momentaneous temperature at time t (°C), t_k is the beginning of a year and t_{k+1} is the end of the year.

6.6 Growth

6.6.1 General Principles

The growth of the various plant compartments of a tree is based on the functional balance principle (Brouwer 1962). A balance is assumed to exist between the needles and the roots responsible for nutrient uptake when the nutrient requirement of growth is matched by nutrient uptake and relocation from senescing structures. In other words it is assumed that the total quantity of nutrients in plant is the sum of a product between the masses of plant compartments and their nutrient concentrations which are assumed to be constant but specific to each compartment (e.g. Mälkönen 1974). It is further assumed that nutrients are taken up from the soil in fixed proportions and that it is actually nitrogen availability that dominates the growth response.

The woody structure is assumed to be balanced when regular but not necessarily equal ratios exist between the sapwood cross-sectional areas of the different tree parts and the needle biomass at the end of the pipe. (see Chapter 5).

6.6.2 The Needle Mass–Fine Root Ratio

The total amount of nitrogen in a plant is the sum of nitrogen concentrations of plant compartments times their mass. The change in the plant nitrogen content, ie. uptake minus loss, is the sum of the changes in the sizes of plant compartments times their concentration. Nitrogen uptake is naturally proportional to growing fine roots in soil but nitrogen loss is somewhat more problematic to describe. It is related to the senescence of various plant compartments but it seems that also considerable leaching of nutrients takes place from foliage (Mälkönen 1974, Helmisaari and Mälkönen 1989) Furthermore, a considerable proportion of nutrients is relocated from the senescing structures back to use by other parts of the tree (e.g. Helmisaari 1990). If we assume that relocation takes place only from senescing needles we can describe the balance assumption as follows

$$U - L = e_r(G_r + X_r - S_r) - \sum_j \pi_j S_j - (1 - u_n)\pi_n S_n = \sum_i \pi_i (G_i - S_i) \qquad (6.19)$$

where j = b, s, c, r and i = n, b, s, c, r , U and L are the nitrogen uptake and loss respectively, of a tree (kg N tree^{-1}), e_r is the biomass specific annual nitrogen uptake (kg N kg DM^{-1}), π_i is the nitrogen concentration in plant compartment i (kgN kg DM^{-1}), and u_n is the proportion of nitrogen relocated from senescing needles.

This simplifies into

$$e_r(G_r + X_r - S_r) + u_n \pi_n S_n = \sum_i \pi_i G_i \qquad (6.20)$$

where i = n, b, s, c, r.

The fine roots can interact with each other, while the fine root density increases in the soil (Fitter and Hay 1987). This phenomenon is taken into account by assuming that nutrient uptake is directly proportional to the mass of fine roots if the fine root density, F_d, (kg/m^2), is below threshold value D_r and at root densities exceeding this threshold value the efficiency of roots is determined by a negative exponential function on the mass of fine roots as follows:

$$e_r = \begin{cases} e^*{}_r, & \text{when } F_d \le D_r \\ e^*{}_r e^{-k_r(F_d - D_r)}, & \text{when } F_d > D_r \end{cases} \qquad (6.21)$$

where $e^*{}_r$ is a parameter describing the fine root mass specific annual nitrogen uptake (kg N kg DM^{-1}) without competition. and k_r is a parameter describing the slope steepness in the decrease of

nutrient uptake efficiency by fine roots due to resource depletion by the uptaking organs (m^2 kg^{-1}).

Most of the nutrients are taken up by the youngest fine roots due to changes in the root morphology as they age and because of the inefficient transport processes in soil which facilitate resource depletion around the uptaking roots (e.g. Nye and Tinker 1977, Clarkson and Hanson 1980, Clarkson 1985). For these reasons it was assumed that the root senescence equals the standing biomass (ie. $X_r - S_r = 0$) and we can simplify the annual uptake further

$$U = e_r G_r \tag{6.22}$$

Now we can rearrange Eq. (6.20) and we get an expression for fine root growth as a function of growth of other plant compartments, their nitrogen concentration, the fine root mass specific nitrogen uptake rate and the relocation of nitrogen from senescing foliage.

$$G_r = \frac{\sum_j \pi_j G_j - u_n \pi_n S_n}{e_r - \pi_r} \tag{6.23}$$

where $j = n, b, s, c$.

6.6.3 Formation of Wood Structure

Chapter 5 demonstrates that there are quantitative relationships between the components of a tree. The foliage biomass of a branch (X_{nb} in Fig. 6.3) and the cross-sectional area of the branch at the base of its crown (A_b) seem to be linearly correlated. The total branch cross-sectional areas (SA_b) of the tree crown and the stem cross-sectional area at the base of the living crown (A_s) are linearly correlated. Thus the total foliage biomass of the crown (X_n) is also linearly related to stem cross-sectional area. In addition, the total cross-sectional area of transport roots (SA_c) and the stem cross-sectional area at crown base (A_s) seem to be linearly related (Fig. 6.3). These regularities of structure can be used to derive the growth of woody structure as a function of foliage growth (see Hari et al. 1985, Valentine 1985, Mäkelä 1986, 1988).

The new thickening growth of branches, stem and transport roots can be derived from the new growth of foliage assuming that a regular ratio between the number of needles and the cross-sectional area of wood supplying them with water subsists and that this relationship remains unchanged from year to year (see also Mäkelä 1986, Valentine 1985). The derivation of the above relationship follows the lines descibed by Mäkelä (1986).

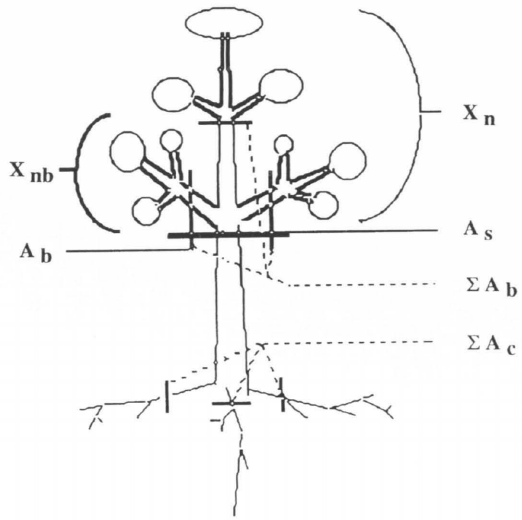

Fig. 6.3. The division of the tree into foliage, branches, stem and transport roots. A_b, A_s and A_c stand for branch, stem and transport root cross-sectional areas respectively, W_n for the foliage mass of the whole tree and W_{nb} for the foliage mass of one branch.

The cross-sectional area of water-transporting wood is a function of foliage mass:

$$A_{sw} = \alpha_{sw} X_n \tag{6.24}$$

By multiplying the sapwood area, A_{sw}, by the length of the water-conducting path, l_{sw}, and the wood density, γ_{sw}, we get the biomass of the water-transporting wood

$$X_{sw} = A_{sw} l_{sw} \gamma_{sw} = \alpha_{sw} l_{sw} \gamma_{sw} X_n \tag{6.25}$$

We can write the growth of the stem mass of the year k+1 as a function of needle mass growth and senescence if the ratio, α_{sw}, remains constant from year to year and the role of transport path

length growth is insignificant in the annual wood growth

$$G_{sw} + X_{sw} - S_{sw} = \alpha_{sw} \gamma_{sw} l_{sw} (G_n + X_n - S_n) \tag{6.26}$$

and from this we get

$$G_{sw} = \alpha_{sw} \gamma_{sw} l_{sw} (G_n - S_n) + S_{sw} \tag{6.27}$$

From the empirical work it became clear that the ratio between the water transporting wood cross-sectional area and the foliage biomass is very different in branches, stem and transport roots (see Chapter 5 and Hari et al. 1986a, see also Figure 6.3). We must therefore write Eq. (6.27) separately for all these components (ie. G_{sw}= G_b+G_s+G_c), obtaining

$$G_b = \alpha_b \gamma_b l_b (G_n - S_n) + S_b \tag{6.28}$$

$$G_s = \alpha_s \gamma_s h_{med} (G_n - S_n) + S_s \tag{6.29}$$

$$G_c = \alpha_c \gamma_c l_c (G_n - S_n) + S_c \tag{6.30}$$

6.6.4 The Distribution of Growth

It is possible to calculate the growth based on the carbon balance and the growth Eqs. of various organs. To simplify the notation let us write:

$$T_i = \alpha_i \gamma_i l_i \tag{6.31}$$

for i = b,s,c ie. for branches, stem and coarse roots. We can now substitute the expressions from eqs (6.28–30) for G_b, G_s and G_c into Eq. (6.23) to get the fine root growth as a function of foliage growth, nutrient uptake efficiency and senescence of different plant compartments:

$$G_r = \frac{\left(\pi_n + \sum_i T_i \pi_i\right) G_n - \left(u_n \pi_n + \sum_i T_i \pi_i\right) S_n + \sum_i S_i \pi_i}{e_r - \pi_r} \tag{6.32}$$

We can rearrange Eq. (6.5) as follows:

$$G_n \omega_n^{-1} = (P - R) - (G_b \omega_b^{-1} + G_s \omega_s^{-1} + G_c \omega_c^{-1} + G_r \omega_r^{-1}) \tag{6.33}$$

We can substitute G_b, G_s, G_c and G_r in Eq. (6.33) with expressions from Eqs. (6.28–30) and (6.32). Now we have foliage growth, G_n, as a function of net annual photosynthetic production, senescence of different plant compartments, transport path length and nutrient uptake efficiency. Since the growth of all other biomass compartments depends on the foliage growth, we can write the growth of the whole tree using Eqs. (6.28) to (6.30), (6.32) and (6.34).

$$G_n = \frac{(P - R) + S_n \left(\sum_i T_i \omega_i^{-1} + \frac{\pi_n u_n \omega_r^{-1} + \omega_r^{-1} \sum_i \pi_i T_i}{e_r - \pi_r} \right) - \left(\sum_i S_i \omega_i^{-1} - \frac{\omega_r^{-1} \sum_i \pi_i S_i}{e_r - \pi_r} \right)}{\left(\omega_n^{-1} + \left(\sum_i T_i \omega_i^{-1} + \frac{\pi_n \omega_r^{-1} + \omega_r^{-1} \sum_i \pi_i T_i}{e_r - \pi_r} \right) \right)} \tag{6.34}$$

where i=b, s, c.

As can be seen from Eq. (6.34), when either the pipe cost per unit length increases or pipe length increases, the relative significance of foliage senescence also increases (both increase the value of T). When the nutrient uptake rate is low (ie. low e_r–π_r value), the senescence of both foliage and other structures have more importance com-

pared with the production. The influence of nutrient relocation from the dying needles on foliage growth is also higher when the nutrient uptake rate per unit mass of fine roots is low. Increased foliage senescence would generally tend to increase allocation to needles while increased senescence of the woody component would decrease it.

6.6.5 The Length of Different Organs

6.6.5.1 Average Lengths

For the sake of simplicity we use only the average length of branches, stem and transport roots in the model structure. The average height of the stem (h_{med}) was calculated as the average height of the needle mass of the crown. The average height is then

$$h_{med} = \frac{\int_{l_{cb}}^{h} \chi_m(z) z\, dz}{X_n} \qquad (6.35)$$

where $\chi_m(z)$ is the height distribution of the needle mass of a tree (see Eq. 6.2), h is the tree height and l_{cb} is the crown base height. The height growth and pruning limit height growth are needed to calculate the average tree height. However, for the transport roots and branches only average lengths are used so that the length growth of these organs in the model was the growth of average length of branches and transport roots.

6.6.5.2 Height Growth

It was assumed that the height growth of the tree depended linearly on the diameter growth when trees were growing in open conditions without interaction between them (Ek 1971). The light competition from neighbouring trees was assumed to increase this ratio (Kellomäki and Kanninen 1980). The amount of increase depended on the steepness of the light gradient between the centre of the upper third of the crown and that of the lower third. The above considerations yielded following Eq.:

$$\Delta h = \Delta d_s(\beta_{hd} + DI) \qquad (6.36)$$

where Δh is height, Δd_s the diameter growth of a tree (both in m), b_{hd} is the ratio between height and diameter in open-grown trees and DI is the increase in height growth relative to diameter growth resulting from stand density.

The diameter growth of the stem (Δd_s) follows directly from the structural regularities. The new diameter must fulfil the requirements specified in section 6.6.3. Thus the stem area growth must be proportional to a) the change in the foliage biomass of the tree above the point of reference and b) the conversion of sapwood into heartwood. In Eq. (6.37) the senescence of foliage and sapwood to heartwood turnover are related to give variable RL_{bs}. It gives directly the amount of senescing folige that releases transport structure to reuse, ie. the amount of new sapwood required is the difference between foliage growth and this released sapwood multiplied by the proportionality coefficient a_s. The derivation of RL_{bs} is described in Eq. (6.50). Now by adding the new area to the existing area we can also get the diameter growth assuming a circular cross-section for stems

$$\Delta d_s = \left(\sqrt{\frac{(G_n - RL_{bs})\alpha_s + \frac{\pi d_s(k)^2}{4}}{4\pi}} \right) - d_s(k) \qquad (6.37)$$

The density effect (DI) is assumed to be mediated by the difference in the light gradient of the tree crowns in different size classes. In very shaded or very open conditions, the light gradient is small, so that height growth is supressed. In dense, even-aged stands, on the other hand, the light gradient can be very steep and the height growth relative to diameter growth is accelerated. The following Eq. was used to describe this:

$$DI = \frac{\beta_l(e^{-kB(lu)} - e^{-kB(ll)})}{h - l_{cb}} \qquad (6.38)$$

where b_l is the light gradient steepness multiplier (m) and lu and ll are the centre points of the upper and lower thirds of the crown of a tree and k is the light extinction coefficient expressed in biomass per unit of land area.

6.6.5.3 Shoot and Root Elongation

The growth of the average length of branches was calculated similarly except that no density dependent effect existed, ie. it was assumed that the length/diameter ratio of branches would remain constant. This yielded the following Eq.:

$$\Delta l_b = \Delta d_b \beta_{ld} - l_b K_{lr} \qquad (6.39)$$

where Δl_b and Δd_b are the average length and diameter growth of branches (m), β_{ld} is the length diameter ratio of branches, K_{lr} is the reduction in the average length of branches due to self-pruning and l_b is the present average length of branches.

For the sake of simplicity the diameter growth of branches (Δd_b) was derived from their biomass growth by assuming a constant form factor for them (ie. a constant ratio between the cylinder determined by the basal area of the branch and branch length and its true volume). It was also assumed that the new extension growth is only a minor proportion of the total mass growth of branches. Now the new mass (G_b+X_b) divided by the branchwood density (γ_b) gives the total branchwood volume that has to be divided by the number of branches (n_b) to get the average volume. The average branch volume divided by the branch length (l_b) and form factor (ff) gives the new basal area of the branch, from which the diameter can be obtained assuming circular geometry. Initially, this model may overestimate the diameter growth if the average length of branches is about the same magnitude as the new length growth. However, this accelerates the branch length growth as well which results quite quickly in the situation in which the assumptions of the model hold approximately.

$$\Delta d_b = \frac{\sqrt{G_b + X_b} - \sqrt{X_b}}{\sqrt{4\pi ff \gamma_b l_b n_b}} \qquad (6.40)$$

In Eq. (6.39) the average branch length growth was calculated by adding the average length growth due to the diameter growth to the existing average branch length and by subtracting the effect of dying branches on the average length.

Since the model used the average branch length, the effect of self-pruning of tree crowns on the length also had to be considered. It is assumed that the crown consists of a conical upper part and cylindrical lower part. In the conical upper part

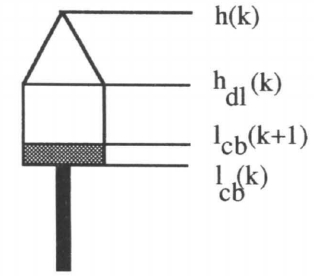

Fig. 6.4. Schematic presentation of the branch length in the tree crown. For symbols, see the text.

the branch length is proportional to the distance of the branch from the top of the tree and in the cylindrical lower part it remains constant. It is also assumed that the number of branches within the crown is proportional to its length. Self-pruning decreases the number of branches that have attained more or less constant length (see Fig. 6.4). The new average branch length is thus proportional to a) the area of a triangle formed by the height of the conical part (h–h_{dl}, where h_{dl} is the lower limit of the conical part of the crown (see Fig. 6.4)) and the maximal branch length at the bottom of the conical part and b) the area of a square formed by the maximal branch length and the height of the cylindrical part of the crown (h_{dl}–l_{cb}). Self-pruning affects the crown length and the area of the cylindrical part. Since we know the change in the pruning limit we can also calculate the new average branch length relative to the old length as follows:

$$K_{lr} = \frac{h(k)/2 - l_{cb}(k+1) + h_{dl}(k)/2}{h(k)/2 - l_{cb}(k) + h_{dl}(k)/2} \cdot \frac{h(k) - l_{cb}(k)}{h(k) - l_{cb}(k+1)} \qquad (6.41)$$

The number of branches per tree crown (n_b) was calculated assuming that it was proportional to the length of the living crown and that each year a constant number of new branches (β_{pw}) would be formed. This yielded the following Eq.:

$$n_b(k+1) = \left(\frac{h(k) - l_{cb}(k+1)}{h(k) - l_{cb}(k)} \right) \cdot n_b(k) + \beta_{pw} \qquad (6.42)$$

where h and l_{cb} are the height of the tree and the height of the pruning limit respectively (see also Figure 6.4).

The length growth of the transport roots was calculated from the fine root density of the stand. It was assumed that the fine roots of the same tree always fill new soil volume at the same density. It was also assumed that 50 % of the new fine roots are growing in the space already occupied by the transport roots and 50 % grow into new soil volume outside the circle occupied by the transport roots in a circular fashion. From these premises the following Eq. was constructed:

$$\Delta l_c = \sqrt{l_c^2 + \frac{G_f / D_r}{2\pi}} - l_c \qquad (6.43)$$

where D_r is a parameter describing the density by which the fine roots fill new soil volume. It is also the threshold density for root competition (see Eq. 6.32).

6.6.5.4 Pruning Limit

The change of pruning limit, Δl_{cb}, is required to enable calculation of the distribution of growth as seen in the previous chapters. Apart from its importance in determining the average lengths of wood in stem and in branches to support the needles of a tree crown, the pruning limit change in our model is associated with the conversion of sapwood to heartwood. Therefore the formulation of its dynamics has considerable influence on the overall simulated growth and development of the tree stands.

We assumed that the annual photosynthetic production of the needles at the pruning limit should be at least a given proportion of the average annual photosynthetic production of the needles of the crown. The above principle was simplified from a cost-benefit formulation by Nikinmaa and Hari (1990) and Nikinmaa (1990) in which a special case of optimal distribution of foliage in the crown was assumed.

The pruning limit gets higher if the amount of light at the limit is too small to facilitate the required annual photosynthetic production, which is a given proportion of the average photosynthetic production of the crown (P/X_n). The photosynthetic production of the needles at the crown base is estimated for the sake of simplicity by an exponential function along the lines of Lambert-Beer's law (Monsi and Saeki 1953) assuming a linear photosynthetic light response. One lifts the pruning limit until the foliage layer is so thin that enough light passes through it. To simplify the treatment it is assumed in this sub-model that the amount of foliage above a certain point in the canopy is directly proportional to the distance of this point from the top of the canopy. However, it is assumed that in the shade crown where pruning takes place there is less foliage per unit layer than in the sun crown. The difference is described by parameter χ_{dr} which is the relationship between foliage mass per average unit layer in the crown and that at the crown base.

Now we have an expression for light penetrating through canopy and photosynthetic production at the crown base derived from this as a function of crown base height and an expression for the photosynthetic production required. From this we can solve the new pruning limit height change as follows:

$$\Delta l_{cb} = H_{\max} + \ln\left[\left(\frac{P}{P_0}\right)\frac{1}{\delta X_n}\right]\left(\frac{h_{\max} - l_{\min}}{\chi_{dr} k Y_n}\right) - l_{cb} \qquad (6.44)$$

where the logarithm term describes the photosynthetic production required and the term in brackets describes the light climate at the lower canopy. In the Eq., l_{cb} is the height of the pruning limit and Δl_{cb} is the change in it; $h_{\max}$ is the maximum height of the stand and $l_{\min}$ the lowest present pruning limit of the stand, P is the annual photosynthetic production of the tree in question (kg C) and P_o(kg C kg DM^{-1}) is the annual photosynthetic production of unit mass of needles in nonshaded conditions, X_n is the needle biomass of the tree (kg) and δ is a parameter giving the production requirement of photosynthesis at the crown base as compared to the crown average, χ_{dr} describes the ratio between the average needle mass per unit height in the canopy and that at the crown base.

6.7 Senescence

As can be seen from Eqs. (6.28–30, 6.32, 6.34), the determination of senescence of different plant compartments also greatly affects the new growth in the present approach. The senescence of needle biomass is a linear function of their biomass in the model ie.

$$S_n = m_n X_n \qquad (6.45)$$

where m_n is the senescence rate parameter ($1/a$). As mentioned in section 6.6.2, all the fine roots formed during a growing period would become non-functional during the same period. The above is done by equating the initial fine root mass with the annual senescence, ie.:

$$S_r = X_r \qquad (6.46)$$

The treatment of branchwood, stemwood and transport root wood senescence is a more complicated matter. "Stemwood senescence" is understood as the conversion of water-conducting sapwood into non-conducting wood which consists of the "real" heartwood and the transition zone between heartwood and sapwood. In branchwood and transport root senescence, a proportion of twigs and branches which die and become detached from the tree are also included in senescence.

For the woody structures, ie. branches, stem and transport roots, the senescence of those organs that do not die completely is calculated as the difference between the wood biomass associated with the needle biomass senescence according to the pipe model theory and the proportion of that wood biomass which is reused for water supply of existing and new needles. From these principles we can write for branches, stem and transport roots

$$S_b = (S_n - RL_{bs})\alpha_b \gamma_b l_b \qquad (6.47)$$

$$S_s = (S_n - RL_{bs})\alpha_s \gamma_s h_{med} \qquad (6.48)$$

$$S_c = (S_n - RL_c)\alpha_c \gamma_c l_c \qquad (6.49)$$

where RL_{bs} is the proportion of dying needles that release transport structure for reuse in the branches and stem and RL_c is that for transport roots (the definition of RL´s is given in Eqs. (6.50 and 6.51).

The proportion of reuse of transport structure in the stem is assumed to depend on the crown dynamics. In other words, as the empirical results of this project suggested (see section 5 and Hari et al. 1985, Kaipiainen and Hari 1985) the tree rings become non-conducting as the whorl of branches which was formed at the same time dies off. In the model this is interpreted to mean that the needle biomass which died below the new pruning limit, ($l_{cb}(k+1)$), does not release transport structure for reuse.

In older trees the above gives insufficient sapwood conversion since heartwood is also formed in the branches. So as to get the total proportion of dying needles releasing transport structure for reuse in the stem, both of these aspects have to be included. This is expressed in the model as follows:

$$RL_{bs} = (1 - m_b)\left(S_n - \int_{l_{cb}(k)}^{l_{cb}(k+1)} \chi_m(z)\,dz\right) \qquad (6.50)$$

where the multiplier m_b is the proportion of heartwood formation associated with the foliage senescence within a living crown and the second term in parentheses describes heartwood formation in the stem due to self-pruning. $l_{cb}(k)$ and $l_{cb}(k+1)$ are the pruning limit height at age k and $k+1$ and χ_m is the needle mass height distribution function (see Eq. 6.2).

It was assumed that as the average age of transport roots approaches some notional maximum, the proportion of sapwood turning into heartwood associated with foliage senescence would increase:

$$RL_c = \left(\frac{d_{cm} - d_c}{\theta + (d_{cm} - d_c)}\right) S_n l_c (1 - m_c) \qquad (6.51)$$

where d_{cm} is the maximum age of transport roots, d_c is the average age of transport roots, m_c is the proportion of needle senescence associated with heartwood formation in transport roots and θ is a parameter.

6.8 Tree Mortality

The self-thinning of stands, ie. the reduction in the number of stems per size class from natural causes is denoted by M_1. The number of stems can also decrease because of human intervention for which a parameter Th_1 is used. Then

$$N_l(k+1) = (1 - M_1(k) - Th_1(k))N_l(k) \qquad (6.52)$$

The prescribed thinnings, Th, are given functions of time for each size class. Self-thinning, M, has to be related to the dynamics of the stand. This process is not well understood, but ultimately it must be connected with the carbon balance so

that when respirational requirement surpasses photosynthetic production the tree will die. In the present approach this is approximated by the assumption that when the needle mass growth in a size class is smaller than a defined proportion of needle senescence, then natural deaths occur, ie.

$$M_l(k) = \begin{cases} m_l(t_{mr}S_n - G_n) & \text{if } G_n \le t_{mr}S_n \\ 0 & \text{if } G_n \ge t_{mr}S_n \end{cases} \quad (6.53)$$

where m_l is the mortality rate parameter (1/ kg DM tree^{-1}) and t_{mr} is the threshold parameter.

This version of the model has been written with Simnon software (Elmqvist et al. 1990). Each of whose 4 size classes has 20 state variables. The total number of parameters is 53. Appendix 6.1 presents the variable and parameter list of the model.

6.9 Final Remarks

Our main objective was to build a model which could simulate the growth of Scots pine stands in very different climatic regions. Until now we have described the core model, ie. those general, qualitative relationships between structure and function which we assume to be the same for Scots pine growing in different conditions. In the next chapter we apply the model to simulate growth and development of those Scots pine stands where the measurements resulting from this cooperative effort were made.

Our model is very simple with respect to determination of inflow and outflow. Basically, it is assumed that the environment can be described by two factors: a) the potential behaviour of the plant organ under the given conditions without competition effect and b) the competition effect due to depletion of desirable resources that causes deviations from the potential uptake. This differs from the more detailed models in that both the changes in the environment and the plants acclimation or adaptation are aggregated in the potential behaviour and in competition responses. In order to simulate the geographic performance of trees one needs to conduct a variety of measurements in a range of locations to derive both the potential behaviour and the competition effect. Alternatively, one could use more detailed models which calculate photosynthetic production under different conditions, and create a "metamodel" based on the results of these simulation runs as a function of relevant variables (Mäkelä 1990, Berninger, in print).

The present model was constructed emphasizing the balance between the detailed description of the various parts of the model. It was felt at the beginning of this work that the structural growth was the least known part. At the moment, the growth of different plant compartments is indirectly derived from process-based considerations but quite a lot more work is still needed before the functional and structural connections of wood are known in the same detail as those of needles. However, we feel that this line needs to be followed, since the xylem and phloem have a very important role in the entire tree's functioning.

Among the major tasks for improving the model in the future is a better description of the nutrient dynamics of trees and especially the interaction between soil and plant and between different nutrients. Even the present simple approach can offer some possibilities in this respect, but nutrient uptake clearly needs to be related to soil conditions before realistic, localised simulations can be done.

Despite the many problems still involved in predicting scots pine growth in different climates, we feel that the present analyses are a first step in that direction. In the following chapter´s application of the model to describing the geographic variation of the growth and development of Scots pine stand we discuss in more detail the possibilities of this approach and also try to tacle the problems involved making predictions.

References

Berninger, F., in print. Effects of drought and phenology on GPP – a simulation study along a geographical gradient. Accepted for publication in the Functional Ecology.

Brouwer, R. 1962. Distribution of dry matter in the plant. Netherlands journal of agricultural sciences 10: 361–376.

Chapin III, F.S. 1989. The cost of tundra plant structures: evaluation of concepts and currencies. Am. Nat. 133(1): 1–19.

Clarkson, D.T. 1985. Factors affecting mineral acquisition by plants. Annual review of Plant Physiology. 36: 77–115.

— & Hanson, J.B. 1980. The mineral nutrition of higher plants. Annual Review of Plant Physiology. 31: 239–298.

de Wit, C.T. 1982a. Simulation of living systems. In: Penning de Vries, F.W.T. & H.H, v.L. (eds). Simulation of plant growth and crop production. Pudoc, Wageningen. p. 3–8.

— 1982b. Coordination of models. In: Penning de Vries, F.W.T. & van Laar, H.H. (eds). Simulation of plant growth and crop production. Pudoc, Wageningen.

Ek, A.R. 1971. Size age relationships for open grown red pine. The University of Wisconsin, Forestry Research Notes 156: 4.

Elmqvist, H., Åström, K.-J., Schönthal, T. & Wittenmark, B. 1990. Simnon TM, User´s guide for MS-DOS computers. (SSPA systems, Göteborg, 1990).

Fitter, A.H. & Hay, A. 1987. Environmental physiology of plants. Academic Press, London.

Ford, E.D. & Sorrensen, K.A. 1992. Theory and models of inter-plant competition as a spatial process. In: DeAngelis, D.L. & Gross, L.J. (eds). Individual based models and approaches in ecology. Chapman and Hall, New York London p. 363–407.

Hari, P. 1980. The dynamics of metabolism in a plant community. Flora 170: 28–50.

— , Heikinheimo, P., Mäkelä, A., Kaipiainen, L., Korpilahti, E. & Samela, J. 1986a. Trees as water transport system. Silva Fennica 20: 205–210.

— , Mäkelä, A., Korpilahti, E. & Holmberg, M. 1986b. Optimal control of gas exchange. In: Luxmoore, R.L., Landsberg, J.J. & Kaufman, M.R. (eds). Coupling of Carbon, Water and Nutrient Interactions in Woody Plant Soil Systems. Heron Publishing, Victoria. p. 169–175.

— , Kaipiainen, L., Korpilahti, E., Mäkelä, A., Nilson, T., Oker-Blom, P., Ross, J. & Salminen, R. 1985. Structure, radiation and photosynthetic production in coniferous stands. Helsinki, 233 p.

— , Kellomäki, S., Mäkelä, A., Ilonen, P., Kanninen, M., Korpilahti, E. & Nygren, M. 1982. Dynamics of early development of tree stand (in Finnish). Acta Forestalia Fennica 177. 39 p.

— , Nikinmaa, E. & Korpilahti, E. 1991. Modeling: Canopy, photosynthesis and growth. In: Raghavendra, A.S. (ed). Physiology of trees. John Wiley & Sons, New York. p. 419–444.

— , Nikinmaa, E. & Mäkinen, M. 1989. The construction of European pine stand model. In: Schmidt, P., Oldeman, R.A.A. and Teller, A. (eds). Unification of European forest pattern research. Pudoc, Wageningen. p. 67–82.

Helmisaari, H.-S. 1990. Nutrient retranslocation within Pinus sylvestris. D.Sc.-thesis, University of Joensuu, Publications in Science, Joensuu. 13 p.

— & Mälkönen, E. 1989. Activity and nutrient content of throughfall and soil leachate in three Pinus sylvestris stands. Scand. J. For. Res. 4: 13–28.

Huston, M.A., DeAngelis, D.J. & Post, W. 1988. New computer models unify ecological theory. BioScience 38: 682–691.

Kaipiainen, L. & Hari, P. 1985. Consistencies in the structure of Scots pine. In: Tigersted, P., Puttonen, P. & Koski, V. (eds). Crop physiology of forest trees. Helsinki University Press, Helsinki. p. 32–37.

Kellomäki, S., Hari, P., Kanninen, M. & Ilonen, P. 1980. Ecophysiological studies on young Scots pine stands: II. Distribution of needle biomass and its application in approximation light conditions inside the canopy. Silva Fennica 14: 243–257.

— & Kanninen, M. 1980. Eco-physiological studies on young Scots pine stands: IV Allocation of photosynthates for crown and stem growth. Silva Fennica 14: 397–408.

— , Salminen, R., Hari, P., Ventilä, M., Kanninen, M., Kauppi, P. & Smolander, H. 1979. A method for approximating the photosynthetic production of stand members inside the canopy. J. Appl. Ecol. 16: 243–252.

Korpilahti, E. 1988. Photosynthetic production of Scots pine in the natural environment. Acta Forestalia Fennica 202. 71 p.

Linder, S. & Axelsson, B. 1982. Changes in carbon uptake and allocation pattern as a result of irrigation and fertilization in a young Pinus silvestris stand. In: Waring, R.H. (eds). Carbon uptake and allocation in subalpine ecosystems as a key to management. Forest research laboratory, Corvallis, Oregon. p. 38–42.

Mäkelä, A. 1986. Implications of pipe model theory on dry matter partitioning and height growth of trees. J. Theor. Biol. 123: 103–120.

— 1988. Models of pine stand development: An ecophysiological systems analysis. University of Helsinki, Department of Silviculture, Research notes 62, 267 p.

— 1990. Adaptation of light computations to stand growth models. Silva Carelica 15: 221–239.

— & Hari, P. 1986. Stand growth model based on carbon uptake and allocation in individual trees. Ecol. Modelling 33: 205–229.

Mälkönen, E. 1974. Annual primary production and nutrient cycle in some scots pine stands. Commun. Inst. For. Fenn. 84(5). 87 p.

Mohren, G.M.J. 1987. Simulation of forest growth, applied to Douglas fir stands in the Netherlands. Pudoc, Wageningen, 184 p.

Monsi, M. & Saeki, T. 1953. Über die Lichtfaktor in der Pflanzengesellschaften und seine Bedeutung für die Stoffproduktion. Japanese Journal of Botany 14:22–52.

Nikinmaa, E. 1990. Application of cost-benefit principle on stand growth: A carbon budget model approach. Silva Carelica 15: 155–166.

— & Hari, P. 1990. A simplified carbon partitioning model for Scots Pine to address the effects of altered needle longevity and nutrient uptake on stand development. In: Dixon, R.K., Meldahl, R.S., Ruark, G.A. & Warren, W.G. (eds). Process modelling of Forest Growth Responses to Environmental Stress. Timber Press, Portland, Oregon. p. 263–270.

Nilsson, T. 1977. The penetration of solar radiation into plant canopies (in Russian). Inst. Phys. Astron., Estonian Acad. Sci., Tartu.

Nye, P.H. & Tinker, P.B. 1977. Solute movement in the soil-root system. Blackwell Scientific Publications. Oxford, England, UK. 342 p.

Oker-Blom, P. 1986. Photosynthetic radiation regime and canopy structure in modelled forest stands. Acta Forestalia Fennica 197. 44 p.

— , Lappi, J. & Smolander, H. 1991. Radiation regime and photosynthesis of coniferous stands. In: Myneni, R.B. & Ross, J. (eds). Photon-vegetation interactions: applications in optical remote sensing and plant ecology. Springer Verlag, Berlin Heidelberg. p. 469–499.

Penning de Vries, F.W.T. 1975. The cost of maintenance processes in plant cell. Ann. Bot. 39: 77–92.

— , Brunstig, A.H.M. & Van Laar, H.H. 1974. Products, requirements and efficiency of biosynthesis: A quantitative approach. J. Theor. Biol. 45: 339–377.

Ross, J. 1981. The radiation regime and architecture of plant stands. Junk Publishers, The Hague, 391 p.

Schmidt, P., Oldeman, P.A.A. & Teller, A. (eds.) 1989. Unification of European forest pattern research. Pudoc, Wageningen.

Skre, O. 1991. Physiology of plant survival under cold conditions with particular reference to dark respiration as a factor limiting growth at timber line. A literature review. Commun. Skogsfors 44(1): 1–34.

Sprugel, D.G., Hincley, T.M. & Schaap, W. 1991. The theory and practise of branch autonomy. Annu. Rev. Ecol. Syst. 22: 309–334.

Valentine, H.T. 1985. Tree-growth models: derivations employing pipe model theory. J. Theor. Biol. 117: 579–584.

Appendix 6.1 Variable list of the model

Variable	Explanation	Unit
A_i	sapwood area of plant compartment i of a tree, i = b,s,c,sw	m^2
a_i	allocation coefficients of carbohydrates to plant compartment i, i = n,b,s,c,r	
$B(z)$	foliage biomass per unit stand area in layer (h_{max},z)	kg DM m^{-2}
DI	increase in height growth relative to diameter growth due to stand density	
D_r	density at which roots of a tree grow	kg DM m^{-2}
d_s	tree stem diameter at the base tree	m^2
e_r	annual nutrient uptake per unit mass of fine roots, without competition	kg N kg DM^{-1}
e_r^*	annual nutrient uptake per unit mass of fine roots, with competition	kg N kg DM^{-1}
F_d	soil fine root density per unit stand area	kg DM m^{-2}
ff	branch form factor	
G_i^l	annual growth of plant compartment i of a tree in size class l, i = n,b,s,c,r,sw	kg DM $tree^{-1}$
h	tree height	m
h_{dl}	lower height limit of the conical part of a crown	m
h_{max}	maximum canopy height	m
h_{med}	average tree stem height	m
I	irradiance	µmol m^{-2} s^{-1}
k	light extinction co-efficient (on mass bases)	1/kg Dm m^{-2}
k_r	nutrient interception decrease coefficient	m^2 kg^{-1}
K_{lr}	proportional branch length reduction due to self- pruning	
L	annual tree nutrient loss	kg N $tree^{-1}$
$LAI(z)$	cumulative leaf area index in layer (h_{max},z) per stand area unit	m^2m^{-2}
l_i	length of plant compartment i, i = b,c,sw	m
l_{cb}	lower limit of living tree crown	m
ll	centre point of the lower third of a tree crown	m
l_{min}	minimum canopy height	m
lu	centre point of the upper third of a tree crown	m
M	reduction in number of stems due to self thinning	trees m^{-2}
m_b	proportion of needle senescence associated with heartwood formation initiating in branches	
m_c	proportion of needle senescence associated with heartwood in transport roots	
m_n	needle senescence parameter	
m_t	mortality rate parameter	trees m^{-2} $kgDM^{-1}$
N_l	number of class l size trees	trees m^{-2}
n_b	number of branches per tree crown	
P_l	annual photosynthetic production of class l size tree	kg C $tree^{-1}$
P_0	annual photosynthetic production per unit leaf area in unshaded conditions	kg C m^{-2}
P_0^*	annual photosynthetic production per unit mass of leaves in unshaded conditions	kg C kg DM^{-1}
$p(x,t)$	photosynthetic production at point x at moment t	kg C m^{-3} s^{-1}
R_l	annual tree maintenance respiration	kg C $tree^{-1}$
RL_{bs}	amount of senescing needles associated with transport capacity reuse in branches and stem	kg DM
RL_c	number of senescing needles associated with transport capacity reuse in transport roots	kg DM
r_{gi}	growth respiration per unit mass of structure	kg C kg DM^{-1}
r_{mi}	maintenance respiration per unit mass of structure	kg C kg DM^{-1}
S_i^l	senescence of plant compartment i of a class l size tree, i = n,b,s,c,r,sw	kg DM $tree^{-1}$
TR_i	nutrient translocation from biomass compartment i, i=n,b,s,c,f	kg N
$T(t)$	momentary temperature at time t	°C
TB	maintenance respiration base temperature parameter	°C
t	time	s
Th_l	annual reduction of number of stems in size class due to human intervention	trees m^{-2}
t_{mr}	mortality threshold parameter	
U	tree nutrient uptake	kg N $tree^{-1}$

u_n	proportion of nutrient relocation from senescing needles	
X_i^l	plant compartment biomass i of a class 1 size tree, $i = n,b,s,c,r,sw$	kg DM tree^{-1}
Y_i	stand level biomass of plant compartment i, $i = n,b,s,c,r$	kg DM m^{-2}
α_i	ratio between the sapwood area of plant compartment i and the foliage biomass, $i = b,s,c,sw$	m^2 kg DM^{-1}
β_{hd}	height diameter ratio of open-grown trees	
β_l	light gradient steepness multiplier	m
β_{ld}	branch length diameter ratio	
β_{pw}	average number of branches per whorl	
$\chi(x)$	needle area in unit stand volume at point x	m^2 m^{-3}
χ_{dr}	ratio between average foliage mass density in the canopy and in the shade canopy	
$\chi'(z)$	needle area in a unit depth layer of a class l size tree at height z	m^2 m^{-1}tree^{-1}
$\chi_m^l(z)$	needle mass in an unit depth layer of a tree of the size class l at height z	kg m^{-1}tree^{-1}
δ	photosynthetic production requirement at the crown base relative to the crown average	
γ_i	bulk density of wood in plant compartment i, $i = b,s,c,sw$	kg m^{-3}
γ_i	nutrient concentration in plant compartment i, $i = n,b,s,c,r$	kg N kg DM^{-1}
θ	age when 50 % of the needle senescence is associated with heartwood formation in transport roots	a
τ	degree of interaction	
τ^*	empirically determined degree of interaction on leaf area bases	
τ_m^*	empirically determined degree of interaction on leaf biomass bases	

Subscripts, superscripts and indexes:

n	needles	l	size class
b	branches		
s	stem	k	year
c	coarse roots	z	height
r	fine roots	x	point
sw	sapwood		

7 Geographic Aspects of the Growth of Scots Pine; Results of Simulations

Eero Nikinmaa

7.1 Introduction

One of the main aims of our work was to predict how Scots pine stands grow in different parts of its range. The previous chapter outlined a dynamic, process-based stand growth model used for these purposes. In this chapter we use the model to simulate the growth of Scots pine stands for those locations where the empirical measurements of this project were performed (see Chapter 5) and evaluate how well the approach in Chapter 6 is able to describe stand growth and development in these conditions.

The evaluation of a process-based models is related to that of a suggested theory (e.g. Nikinmaa 1992). It is not enough that model accurately predict a single factor at any given time. Most of the process-based models are rather complicated and heavily parametrized and with a suitable fitting procedure it is possible to produce practically any single feature very realistically. A good process-based model should however be able to realistically predict the behaviour of all those components included in the analyses simultaneously.

A test of realistic behaviour incorporating as many variables as possible gives some support to the rationale of the model structure selected. Only then we are able to proceed towards more rigorous testing of how accurately a model can predict certain observed developments. This latter question relates much to the problems of describing the initial state and the local parameter values as to the model structure itself. Unfortunately, the model definition, when it is derived from theoretical considerations often includes such parameters and state variables as are not routinely measured. These problems make exact comparisons with observed values difficult, not to mention that appropriate long term measurement series from single stands are either rather rare, or are difficult to access. Formal sensitivity and uncertainty analyses can help in the evaluation of the effects of parameter values on the outcome of the simulation runs.

In this study we pay most attention to the qualitative analyses of model behaviour against the sketchy general knowledge of the geographical features of Scots pine growth. We also analyse the sensitivity of the results to the geographic variation introduced into the parameter values. The earlier analyses by Mäkelä (1988) and Sievänen (1992) have shown that a very similar approach is well able to describe stand growth for one location. In this work, as in the previous work by Nikinmaa (1992), the first attempt is made to explore a more general applicability of the approach to Scots pine growth. The model is first initialized and the geographical features are introduced into the analyses. This is followed by a description of the model behaviour for the different locations and a limited test of how well the results agree with growth and yield table information. The sensitivity of model response to key parameters follows next and, finally, the results are discussed with special emphasis on the problems of the geographical application and their potential effects on the simulation results as well as to new and interesting research questions that arise from the results.

7.2 Geographical Variation of Model Parameter Values

The Scots pine stand growth was simulated for conditions corresponding to those of Lapland, (Muddusniemi, 69°N, 27°E), Southern Finland, (Hyytiälä, 62°N, 24°E), Russian Karelia, (Petrozavodsk, 62°N, 34°E) and South Russia, (Voronez, 52°N, 40°E). The same model structure was applied to all stands. The differences between the locations were introduced into the analysis with location-specific parameter values. Long-term series of temperature data from Murmansk, Jyväskylä, Petrozavodsk and Voronez which are all situated quite close to the experimental stands were used to derive the different growing conditions for the sites. The measurements performed at the experimental sites were used to describe the architectural and structural differences in trees between locations (see Tables 7.1 and 7.2 and Chapters 5 and 6).

The functional parameters describing the process rates of the model were modified according to the growing season length of each location. The parameter values of photosynthetic production, respiration and nutrient uptake (P_0, r_{mn}, r_{mb}, r_{ms}, r_{mc}, r_{mf}, m_n and e_r^*) were derived so that the values from Hyytiälä were used as the reference values. The values for other locations were adjusted by multiplying the Hyytiälä values by the relative length of the growing season of each location with respect to Hyytiälä. The length of growing season for each location was calculated from the daily average temperatures of extended series of weather data using a threshold temperature of 5°C (see Table 7.1 and Chapter 2).

Table 7.1 The length of the growing season in different locations assuming different threshold temperatures.

Location	Length of the growing season with different threshold temperatures (days)		
	0°C	+3°C	+5°C
Murmansk	165	144	117
Jyväskylä	223	179	160
Petrozavodsk	209	169	150
Voronez	241	210	200

Actual measured values from different locations were used for the structural parameters ($\alpha_b\gamma_b, \alpha_s\gamma_s, \alpha_c\gamma_c$) (see Chapter 5). However, it was assumed that the wood density would not change between locations. Hakkila (1979) has observed that in Finland there is about 10 % increase in wood density from north to south. On the other hand, the wood density decreases as the tree ring width increases (Hakkila 1968). Tree ring width increased from north to south. Since no wood densities were measured from the various sites, it was assumed that these opposing trends would cancel out each other.

Table 7.2 The varying parameter values for different locations. *P0* stands for potential annual photosynthetic production in unshaded conditions (kg C/kg dm) , r_{mn}, r_{mb}, r_{ms}, r_{mc} and r_{mf} stand for annual weight-specific maintainance respiration of needles, branches, stem, coarse roots and fine roots respectively (kg C/kg C), m_n1–3 are the proportions of needlemass that die annually from needles of different age classes (1/a), e_r^* stands for the fine-root weight-specific annual nutrient (here nitrogen) uptake (kg N/kg dm), b_{pw} is the average number of branches in a whorl and $\alpha_b\gamma_b$, $\alpha_S\gamma_S$, $\alpha_c\gamma_c$ stand for dry matter required in the stem, branches and coarse roots respectively, per unit length of organ per unit mass of needles (kg dm/m /kg dm)).

Parameter	Location			
	Muddusn.	Hyytiälä	Petrozavodsk	Voronez
P_0	1.98	2.72	2.56	3.4
r_{mn}	0.10	0.14	0.13	0.175
r_{mb}	0.015	0.02	0.019	0.025
r_{ms}	0.015	0.02	0.019	0.025
r_{mc}	0.015	0.02	0.019	0.025
r_{mf}	0.35	0.48	0.45	0.6
m_n1	0	0.05	0.05	0.1
m_n2	0.05	0.2	0.2	0.4
m_n3	0.3	0.4	0.4	0.8
e_r^*	0.0106	0.0145	0.0136	0.018
b_{pw}	3	4	4	6
$\alpha_S\gamma_S$	0.98	0.78*	0.87*	0.35
$\alpha_b\gamma_b$	0.89	0.89*	0.89*	0.54
$\alpha_c\gamma_c$	0.45	0.45	0.45	0.64

* Values from Hari et al. (1985) were used to determine the needlemass branch cross-sectional area ratio.

The parameter set used for simulating the growth of the Hyytiälä stand and the sources from which the parameters are derived are presented in Appendix 7.1. The parameters which were varied from one location to another together with the values used are set out in Table 7.2. It must be noted here that root competition was written out of these simulations by assigning the "nutrient interception extinction" coefficient 0 (parameter k_r, Eq. (21), Chapter 6)

7.3 Model Initialization and Simulation Runs

Initial conditions for the simulations were the same for each location. Since the overall development of the stand was considered, the initial state of the stand selected corresponds to an early established seedling stand. There were 2000 seedlings which had 0.1 kg dm of needles, branches, stem, coarse roots and fine roots. The seedlings were divided into four size classes. The height of the biggest size class was 0.5 m and the smaller size classes had heights of 90, 80 and 70 % of the biggest size class respectively. These are henceforth called size classes 1 to 4.

The initial average branch length of the seedlings was 0.1 m and the average coarse root length also 0.1 m. The initial pruning height of the seedlings was 0.1 m and the seedling age at the beginning of the simulations was estimated to be 5 years in Voronez, 10 years in Hyytiälä and Petrozavodsk and 15 years in Muddusniemi. Finally, the initial number of branches was set at 20.

The stand growth and development was simulated for the different locations using the parameter sets described. Sensitivity analyses of the model were done for Hyytiälä and for Voronez with respect to the root functioning parameter and the parameter affecting sapwood conversion to heartwood and that of needle senescence which have been shown to be most critical values in previous studies using the same approach (Mäkelä 1988). Finally, separate sensitivity analyses of the model were done in which the sets of functional and structural parameters that were used to introduce the geographical variation into the study were varied one at a time.

The following chapter gives the results of the simulations. First I set out the simulated development of stand and tree class level characteristics and compare them against growth and yield table data. I then give a brief account of how the growth driving processes ie. photosynthetic production, respiration and allocation of carbohydrates vary over time. The final part of the results consists of the sensitivity simulations.

7.4 Results

7.4.1 Regional Differences in Stand Growth

The more southerly the growing site the faster the stand developed and the higher the biomasses attained after 100 simulated years. The biggest difference was between the Muddusniemi stand and the others, although with respect to needle biomass and coarse root biomass the Voronez stand differed considerably from those of Hyytiälä and Petrozavodsk. The development of the total stand biomasses of different biomass compartments and the height growth of the biggest size classes are presented in Fig. 7.1 a–f.

The simulated stand needle masses in Hyytiälä seemed low compared to Ilonen's observations (1981). However, it must be noted that the simulated needle masses are annual minimum values. If the annual mortality is added to those values then the maximum annual needle mass is close to the observed values.

A similar peak in needle mass as obtained in the simulations has been observed for Scots pine in Sweden (Albrektsson 1980). Assuming that the stand basal area also reflects changes in the stand needle biomass, the Ilvessalo's results (1937) show similar trends to those simulated when moving from poorer to better growing conditions (Kuuluvainen 1991). The simulated needle mass peak value at around canopy closure in Voronez was smaller, however, than the observed value of this study (Chapter 4). The simulated needle mass varied between 1500 and 11500 kg/ha for different soil fertilities in Voronez whereas that observed was about 18500 kg/ha during maximum needle mass. About one third would have to be subtracted from this to get comparable values.

There was a clear intermediate peak value in branchwood biomass in Hyytiälä, Petrozavodsk

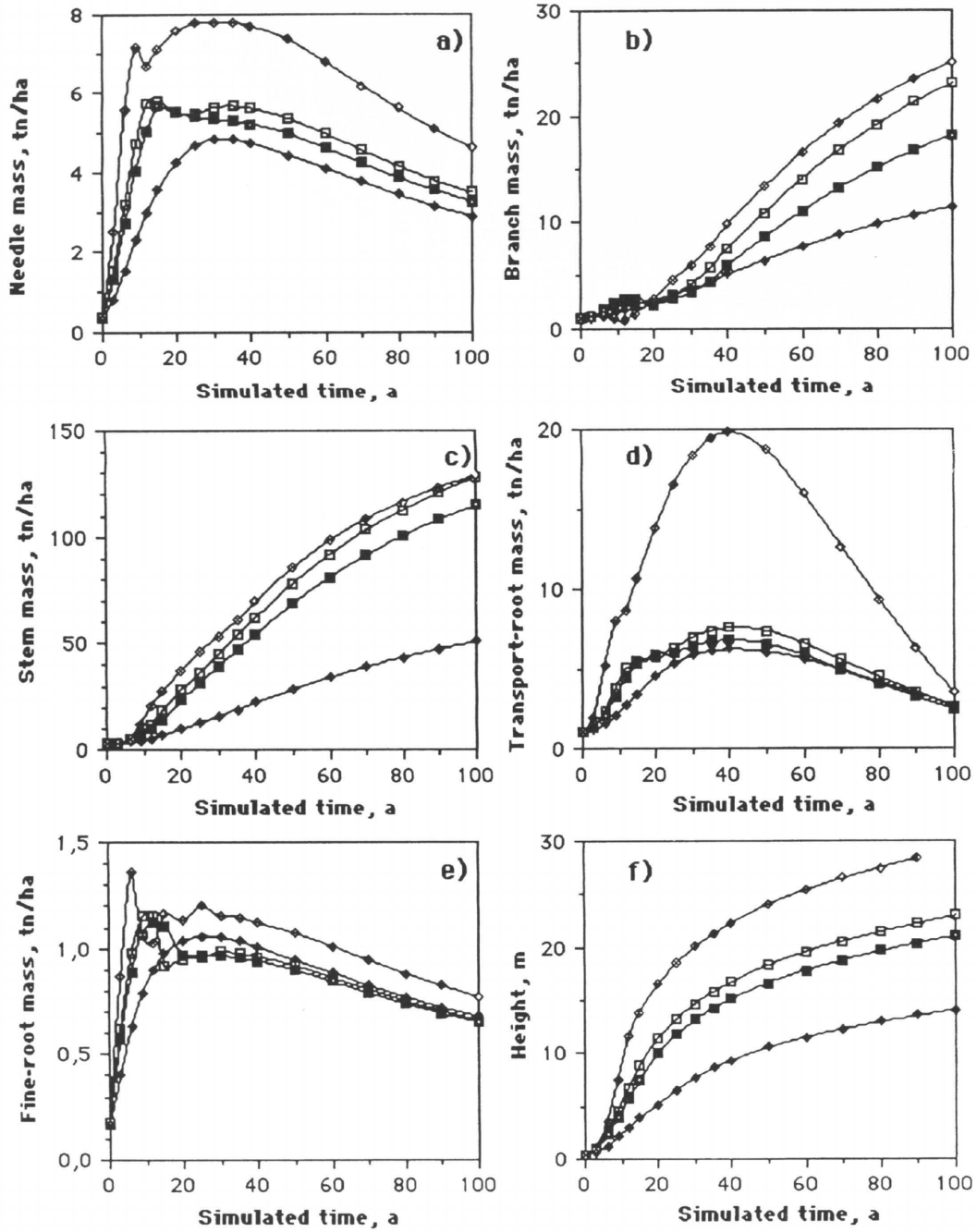

Fig. 7.1. The simulated development of a) needle mass, b) branch mass, c) stem mass, d) transport-root mass, e) fine-root mass, f) height of the trees of biggest size class for Muddusniemi (—◆—), Petrozavodsk (—■—), Hyytiälä (—□—) and Voronez (—◇—).

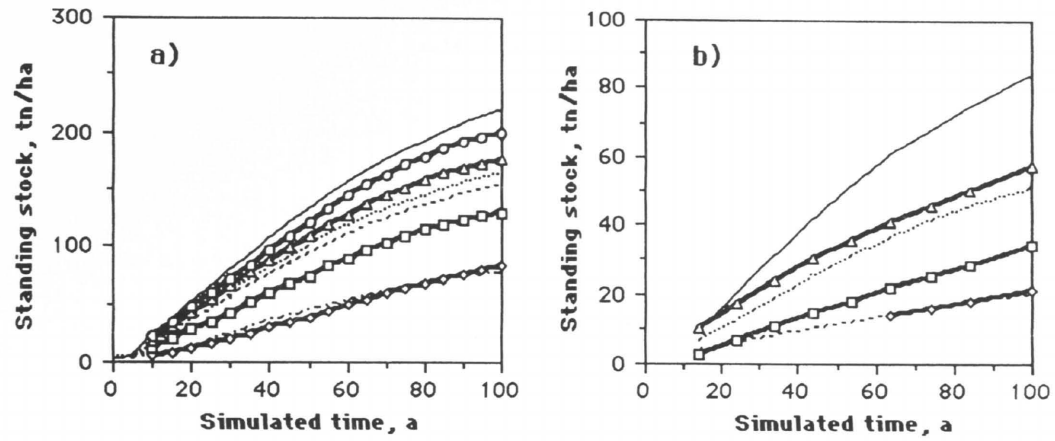

Fig. 7.2. The simulated time development of standing stock (thin lines) and that derived from yield tables (thick lines) for a) Hyytiälä and b) Muddusniemi. The yield table values were redrawn from Ilvessalo (1920) and (1970) for various site types from fertile to poor in southern Finland (OMt (—□—), Mt(—△—), Vt (—■—), Ct (—◇—)) and northern Lapland (EMt (—▲—), ErClt (—■—), Clt (—◇—)).

and Voronez, which occured simultaneously with the needle mass peak value in Voronez and slightly later in Hyytiälä and Petrozavodsk. Hakkila (1971) reports that branch mass of individual trees was about 20 to 25 % of the bole mass (diameter over 6 cm) in southern Finland when the crown ratio of trees is between 40 to 60 % and the same value was 30 to 40 % in northern Finland. The simulated branch mass, which was 20 % of the total stand stem mass in Hyytiälä and 25 % in Muddusniemi is in quite good agreement with that observed.

Despite big differences in needle mass the differences in stand stemwood biomasses were quite small between Voronez, Hyytiälä and Petrozavodsk. The development of the Voronez stand was faster but the biomasses attained values which were close to Hyytiälä values after 100 years of simulations. Quantitative comparisons between southern Russia and Finland were made assuming no nutrient limitation to growth, ie. the parameter value of parameter e_r^* was set high (0.1). Simulations were compared with observations by Kazimirov et al. (1984) who had collected growth and yield data from the most fertile stands from various parts of Russia. The simulated results corresponded closely with the observed values for Karelian conditions. The standing stock was 720 m^3/ha at 100 years when the yield table value was 696 m^3/ha and the respective heights were 36 and 32 metres. The simulations seemed to underestimate the growth in Voronez, as for the needle mass, since the simulated standing stock was 861 m^3/ha whereas the yield table value was 1007 m^3/ha.

Fig. 7.2 presents comparison between simulated and observed standing stocks from Southern Finland and Lapland. The simulated and observed stem masses are fairly comparable, since in the simulation no exact match with observed site types was attempted. The simulated standing stock development is qualitatively equal to that observed and the differences between site types could have been obtained exactly by choosing slightly different root function efficiency (e_r^*) values (see Fig. 7.2a). The observed stem mass is calculated from the reported volume values (Ilvessalo 1920) multiplied by the average stemwood density of pines (Kärkkäinen 1985).

For the Muddusniemi stand a similar comparison was made against the local site types. The parameters were varied as explained in Chapter 7.2. The simulated standing stock values for Muddusniemi corresponded to observed values as in southern Finland, as can be seen from Fig. 7.2b. In other words, the correspondence between simulated and observed site type differences were repeated for Lapland simply by changing the pa-

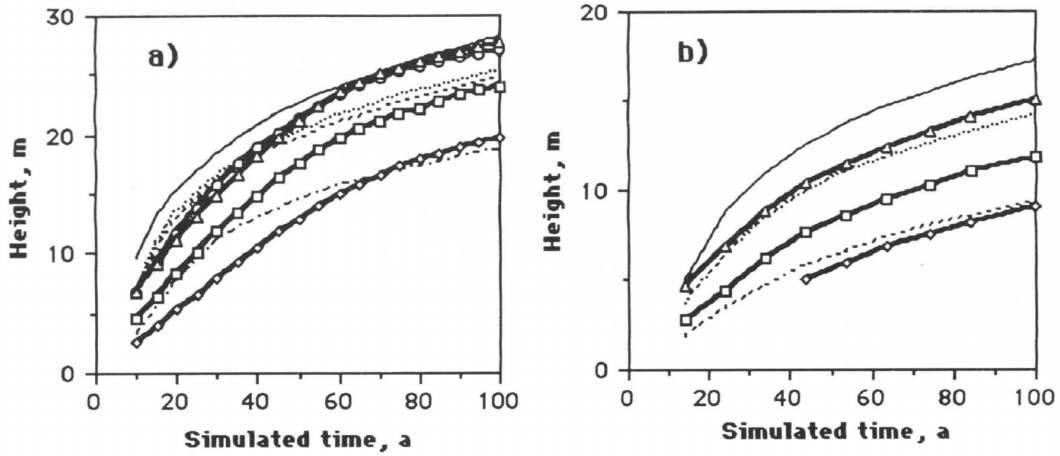

Fig. 7.3. The simulated development of the height of the trees of size class 1 (thin lines) and yield table time development of the average height (thick lines) for a) Hyytiälä and b) Muddusniemi. The yield table values were redrawn from Ilvessalo's (1920, 1970) for different site types from fertile to poor in southern Finland (OMt (—○—), Mt (—△—), Vt (—□—), Ct (—◇—)) and northern Lapland (EMt (—△—), ErClt (—□—), Clt (—◇—)).

rameter values by the relative growing season length and the measured structural differences.

The changing length of the growing season is assumed to affect the average nutrient uptake efficiency of the fine roots in simulations between the locations. The actual fine root biomass turnover within the stands however reaches more or less the same value although there were quite considerable differences in the needle mass between the stands. Linder and Axelsson (1982) estimated the annual fine-root turnover as between 1200 and 2000 kg/ha, which is slightly higher than the simulated values. Direct comparison between the values is difficult, though, since in the model the fine roots are the actively uptaking roots whereas the fine roots in empirical work are usually determined by size.

Changing the parameter values to simulate change in growing conditions had a powerful effect on the dynamics of the height growth of trees. The Muddusniemi stand in particular had much lower height growth than the rest (see Fig. 7.1f). The simulated and yield table estimates of height growth (Ilvessalo 1920, 1970) were compared between southern and northern Finland over the rotation (see Fig. 7.3 a and b). The height growth was initially faster than in growth and yield tables in the south but in later phases gave comparable values. The reported value of the simulations was the height of size class 1, which initially corresponds to the dominant height of the stand. At later phases of stand development it corresponds more to the average height reported in the growth and yield tables because the number of trees in the other size classes has diminished considerably. In Muddusniemi the differences between the size classes were smaller and thus the height of size class 1 corresponded better with the average height (see also Fig. 7.5a). The simulated height growth for Voronez followed a similar qualitative trend as that observed by Kazimirov (1984) for southern Russia.

Fig. 7.4 a, b sets out the development of height and crown base height of size class 1 for Voronez and Hyytiälä and those of size class 1 and 3 in Hyytiälä. The smaller size classes are dominated much faster in the south than in Hyytiälä. In Voronez the smallest size class (4) is practically dead before 20 years of simulation whereas in Hyytiälä the same size class survives more than 50 years of simulation. The pruning limit also rises very fast initially in Voronez compared to Hyytiälä. This coincides with the field observation of this study between locations (see Chapter 5.3). At later phases of stand development, the change of pruning limit seems to slow down considerably in all lo-

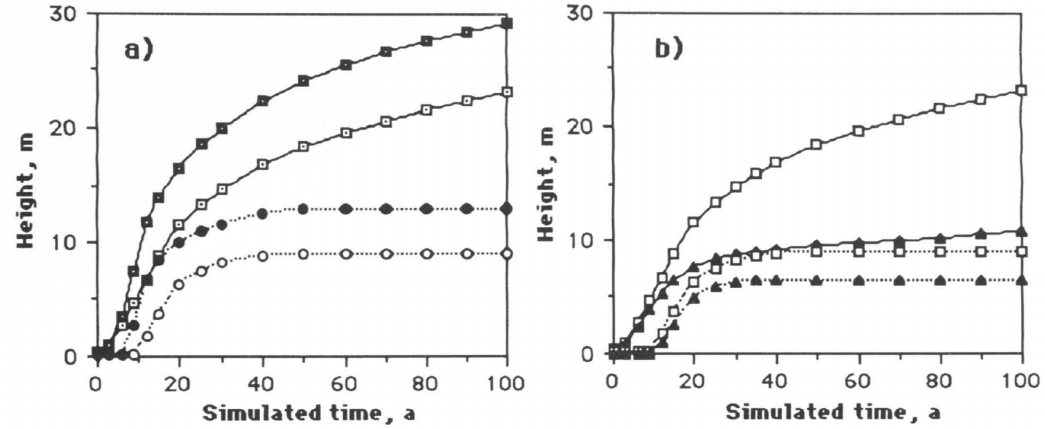

Fig. 7.4. Simulated height (——) and pruning limit (·····) for trees in a) size class 1 in Hyytiälä (□ , ○) and Voronez (■ , ●) and b) the same for size class 1 (□) and 3 (▲) in Hyytiälä.

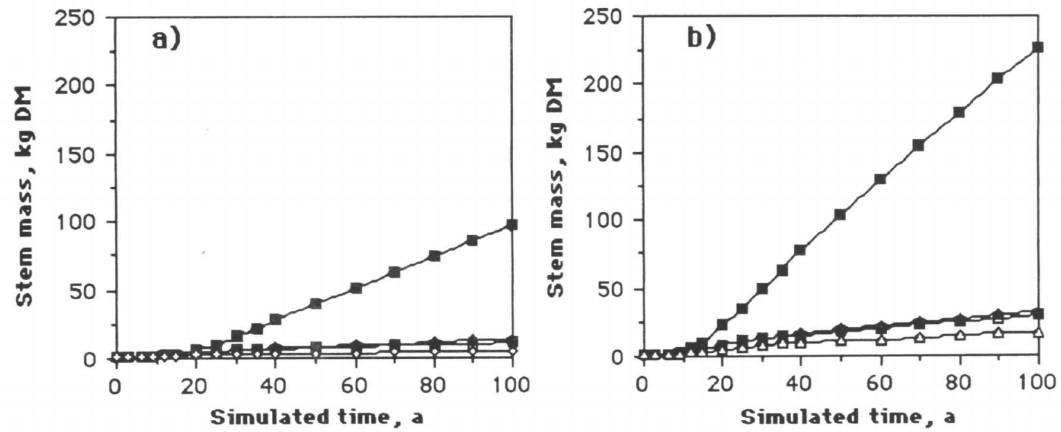

Fig. 7.5. The simulated development of size classes in a) Muddusniemi and b) Hyytiälä (size class 1 (=largest —■—), size class 2 (—□—), size class 3 (—▲—) and size class 4 (= smallest —△—)).

cations. The simulated pruning height development agreed quite well with results observed in Finland (Hakkila et al. 1972).

The development of the pruning limit in the various size classes is initially very similar. However, as the differentiation of trees into dominant and dominated proceeds the pruning limit of the smaller trees also remains lower than that of the dominant trees. Similar behaviour of the pruning limit has been observed in the permanent sample plots in Finland (Ojansuu, pers. comm.).

Fig. 7.5 a and b shows how significant the differentiation of the size classes of trees to the development of stem mass is for Hyytiälä and Muddusniemi, and Fig. 7.6 a and b shows how the number of stems decreases in the size classes at the same locations. At all locations, the stem mass of the dominant trees is far higher than of any other size class. This sharp differentiation is partially an artifact of the model since only four size classes were used. However, the model predicts the often observed phenomenon that the stands become dominated by a few large, evenly distributed individuals as the age increases (see review

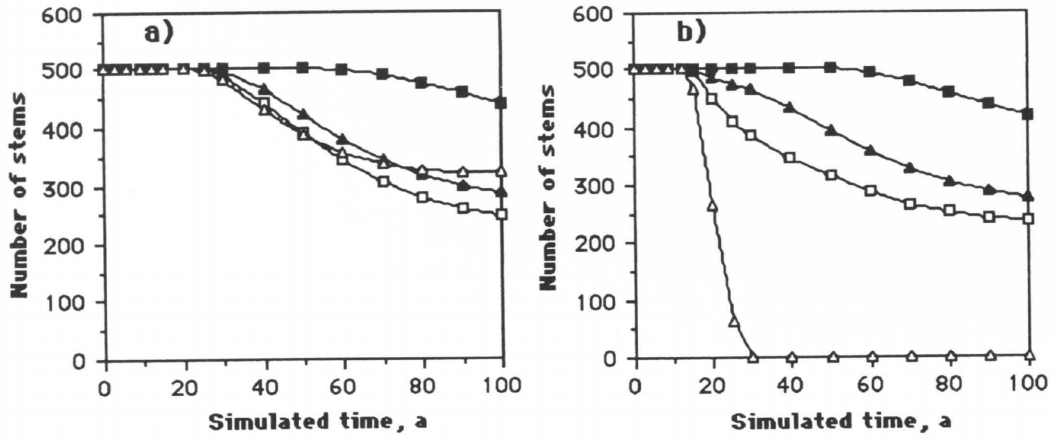

Fig. 7.6. The simulated development of the number of stems in different size classes in a) Muddusniemi and b) Hyytiälä (size class 1 (=largest —■—), size class 2 (—□—), size class 3 (—▲—) and size class 4 (= smallest —△—)).

by Ford and Sorrensen 1992). Further north the differences between the size classes are reduced and the period of co-existence between small and large size classes increases.

The model seems to produce the double-peaked diameter distribution at around canopy closure which has been reported to occur in monocultures under strong competition (Ford 1975). Initially the trees of the larger size classes grow better but when the stand reaches canopy closure, the trees of the second biggest size class (2) start dying first. It seems that they end up in an unfavourable situation since the size they have attained during their early development requires fairly high maintenance and construction cost to keep up with the growth rate, but shading by the largest size class cuts down their production considerably. Trees of size class 3 fare better. Their resource requirement is less because of their smaller size and the light climate is not much worse than for the trees of the size class 2 since the decline of light climate is initially very steep as a function of foliage mass but levels off considerably as the shading biomass increase (see Chapter 6).

7.4.2 Simulated Variation in Photosynthetic Production, Respiration and Carbohydrate Allocation

The simulated growth patterns (Figs 7.1–7.6) are due to the assumptions about photosynthetic production, respiration and carbon allocation which are based on the functional balance principle and pipe model. In this chapter *I* compare the variation of these "driving" processes between the sites.

Fig. 7.7 a shows the development of the annual photosynthetic production in trees of the size class 1 at different locations and Figure 7.7 b shows the maintainance respiration of the existing structures (without new growth) as a function of photoproduction. The annual photosynthetic production is much larger in the south as is the maintenance respiration. However, a larger proportion of the photosynthetic production is used for maintenance respiration of existing structures in the north. This reflects the changes in the proportional amounts of wood, foliage and fine roots between locations. The simulations also suggest that the proportion of maintenance respiration from photosynthetic production increases with the tree size. This seems contrary to the linear relationship suggested between light interception and dry matter production (e.g. Linder 1987) but is consistant with the

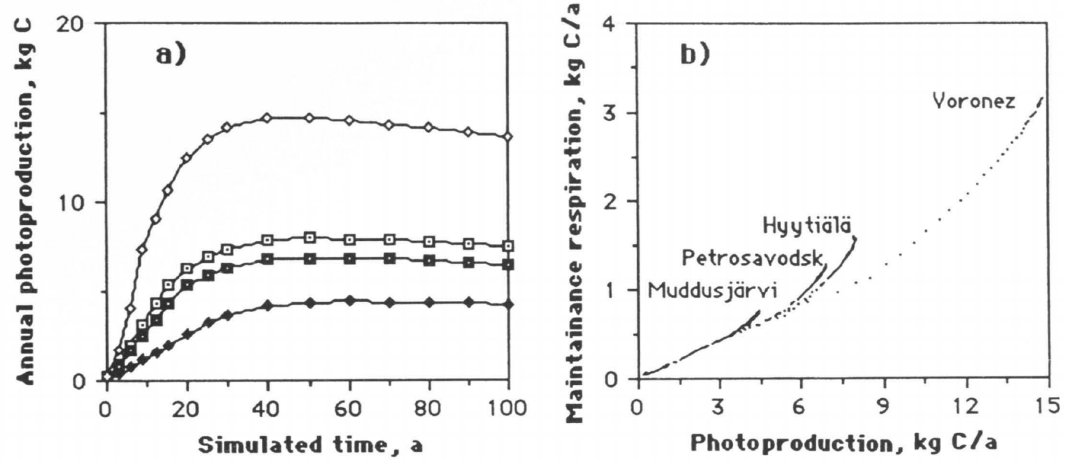

Fig. 7.7. a) The simulated annual photosynthetic production of trees of size class 1 for different locations (Muddusniemi (—✦—), Petrozavodsk (—■—), Hyytiälä (—□—) and Voronez (—◇—)) and b) annual amount of carbon used for maintainance respiration as a function of annual photosynthetic production for the same trees and locations.

generally accepted theory of the development of the costs of maintenance vs. production as a function of size (e.g. Givnish 1988).

The allocation of carbohydrates to the various biomass compartments is very dynamic (Fig. 7.8). The proportion allocated to stem characteristically increases in the early phase of stand development, followed by a more gradual decrease. Other but much smaller changes take place in the allocation to the needles, ie. an initial decrease followed by a stable phase. The same pattern has also been observed with Scots pine in Sweden and in the UK (Albrektson and Valinger 1985, Ovington 1957). A simulated pattern of carbon allocation also produces the trends predicted by Kuuluvainen (1991). Similar trends have previously been produced with a simpler model but stemming from the same principles (Hari et al. 1985, Mäkelä 1990a).

The proportion allocated to fine roots decreases throughout stand development as a bigger proportion of the nutrient demand is supplied by internal circulation. The steady increase of allocation to coarse roots reflects their continuous length growth. More than 45 % of the carbohydrates was finally allocated to fine and coarse roots in Voronez and Muddusniemi and about 30 % in Hyytiälä and Petrozavodsk. The high proportion for Voronez is caused by the relatively large quantity of coarse roots. This follows from the measurements of the coarse root and stem sapwood cross-sectional areas (see Chapter 5). Simulated values fit within the considerable variation of 20 to 60 % reported in the carbohydrates that go below ground in young stands growing on poor soil (Albrektson 1980, Linder and Axelsson 1982, Ford 1975).

The dynamics of allocation to the stem varied markedly between locations. There were no large differences between Voronez, Hyytiälä and Petrozavodsk in the maximum proportion allocated to the stem, the peak occuring only much earlier in Voronez than in the other two places. In Muddusniemi the proportion of stem growth was much lower than in the others most of the time. The large proportion allocated to the fine roots mainly decreased the stem and branch growth, while needle growth remained unaffected.

Figure 7.9 a–d shows the allocation to needles and stem in the different size classes in Hyytiälä and Voronez. In the very early phases of stand growth they are almost identical. As the smaller size class gradually becomes more shaded, the proportion allocated to needles increases as the relative importance of needle senescence becomes higher (see Eqs. (6.28–30), (6.32), (6.34), Chapter 6.6). At some stage the allocation to needles

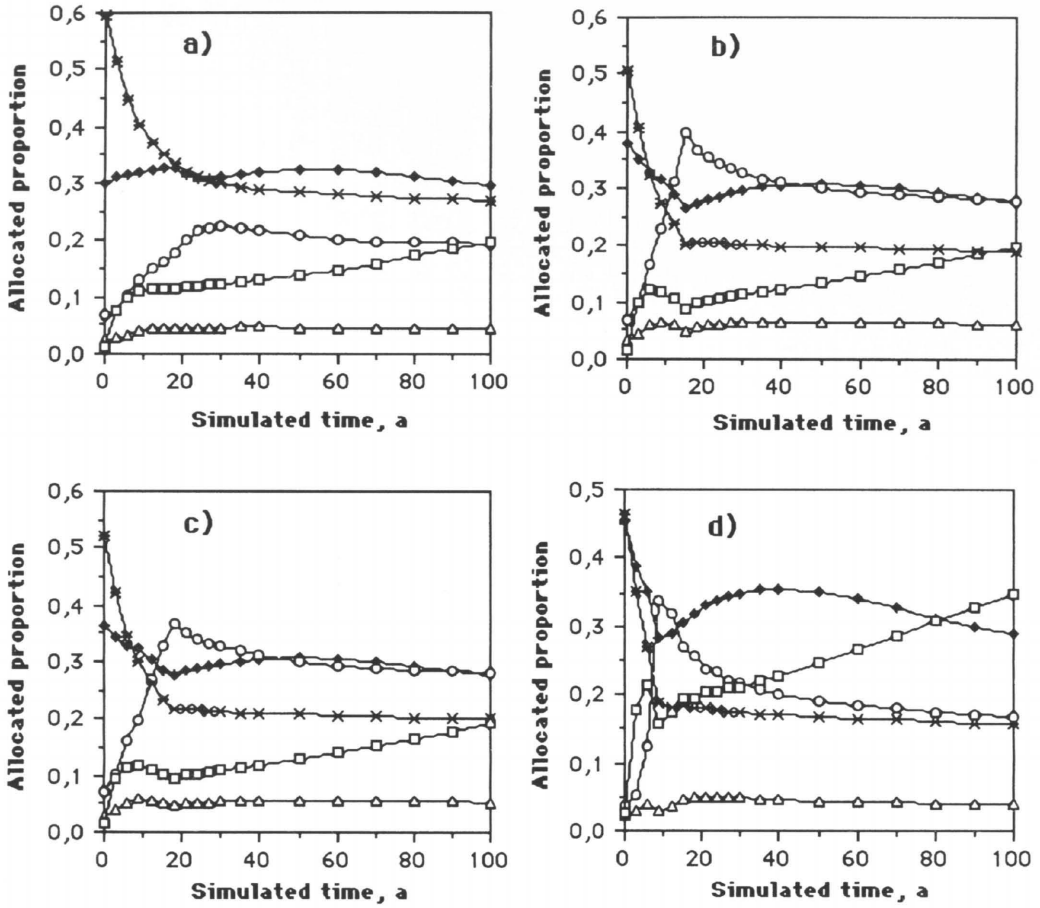

Fig. 7.8. The simulated distribution of carbohydrates to different biomass compartments (needles (—✱—), branches (—△—), stem (—○—), coarse roots (—□—) and fine roots (—✱—)) in a) Muddusniemi, b) Hyytiälä, c) Petrozavodsk and d) Voronez.

starts declining again because the proportional height growth of trees increases in response to increased shading. This goes on until the lack of light becomes too severe to sustain the growth required to maintain the balanced structure. The behaviour of the allocation to stem is the opposite to that of the needles. Development is much faster in Voronez than in Hyytiälä. Fig. 7.9 shows that allocation coefficients show strong oscillations in Voronez where two of the size classes become extinct and one reaches a new equilibrium. These oscillations indicate problems in the carbon balance but are probably caused by the technical simplifications of the model, ie. the small number of size classes, and no immediate connection between extension growth and the mass balances, which were done mainly to avoid iterative model structures.

Supressed trees first increased their allocation to needles and as they became more supressed allocated proportionally more to the stem height growth, until the reducing foliage was no longer able to supply them with enough resources. It is normally reported that the newest needles have the highest priority (e.g. Waring 1987). These results support this observation under moderate shading conditions.

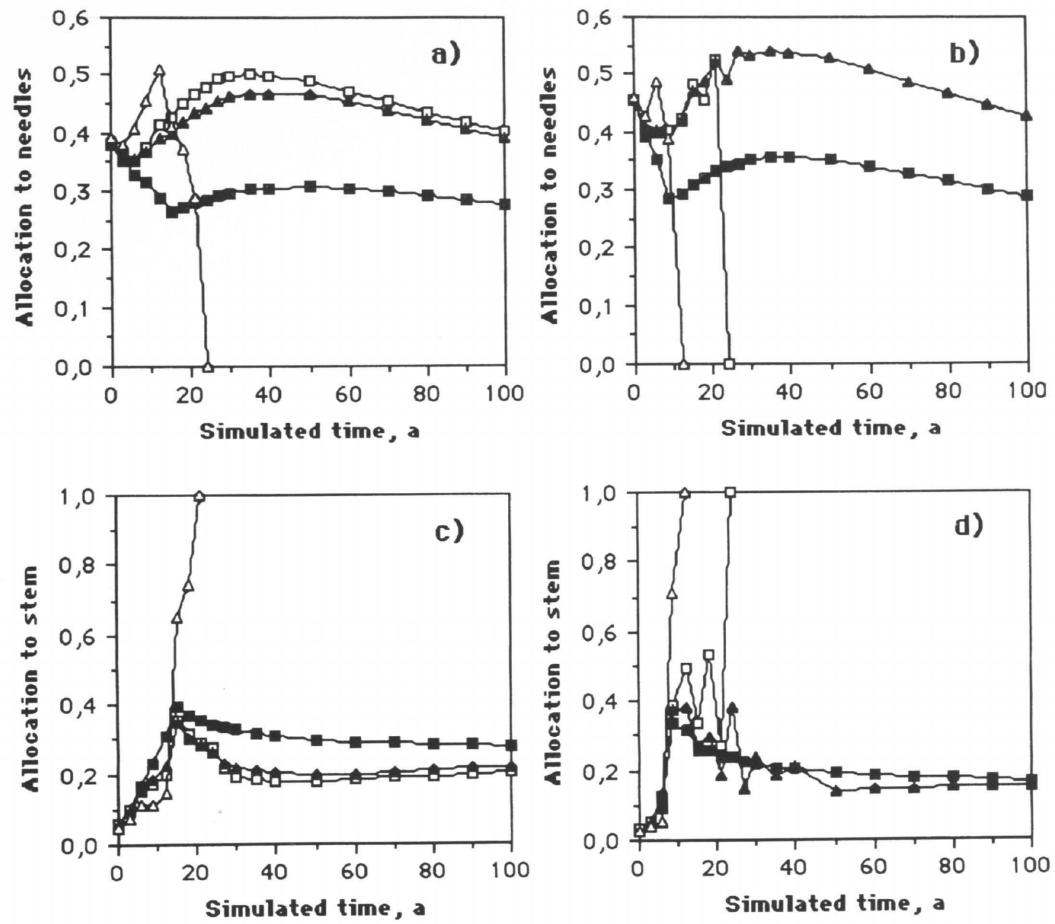

Fig. 7.9. The simulated proportion of carbohydrates distributed to needles in the trees of the different size classes (size class 1 (=biggest —■—), size class 2 (—□—), size class 3 (—▲—) and size class 4 (= smallest —△—)) in a) Hyytiälä and b) Voronez and the same for stem in c) Hyytiälä and d) Voronez.

7.4.3 Sensitivity of the Model to Changes in the Root Functioning and Senescence Parameters

The previous section demonstrated that the model describes multiple features of stand development realistically, as well as giving comparable results with growth and yield table results. However, as previous analyses have shown, the model uses parameters the value of which is still rather uncertain. Those parameters associated with root functions and senescence of different parts of the tree especially have both been proved uncertain and to have considerable influence on the simulation results (Mäkelä 1988).

To get some idea of the effect of these parameters in the geographical results, sensitivity simulations were done changing the fine-root function efficiency (e_r*) and the parameters describing the senescence of different biomass compartments.

The stand development in Hyytiälä and Voronez was simulated using eight levels for fineroot functioning efficiencies. The values ranged from 0.0055 to 0.1 for both locations. At the lowest parameter value the stand needle mass reached almost identical values in both locations (maxi-

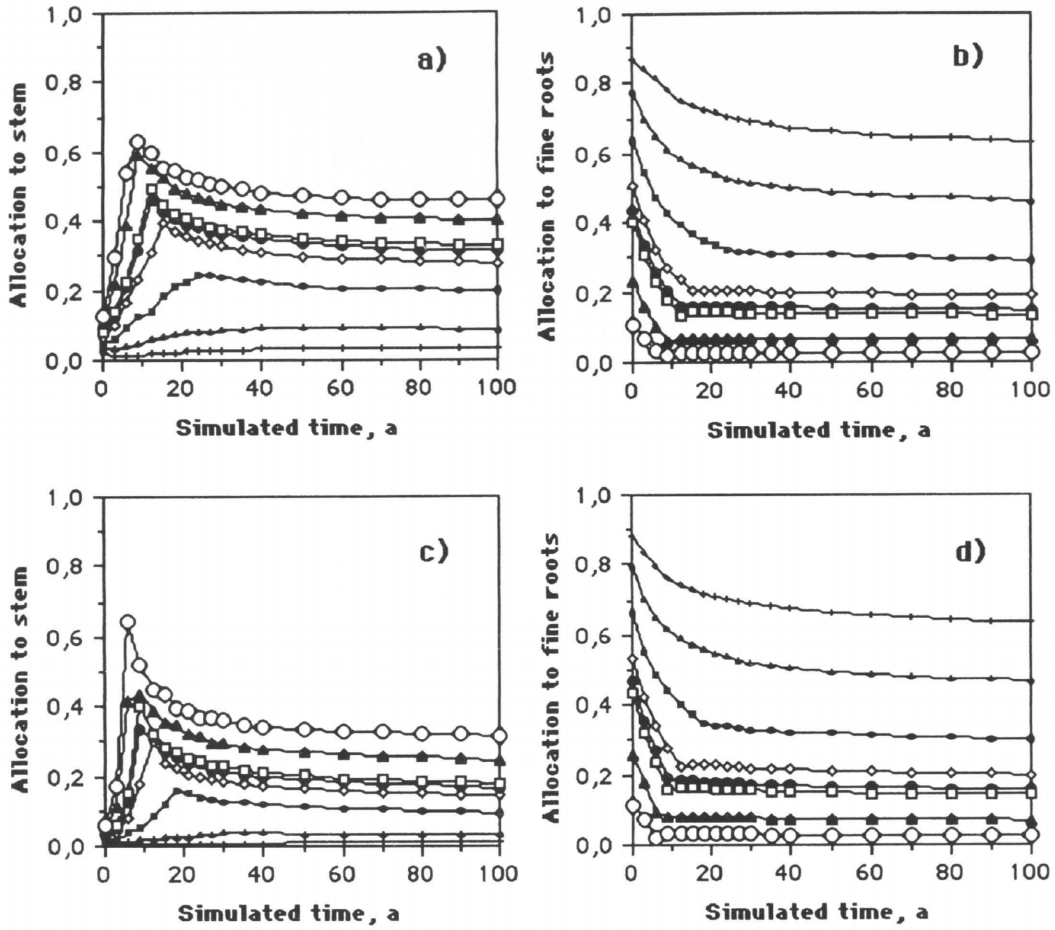

Fig. 7.10. The simulated development of allocation to stem and fine roots as a function of specific root mass nutrient uptake (e_r* 0.0055 (–+–), e_r* 0.007 (–▲–), e_r* 0.01 (–■–), e_r* 0.014 (–◇–), e_r* 0.018 (–●–), e_r* 0.020 (–□–), e_r* 0.040 (–▲–), e_r* 0.100 (–○–)) in Hyytiälä (a and b) and in Voronez (c and d).

mum needle mass about 1.3 tn/ha) but, as the nutrient limitation lessened, the response in the more favourable conditions of Voronez (12 tn/ha) was about double that of Hyytiälä (7 tn/ha). However stand fine root mass first increased then decreased at both locations as the parameter value was increased. It has been observed that the fertilization of a very poor site does not increase the fine root biomass of the stand greatly but that new growth is mainly in above-ground parts (Persson 1980, cited by Linder and Axelsson 1982). The simulated results were consistent with this observation. Although there was some variation in the fine-root mass, the accompanying changes in the above-ground masses dominated the response.

As could be expected stemwood increase was bigger in Voronez than in Hyytiälä as the value of e_r* was changed from 0.0055 to 0.1; however, the difference was not as dramatic as in the needle mass.

Fig. 7.10 a–d depicts allocation to stem and fine roots as the parameter e_r* is changed. The changes affect both the level and dynamics of allocation in both cases. The nutrient availability also reduces growth at low availability more than at

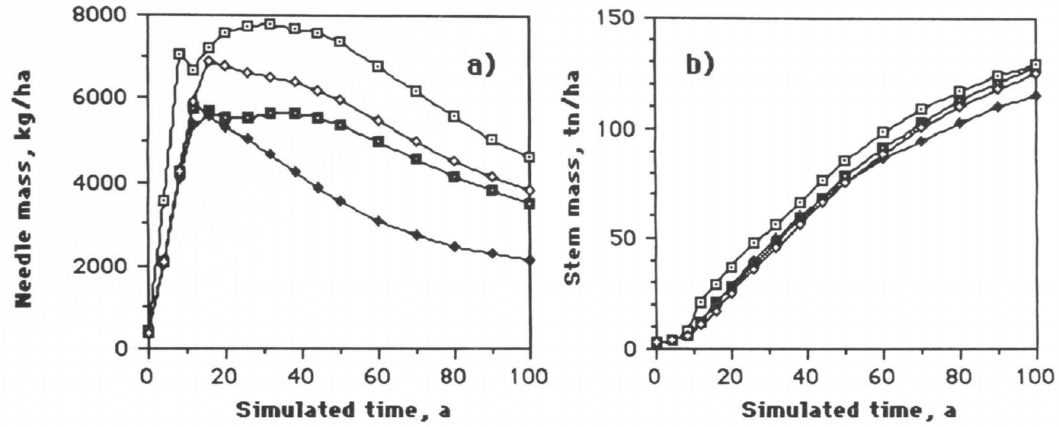

Fig. 7.11. The simulated development of a) needle mass and b) stem mass in Hyytiälä and Voronez assuming different parameter values for sapwood conversion to heartwood (m_b) as a function of foliage senescence (Hyytiälä m_b 0.9 (–■–), Hyytiälä m_b 0.8 (–◆–), Voronez m_b 0.9 (–□–), Voronez m_b 0.8 (–◇–)).

high availability. Changing the root functioning efficiency value from 0.0055 to 0.01 caused about as large a growth increase as when it was changed from 0.01 to 0.1.

The senescence rates have an impact on the state variables both directly through the dynamic Eqs. (Chapter 6, Eq. (6.3)) and indirectly through allocation (Chapter 6, Eqs. (6.28–30), (6.35)). The processes actually bringing about senescence, both of whole individuals and organs of those individuals, are still rather poorly understood. The sensitivity of this model was examined with respect to changes in the parameters which affected senescence of needles, branch and stem sapwood and the mortality of entire trees. We also asked whether those changes would be different depending on the other parameter values which brought about the geographical differences between the Hyytiälä and Voronez stands.

Heartwood formation was divided into two components in the model: that caused by the dying of lower branches in the crown, and that caused by dying of sub-branches (see Chapter 5.2, Kaipiainen and Hari 1985).

The parameter value giving the proportion of senescing foliage that is associated with sapwood turnover to heartwood (see Eqs. (6.47–50) in Chapter 6.7) was varied from 0.1 to 0.2. The change affected foliage biomass at both Hyytiälä and Voronez, being initially stronger in Voronez but at later phases more significant in Hyytiälä (the difference between the simulation runs at 100 years was 40 % in Hyytiälä and 20 % in Voronez) see Fig. 7.11. However, only a slight effect can be seen in the stem biomass, especially in Voronez (3 % in Voronez, 14 % in Hyytiälä).

The change in the parameters affecting the self-pruning of the trees (Chapter 6, Eq. (6.44) δ and χ_{dr}) affected the needle and stem mass both in Hyytiälä and Voronez. The effect was quite similar at both locations. Slowing the crown base change allowed the needle mass to reach a higher level, and the culmination of needle mass occurred at a later phase. However, the change had hardly any effect on the total stem mass, as in the previous case. The main difference between the two aspects of the heartwood formation was that during early stand development the pruning height change was responsible for most of the heartwood formation, whereas at later phases the heartwood formation in branches seemed to dominate. This is, of course, logical since at later ages the pruning limit attains a more or less constant height (see Fig. 7.4).

The effect of needle senescence rate on the stand needle and stem mass was also examined in Hyytiälä and Voronez. At both locations, the basic run (using the parameter set of Table 7.2) was compared with one with a 50 % smaller senescence rate in each needle age class. The effect on

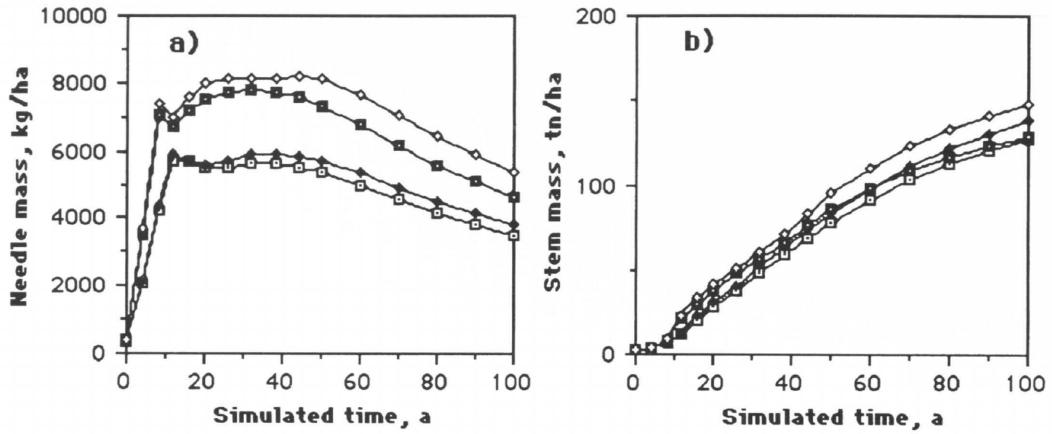

Fig. 7.12. The simulated development of a) needle mass and b) stem mass in Hyytiälä and Voronez assuming different parameter values for needle senescence rate (m_n) (Hyytiälä basic run (–□–), Hyytiälä 50 % less (–♦–), Voronez basic run (–■–), Voronez 50 % less (–◇–)).

stand needle mass was much smaller than when changing the parameters affecting heartwood formation (see Fig. 7.12 a) and was clearly bigger in Voronez than in Hyytiälä. The effects on stem mass however were of the same order of magnitude as changes affecting heartwood formation (see Fig. 7.12 b).

Finally, the sensitivity of the model to the rate of tree mortality was examined by changing the value of the parameter describing how big the needle growth must be compared to senescence in order that no mortality take place (t_{mr}, Chapter 6, Eq (6.54)). The value was changed from 1.0 to 0.9. This change produced about a 10 % difference in the final stem biomass in each case.

7.4.4 The Role of Functional and Structural Parameters in the Simulated Geographical Variation

The manner in which the geographic variation was introduced into the analyses was rather simple, relying on temperature data and structural measurements performed at a single point in the time development of the stand. In the Figs 7.13 and 7.14 an attempt is made to identify those factors causing the differences in simulations between Voronez in southern Russia and Muddusniemi in Finnish Lapland (see also Fig. 7.1 a to f). The simulation runs were repeated at different locations when changing only a) the functional parameters (P_0, r_{mn}, r_{mb}, r_{ms}, r_{mt}, r_{mf}, m_n1–3, e_r*; Fig. 7.13 a–f) and b) the structural parameters (b_{pw}, $\alpha_b\gamma_b, \alpha_s\gamma_s, \alpha_c\gamma_c$; Fig. 7.14 a–f). The functional parameters were those giving the annual rates of input-output processes (e.g. photosynthetic production, respiration, nutrient uptake) and the structural parameters describe the connections between different dimensions of the trees (see Chapter 7.1).

The differences in needle, coarse root and fine root biomasses decreased, whereas that of the stem mass increased considerably between the sites when the functional parameters only were changed compared with the basic run where all the parameters were changed (Figs 7.13 a–f, 7.1 a–f). At the age of 100 years the stem mass of Hyytiälä was about 50 % of the stem mass of Voronez, whereas in the basic run the difference was almost nil. The simulations would thus suggest that considerable overestimations of stem growth may follow if the changes in tree structure are not considered.

There were only minor changes between the Muddusniemi, Hyytiälä and Petrozavodsk simulations for variation in structural parameters between sites, but those of the Voronez stand differed considerably (see Fig. 7.14 a–f). The effect of the north-south change of the structural parameters was reflected as an increase of both the nee-

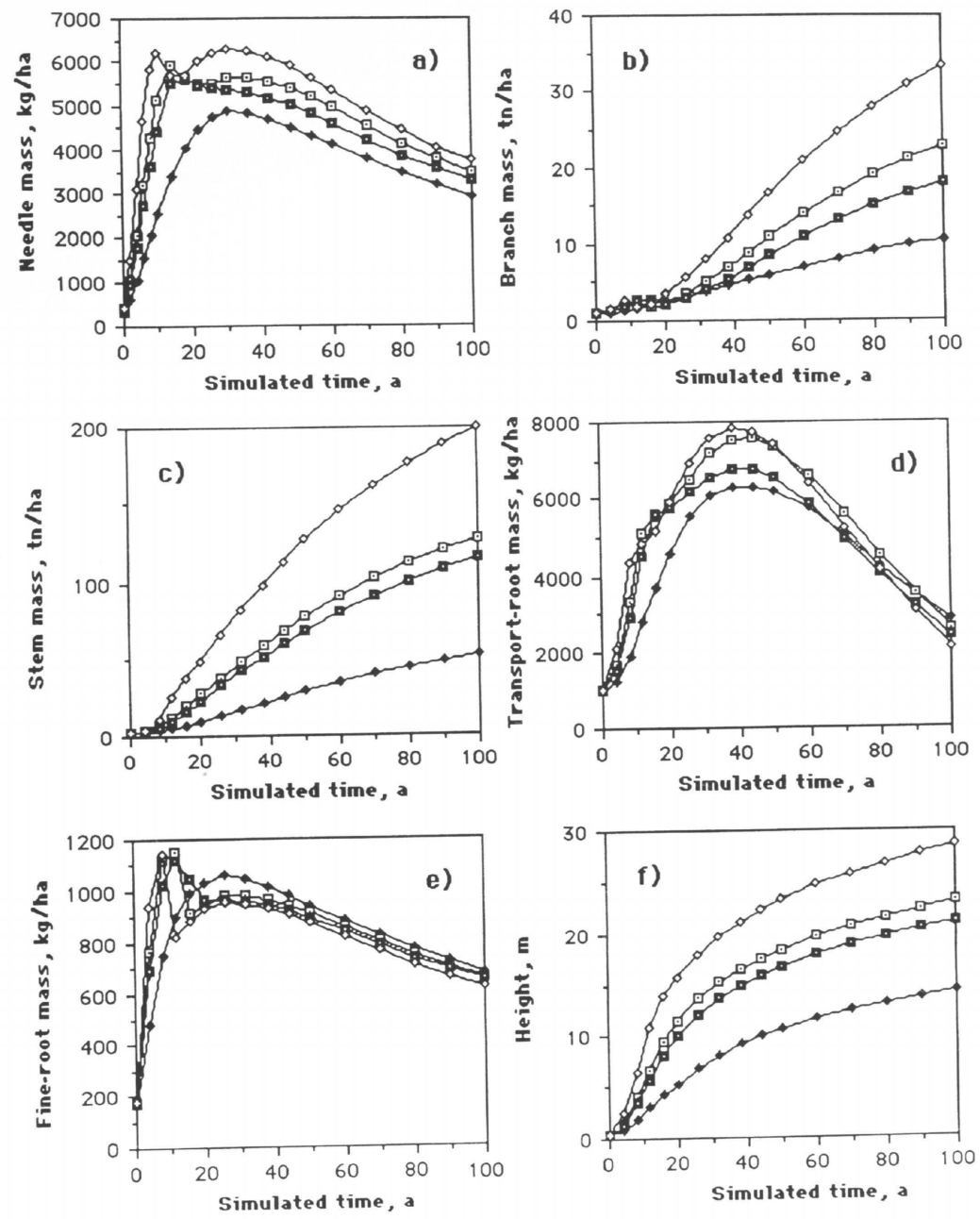

Fig. 7.13. The simulated development of a) needle mass, b) branch mass, c) stem mass, d) transport-root mass, e) fine-root mass and f) height of the biggest size class for Muddusniemi (–♦–), Petrozavodsk (–■–), Hyytiälä (–□–) and Voronez (–◇–) assuming that only the functional parameters vary.

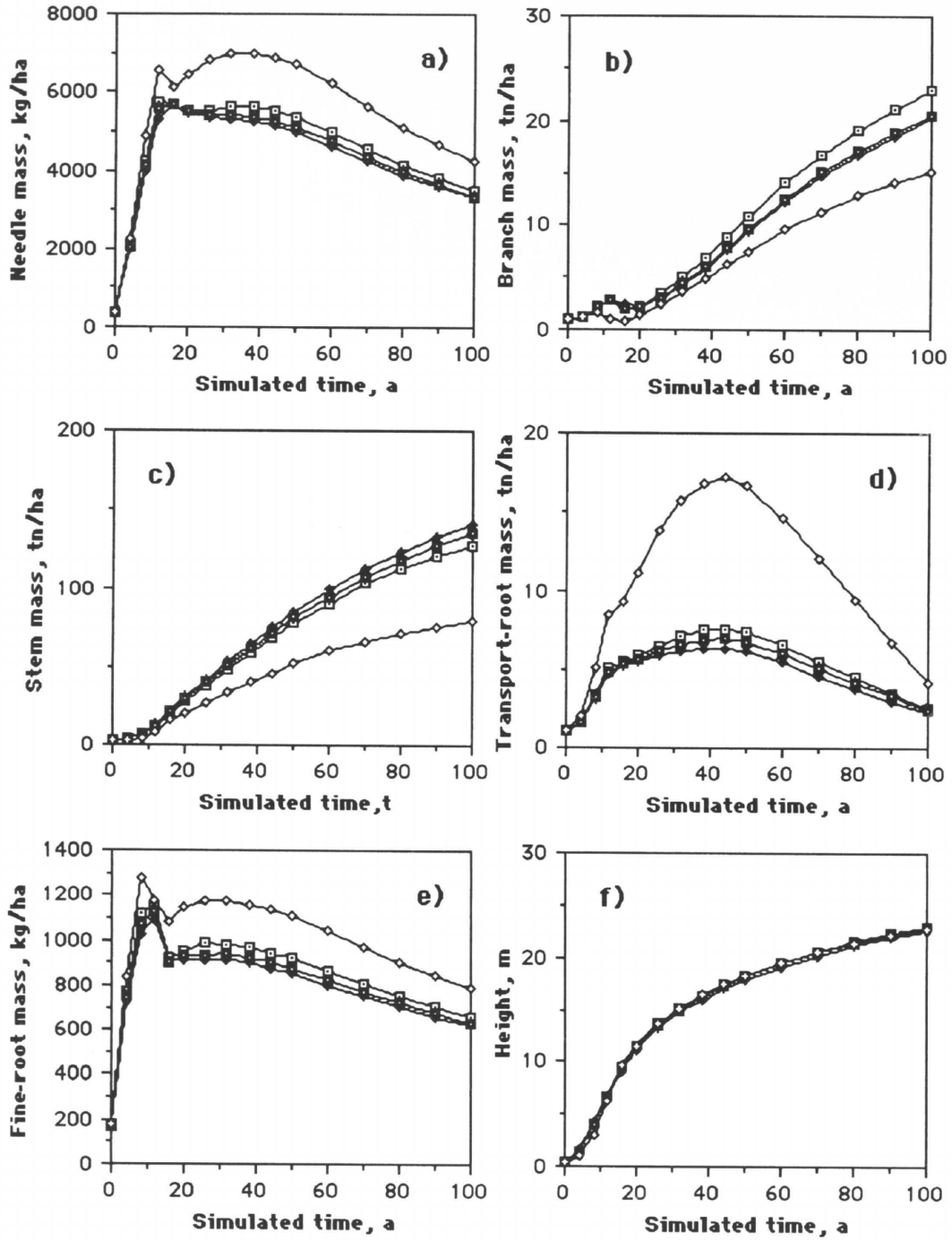

Fig. 7.14. The simulated development of a) needle mass, b) branch mass, c) stem mass, d) transport-root mass, e) fine-root mass and f) height of the biggest size class for Muddusniemi (—✦—), Petrozavodsk (—■—), Hyytiälä (—□—) and Voronez (—◇—) assuming that only the structural parameters vary.

dle and fine-root masses and especially the coarse-root mass. On the other hand, the branch and stem mass decreased considerably. The relative stem mass change between the simulations after 100 years was of the same order of magnitude as the change in the structural parameters whereas change in the coarse-root mass was about three times that of the change in the value of the parameter, which seems rather high. The north to south variation in structural parameters favours both foliage growth and faster initial growth of the stand, but generally decreases wood growth.

7.5 Discussion

Model behaviour

The principal question is how well this approach could account for the trends observed both within a stand as a function of time and between stands growing under very different climatic conditions. It is particularly interesting to see how well this simplified approach could explain the relative geographical differences in Scots pine growth.

From the Hyytiälä simulations it would appear that the model is able to predict different aspects of stand growth realistically using a fixed parameter set. The development of the different biomass compartments (Ilvessalo 1920, Mälkönen 1974, Hakkila 1971, Albrektson 1980, Linder and Axelsson 1982) the height (Ilvessalo 1920) and crown development (Hakkila et al. 1972) and the pattern of carbon allocation to stem (Albrektson and Valinger 1985, Mohren 1987, Ovington 1957) all corresponded quite well with observed patterns. Although these observations were not always from similar conditions as in Hyytiälä, they indicated similar patterns as observed in the geographical simulations. The model also simulated the differences between the site fertility classes (Ilvessalo 1920) consistently with earlier results with similar approach (Mäkelä 1988) after modifying only the root function efficiency. However, the most interesting outcome was that the model was able to describe the standing stock and dominant height development for southern Finland and Lapland when only the structural parameters were varied according to the measurements (see Chapter 5) along with modifying the functional parameters by the relative growing season length (see also Nikinmaa 1992, Ilvessalo 1920, 1970). This is quite a strong test of the model structure.

The model was able to predict qualitative trends observed in Scots pine stand growth in more favourable conditions when compared with Finnish conditions (Ilvessalo 1920, Decourt 1965, Kasimirov et al. 1984), but it did somewhat underestimate these differences. It is clear that if no changes in structural parameter values were made, considerable overestimations would have followed. However, it seems that considering simply increase in growing season length is not adequate to describe the differences in the production conditions further south. Other aspects such as water availability effects on photosynthetic production and differences in light climate and its interaction with stand structure should also be considered when the parameter values are derived for those locations (see Berninger (in print)).

An essential component in this model is the derivation of the growth of different organs from the principle of functional balance. As regards wood structure, the function relative to leaves is assumed to be determined explicitly by the relationship between needle mass and wood cross-sectional area. It is therefore not surprising that the large differences observed in these relationships between southern and northern sites cause very large differences in simulation runs. The higher needle mass per unit area of wood in the south not only caused a more rapid initial growth of the stand but also much reduced stem growth over the simulated time period of 100 years. However, taking no structural changes into account, the simulated stem mass was almost double the value simulated when structural changes were considered.

The measurements showed that more coarse roots were required in Voronez than Petrozavodsk for the same amount of foliage (see Chapter 5). This result, when introduced into the parameter values, made the model very sensitive to the factors affecting coarse root growth. It can be seen for example in the high allocation of carbohydrates to coarse roots in Voronez. This might reflect real-world behaviour, but at the same time it must be noted that the coarse-root wood conversion from sapwood into heartwood was also mod-

elled with only a little information about the real-world phenomena. This sub-model had a big influence on the results, especially for Voronez. For example, by doubling the maximum age of the coarse roots, one obtained about 30 % more final stemwood mass and the allocation to coarse roots at the late phases of simulations dropped to about two-thirds of the values presented here. Considering this modification the final stemwood mass was much closer to the growth and yield table value reported by Kazimirov et al. (1984).

The model follows the outline presented by Mäkelä (1988, 1990a) in many respects. The main differences lie in the more detailed treatment of the nutrient balance of trees and more dynamic treatment of the height and pruning height development. Our simulation results showed that these changes do not qualitatively vary the behaviour of the model very much from the results published by Mäkelä (e.g. 1990a). However, considering the internal circulation of nutrients in trees brings new insights to the role of various nutrient sources on the tree growth. On the other hand, when the height and crown base height development are treated separately, new dynamics are introduced into the stem growth. This also applies to heartwood formation through the connections which the latter is assumed to have with the crown base.

Improvements to the Approach

The model produces qualitatively realistic results, but to produce quantitatively accurate and localized results we need to pay more attention to improving both the description of the input-output processes and the description of stand structure.

The estimation of annual photosynthetic production was done simply by assuming that it is directly proportional to growing season length. The empirical observations from Hyytiälä were corrected by the relative growing season length. It was surprising that this method could produce such good growth estimates. A more analytical method would be to calculate annual unshaded photosynthetic production from short-term step data with more detailed models such as those discussed by Hari et al. (1991). One could calculate the photosynthetic production and water transpiration assuming different foliage biomasses for soils with different water retention capacities under different climatic conditions and use this value as a function of the total foliage mass for the annual photosynthetic production under unshaded conditions (Berninger, in print).

At present the model uses an empirically derived relationship between photosynthetic production and light climate described as a function of the total needle biomass of the stand above the point of reference (Kellomäki et al. 1980). The light response of photosynthesis is thus also included in the model (see Chapter 6.3). In more southerly conditions the interaction curve should not be so convex as it was for Hyytiälä. This is caused both by the higher sun angles and higher incident radiation in the south (Oker-Blom et al. 1989, Kuuluvainen 1992). For the same reasons the homogeneous assumption is less well justified in the south than in the north (Chapter 4). The homogeneity assumption about the canopy might produce overestimates of tree photoproduction especially in the early phases of the stand development, when the canopy has not closed. This would show as too rapid initial growth (Mäkelä 1990b). Higher sun angles in the south would then cause more rapid growth initially with this approach.

The height growth is based on the evidence that open-grown trees might have close to a constant ratio between height and diameter measured at relative height (Ek 1971, Lukkarinen 1993) and that trees in a dominated position show a faster length growth proportionally to photoproduction than the dominant trees (Kellomäki and Kanninen 1980). However, the mechanism of this density effect is poorly known. Deriving length growth from the functional principles is more difficult than the diameter growth since it is also related to the uptake of substances by defining the spatial distribution of the uptaking organs. Until the mechanisms are known, various optimization solutions and game theory may give some insight into the problem. Such theoretical work could provide simple "black box" models, such as used here, derived as alternatives to purely empirical models (Mäkelä 1986, King 1990, Mäkelä and Sievänen 1992).

The simulations produced comparable standing stock values with the growth and yield tables

just by changing the root function efficiency parameter. However, not too much attention should be paid to the absolute values of this parameter. Changes in the values of other parameters which produce the described range of the standing stocks may affect the range of values of this parameter (see e.g. Eq. (6.34), Chapter 6.6). The simulations demonstrated that the model is quite sensitive with respect to this parameter at the range of parameter values that produce realistic stand growth. At the moment there is still no reliable information available on the carbon cost of the nutrient uptake in the roots and how the soil conditions affect this value. The values used here were rough estimates from the work by Mälkönen (1974).

It has been demonstrated that the nutrient concentration in needles may increase as the nutrient availability improves, contrary to the assumption of the constant nutrient concentrations in tissues of different types used in the model (Ingestad and Lund 1986). If this was included, the changes in the fine-root biomass with changes in the root function parameter would be smaller. This would correspond better to the observation of the fertilization experiment of the SWECON project (Linder 1987). Presently it is assumed that the nutrient effects are mainly due to nitrogen. In reality, complex interactions exist between different nutrients which affect for example the nutrient uptake rate (Fitter 1987). Neither does the model presently deal with the possibly very different effect that various nutrients may have on growth.

Presently, the model treats the below ground environment with one parameter that remains constant. However, it is obvious that such constancy is not realistic. The decomposition dynamics of dead organic material produce variable amounts of nutrients for the use of trees over the rotation period of stand (Hari and Nissinen, unpublished results). Empirical observations have shown that at late phases of stand development the proportion of fine roots from the total mass start to increase (Vanninen et al. 1996). Model should be able to account for this type of dynamics once the soil processes are linked with the growth model adequately.

Probably the poorest representation in the model is that of senescence of tree parts and the mortality of whole trees. Equations (6.28–30) in Chapter 6.6 demonstrate that senescence has an important role in growth. High foliage turnover tends to increase foliage growth and to decrease that of other parts, while high turnover of woody components has the opposite effect.

There is experimental evidence that crown base dynamics are related to heartwood formation (see Chapter 5, Kaipiainen and Hari 1985), but more work is needed to reveal the underlying mechanisms and controlling factors before generalizations can be made. The sensitivity analyses performed on the model demonstrated that processes bringing about senescence, particularly of the woody compartments, and their rates have a clear effect on the outcome of the simulations.

Interesting Research Topics Suggested by the Model Simulations

The qualitative behaviour of the model is in reasonable agreement with the observed patterns. This gives reason to put forward some observations on the model behaviour as interesting research problems.

Both the internal circulation of the nutrients and that of structure, in one sense, ie. water transport capacity released by the dying needles to be reused by the new needles, seem to have a powerful influence on carbon distribution. Allocation and its dynamics would thus be very much size dependent. This would need to be taken into account, for example when the performance of different provenances in stem wood production is compared. The environmental conditions in the test fields bringing about marked size differences might completely hide the provenance effect on allocation.

From pipe model theory it follows directly that increased needle mortality as such has rather a small effect on the carbon balance of big trees, if it is not associated with heartwood formation. For example, the higher needle turnover in the south implied a smaller allocation to stem. If dying needles release the transport structure which supplied them for reuse by new needles, the actual compensation of the increased needle senescence would be only the growth of new needles (see Eqs. (6.28–30), (6.34), Chapter 6. 6). However, if needle senescence also implies faster heartwood

formation, as is the case in our model if the needles die in the lower parts of the canopy, then there would have to be considerable formation of new transport capacity in addition to the new needles to maintain the balance between transport capacity and foliage biomass. Since the pruning height of trees is strongly dependent on the total needle mass of the stand, the faster initial development of stands in the south causes a rather large conversion of sapwood to heartwood. This is reflected among other things as a high peak in carbon allocation to stem in the early phase of stand development in Voronez. The above dynamics clearly demonstrate the need to understand the processes bringing out the heartwood formation better.

7.6 Conclusions

The model of the growth and development of Scots pine stands discussed here shows promising flexibility in predicting the performance of pine stands in a variety of conditions. As Mäkelä (1988) concluded, a number of silviculturally important aspects can be accounted for with this basic set of assumptions. A first attempt to use the approach to derive the geographic differences was made here and in earlier work presented by Nikinmaa (1992). The results from both southern and northern Finland were promising but greater changes in the environment caused underestimation of the growth. The very simplistic way of calculating the in- and outflows at different locations could cause the problems in simulating the growth of the southern stands. Conversion of sapwood to heartwood, especially in the coarse roots was another factor that could have caused the deviations of simulated values from the yield table data.

Great emphasis has traditionally been paid to quantifying the actual carbon inflows and outflows in photosynthetic and respiratory reactions. However, as the results of this study show, considerable changes in the allocation patterns may take place, which have marked influence on the simulation outcome as well. It could be that input / output models operating at rather an aggregated level would be accurate enough to match the uncertainty involved in carbon allocation.

The generality of the structural variation needs still to be confirmed. Similar results have been obtained by Berninger and Nikinmaa (1995) and Berninger et al. (1995) from a larger data set in which the locations of this study formed one part. While all of these studies are still based on rather limited data sets, the large differences in the actual dimensions, if persistent, would produce the kind of differences simulated. Thus relating the various parts of trees quantitatively so that functionally reasonable dimensions are matched offers an opportunity to analyse not only the acclimatization / adaptation of plants to their environment but also the implications these have for growth.

To be able to extend these analyses would naturally require information on the structural acclimatization in different environmental conditions and the limits set by such adaptation. To derive functionally reasonable dimensions may be difficult since multiple factors such as hydraulic conductivity, hydraulic safety, mechanical support seem to be involved and in different conditions their importance might change (see Chapter 5). On the other hand, to be able to describe a "reasonable" structure does not guarantee that cambial growth would be able to produce such an outcome in different conditions. Despite of these difficulties, it seems that this route offers an opportunity to evaluate the significance of structural acclimatization on tree growth and functioning. The results show that the approach that we described in Chapter 6 and used in this chapter to predict stand growth gives us new tools to predict stand growth in a variety of conditions and under a variety of management regimes.

References

Albrektson, A. 1980. Total tree production as compared to conventional forestry production. In: Persson, T. eds., Structure and function of northern coniferous forest – an ecosystem study. Ecological Bulletin. Stockholm. p. 315–328.

— & Valinger, E. 1985. Relations between tree height and diameter, productivity and allocation of growth in a Scots pine (Pinus silvestris L.) sample tree material. In: Tigersted, P.M.A., Puttonen, P. & Koski, V. eds., Crop physiology of forest trees. Helsinki University Press, Helsinki. p. 95–105.

Berninger, F. (in print). Effects of drought and phenology on GPP – A simulation study along a geographical gradient. Accepted for publication in the Functional Ecology.

— & Nikinmaa, E. 1995. Foliage area–sap wood area relationships of Scots Pine (Pinus sylvestris) trees in different climates. Can. J. For. Res. 24: 2263–2268.

— , Mencuccini, M., Nikinmaa, E., Grace, J. & Hari, P. 1995. Evaporative demand determines branchiness of Scots pine. Oecologia 102: 164–168.

Decourt, N. 1965. La Pin sylvestre el le Pin laricio de Corse en Sologne. Ann. Sci. Forest. XII(2): 259–318.

Ek, A.R. 1971. Size age relationships for open grown red pine. The University of Wisconsin, Forestry Research Not 156: 4.

Fitter, A.H. 1987. Acquisition and utilization of resources. In: Crawley, M.J. eds., Plant Ecology. Blackwell Scientific Publications, Oxford. p.

Ford, E.D. 1975. Competition and stand structure in some even-aged plant monocultures. J. Ecol. 63: 311–333.

— & Sorrensen, K.A. (1992). Theory and models of inter-plant competition as a spatial process. In: DeAngelis, D.L. & Gross, L.J. eds., Individual based models and approaches in ecology. Chapman and Hall.

Givnish, T. J. 1988. Adaption to sun and shade: a whole plant perspective. Aust. J. Plant physiol. 15: 63–92.

Hakkila, P. 1968. Geographical variation of some properties of pine and spruce pulpwood in Finland. Communicationes Instituti Forestalis Fenniae 66(8). 59 p.

— 1971. Coniferous branches as raw material sources. Communicationes Instituti Forestalis Fenniae 75(1). 60 p.

— 1979. Wood density survey and dry weight tables for pine, spruce and birch stems in Finland. Communicationes Instituti Forestalis Fenniae 96(3). 59 p.

— , Laasasenaho, J. & Oittinen, K. 1972. Branch data for logging work (English summary). Folia Forestalia 147. 15 p.

Hari, P., Kaipiainen, L., Korpilahti, E., Mäkelä, A., Nilsson, T., Oker-Blom, P., Ross, J. & Salminen, R. 1985. Structure, radiation and photosynthetic production in coniferous stands. University of Helsinki, Department of Silviculture. Research Notes 54. 233 p.

— , Nikinmaa, E. & Korpilahti, E. 1991. Modelling canopy, photosynthesis and growth. In: Raghavendra, A. S. ed. Physiology of trees. John Wiley and sons. New York. p. 419–444.

Ilonen, P. 1981. The development of dry matter production of young Scots pine (P. sylvestris) stands (In Finnish). University of Helsinki, Department of Silviculture, M. Sc thesis.

Ilvessalo, Y. 1920. Kasvu- ja tuottotaulukot Suomen eteläpuoliskon mänty-, kuusi- ja koivumetsikoille. Acta Forestalia Fennica 15. 94 p.

— 1937. Growth of natural normal stands in Central North Finland. Communicationes Instituti Forestalis Fenniae 24. 168 p.

— 1970. Natural development and yield capacity of forest stand in mineral soils in Northern Lapland. Acta Forestalia Fennica 108. 43 p.

Ingestad, T. & Lund, A.-B. 1986. Theory and techniques for steady state mineral nutrition and growth of plants. Scand. J. For. Res. 1: 439–453.

Kaipiainen, L. & Hari, P. 1985. Consistencies in the structure of Scots pine. In: Tigersted, P., Puttonen, P. & Koski, V. eds., Crop Physiology of Forest Trees. Helsinki University Press, Helsinki. p. 32–37.

Kärkkäinen, M. 1985. Wood Science (in Finnish). Sallisen kustannus, Sotkamo, 415 p.

Kazimirov, N. I., Zeland, M. G., Liyadinskiy, A. G. & Presnukhin, Y.V. 1984. Potential productivity of pine plantations in European part of USSR. Petrozavodsk. 29 p.

Kellomäki, S., Hari, P., Kanninen, M. & Ilonen, P. 1980. Ecophysiological studies on young Scots pine stands: II. Distribution of needle biomass and its application in approximation light conditions inside the canopy. Silva Fennica 14: 243–257.

— & Kanninen, M. 1980. Eco-physiological studies on young Scots pine stands: IV Allocation of photosynthates for crown and stem growth. Silva Fennica 14: 397–408.

King, D. 1990. The adaptive significance of tree height. Am. Nat. 135: 809–828.

Kuuluvainen, T. 1991. Long-term development of needle mass, radiation interception and stemwood production in naturally regenerated Pinus sylvestris stand on Empetrum-Vaccinium site type in the northern boreal zone in Finland; an analysis based on empirical study and simulation. For. Ecol. Manage. 46: 103–122.

— 1992. Tree architectures adapted to efficient light utilization: is there basis for latitudinal gradients? Oikos: 275–284.

Linder, S. 1987. Responses to water and nutrients in coniferous ecosystems. In: Schultze, E.-D. & Zwölfer, H. eds., Potentials and limitations of eco-

system analyses. Springer Verlag, Berlin–Heidelberg. p. 180–202.
— & Axelsson, B. 1982. Changes in carbon uptake and allocation pattern as a result of irrigation and fertilization in a young Pinus silvestris stand. In: Waring, R.H. ed., Carbon uptake and allocation in subalpine ecosystems as a key to management. Forest research laboratory, Corvallis, Oregon. p. 38–42.
Lukkarinen, E. 1993. Männyn pituus- ja paksuuskasvun suhde. (The relationship between height and thickness growth of Scots pine, in Finnish). Master of Science thesis. Department of Forest Mensuration and Management, University of Helsinki.
Mäkelä, A. 1986. Implications of the pipe model theory on dry matter partitioning and height growth of trees. Jour. of Theor. Biol. 123: 103–120.
— 1988. Models of pine stand development: An ecophysiological systems analysis. University of Helsinki, Department of Silviculture, Research Notes 62. 267 p.
— 1990a. Structural-functional relationships in whole tree growth: resource allocation. In: Dixon, R.K., Meldahl, R.S., Ruark, G.A. & Warren, W.G. (eds). Process modeling of forest growth responses to environmental stress. Timber Press, Portland, Oregon. p. 81–95.
— 1990b. Adaptation of light computations to stand growth models. Silva Carelica 15: 221–239.
— & Sievänen, R. (1992). Height growth strategies in open grown trees.Journal of Theoretical Biology 159: 443–467.
Mälkönen, E. 1974. Annual primary production and nutrient cycle in some Scots pine stands. Communicationes Instituti Forestalis Fenniae 84(5).
Mohren, G.M.J. 1987. Simulation of forest growth, applied to Douglas fir stands in the Netherlands. Pudoc, Wageningen, 184 p.
Nikinmaa, E. 1992 Analyses of the growth of Scots pine; matching structure with function. Acta Forestalia Fennica 235. 68 p.
Oker-Blom, P., Pukkala, T. & Kuuluvainen, T. 1989. The relationship between radiation interception and photosynthesis in forest canopies: effect of stand structure and latitude. Ecol. Modelling.
Ovington, J. 1957. Dry matter production by Pinus sylvestris. Ann. Bot. 21: 287–314.
Sievänen, R. 1992. Construction and identification of models for tree and stand growth. Doctor of Technology thesis. Helsinki University of Technology. Automation technology laboratory. Series A: Research Reports 9.
Vanninen, P., Ylitalo, H., Sievänen, R. & Mäkelä, A. 1996. Effects of age and site quality on the distribution of biomass in Scots pine (Pinus sylvestris L.). Trees 10: 231–238.
Waring, R.H. 1987. Characteristics of trees predisposed to die. BioScience 37(8): 569–574.

Appendix 7.1 The parameter lists of model with values for Hyytiälä.

Parameter name	Symbol	Unit	value	Source
Unshaded annual photoprod.	P_0	kgC/kgDm/a	2.72	Korpilahti (1988)
Growth respiration	r_g	kgC/kgC(str.)/a	0.25	Mohren(1987)/Hari et al. (1982)
Maintenance respiration, needle	r_{mn}	kgC/kgC(str.)/a	0.14	Mohren(1987)/Hari et al. (1982)
Maintenance respiration, branch	r_{mb}	kgC/kgC(str.)/a	0.02	Schäfer et al. (1990)/Mohren (1987)
Maintenance respiration, stem	r_{ms}	kgC/kgC(str.)/a	0.02	Schäfer et al. (1990)/Mohren (1987)
Maintenance respiration, coarse roots	r_{mc}	kgC/kgC(str.)/a	0.02	Schäfer et al. (1990)/Mohren (1987)
Maintenance respiration, fine roots	r_{mf}	kgC/kgC(str.)/a	0.48	Schäfer et al. (1991)/Mohren (1987)
Carbon content, dry matter		kgC/kgdm	0.5	Linder & Axelsson (1982)
Nitrogen content of needles	π_n	kgN/kgdm	0.011	Mälkönen (1974)
Nitrogen content of branches	π_b	kgN/kgdm	0.004	Mälkönen (1974)
Nitrogen content of stem	π_s	kgN/kgdm	0.0007	Mälkönen (1974)
Nitrogen content of trans. roots	π_c	kgN/kgdm	0.0013	Mälkönen (1974)
Nitrogen content of fine roots	π_f	kgN/kgdm	0.004	Mälkönen (1974)
Nutrient uptake per fine-root mass per year	e_r*	kgN/kgdm	0.006–0.02	Mälkönen (1974)
Nitrogen relocation %	u_n		70	Helmisaari (1990)
Threshold fine-root density	D_r	kg/m^2	0.1	Estimated from Persson (1980)
Nutrient uptake "extinction" coefficient	k_r	1/kg	0.	
Branch mass / unit length/ needlemass	$\alpha_b\gamma_b$	m^{-1}	0.89	Hari et al. (1985), Kärkkäinen (1985),
Stem mass / unit length / needle mass	$\alpha_S\gamma_S$	m^{-1}	0.78	Hari et al. (1985), Kärkkäinen (1985),
Transport root mass / unit length / needle mass	$\alpha_c\gamma_c$	m^{-1}	0.45	Hari et al. (1985), Ilvesniemi (pers.com.)
Diameter height ratio of open grown trees	β_{hd}	–	25	Sievänen (pers. com.)
Light gradient multiplier	β_l	–	250	Estimated from volume tables
Light extinction coefficient in biomass bases	k	1/kg	0.0002	Stenberg (pers.com.)
Diameter / length ratio, branches	β_{ld}	–	100	Author's studies (limited sample)
Branches per whorl	β_{pw}	–	4	This study
Lower limit of conical part of crown	h_{dl}	–	0.4	Author's studies (limited sample)
Ratio between foliage average mass density in the canopy and in the shade canopy	χ_{dr}		2	Estimation
Photosynthetic production requirement at the crown base relative to that on average in the crown	δ	–	2	Estimated from Nikinmaa and Hari (1990)
Needle density on the average in the crown/ that at crown base	χ_{dr}		0.5	Estimated, Ilonen (1981)
Needle mass mortality proportion by age classes:				
1	$n1$		0.05	Estimated from field data
2	$n2$		0.2	Estimated from field data
3	$n3$		0.4	Estimated from field data
4	$n4$		1.0	Estimated from field data
Proportion of needle senescence associated with heartwood formation in branches	m_b		0.1	Estimation
Maximum age of coarse roots	d_{cm}		150	Estimation
Average age of coarse roots when 50 % of needle senescence is associated with heartwood formation in coarse roots	θ		135	Estimation
Initial proportion of needle senescence associated with heartwood formation in coarse roots	m_c			
Senescence of fine roots	m_f		1.0*	*Model assumption, see text, estimation, Persson (1980)
Tree mortality threshold parameter	t_{mr}		1.0	Estimation
Tree mortality rate parameter	m_t		1.0	Estimation
Needle area distribution parameters	p,q		1.0	Hari et al. (1982)

8 Concluding Remarks

Pertti Hari, Leo Kaipiainen,
Paavo Pelkonen and Juhan Ross

Wood production has received the main attention in the studies of forests ecosystems. This is natural since wood is and has been a very valuable raw material for many purposes. Immediately with economic value enters the will to manage the resource. Management requires fairly detailed knowledge of the production process. Standing volume and annual yield have been relatively easily measurable quantities and have thus received a major attention in the analysis of forests functions. In fact, forest mensuration is planned to serve these characteristics from forests. There are empirical relationships between the dimensions of trees and growth. Regression models can be constructed using these observations. This kind of empirical modelling has dominated growth and yield studies during last decades.

The most demanding use of models, ie. analysis of the effects of treatments on growth of stands, requires models which are constructed using real causal relationships between the growth and the properties of the stand. This kind of causal analysis is missing in the empirical growth and yield models. This has resulted in quite douptfull applications when empirical models have been used outside their methodological limitations. The reason for this undesirable fact is that the biological research has been unable to provide the necessary knowledge for the basis of models. Traditionally the approach in the ecological research has concentrated on finding out the "players" of the ecosystems and not so much the "rules of the game".

Quantitative methods have increasingly been applied in field studies since late sixties and clear quantitative regularities have been detected. This has changed the situation and quantitative information is available for analysis and modelling of growth and development of stands.

Our methodological aim was to utilize the common structural and metabolic features of all Scots pine stands. Thus key phenomena had to be selected and field methods applicable in rather primitive field conditions had to be developed. The selection of simple set of key variables and processes enabled collection of coherent data sets that cover the hole growing area of the tree species under study.

The work concentrated on above ground tree parts and carbon balance. There were double fold reasons for this division. First of all, a coherent treatment of soil properties and plant growth in natural environments is still to be developed. The kind of experimentation and field work involved in those activities were clearly out of the financial and human resources of this project. On the other hand, we also wanted to study how well fairly detailed analyses of above ground structure and main tree functions could be used to describe the site conditions.

Structural and physiological analyses alone do not allow us to predict growth. We need to have means of connecting different things together. The development of systems analyses after the second world war has brought us new tools to connect material flows of entire plants. However, it has been only with the development of computing capacities that these methods have become feasible and rather simple to use for ecological applications as well. This may be one of the main reasons for the rather limited use of causal models in tree and stand growth studies.

As a part of our work we developed a simple process-based stand growth model that could be parametrized for different locations where Scots pines grow naturally. The model development was backed up by simultaneous experimental work in which some of the ideas behind the model were tested. Also new improvements to the concepts

were made that were not yet considered in the present version of the model. However, they allowed us to estimate the effect of these findings on the simulation results.

Experimentally the main results were the development of photosynthesis field measurement system that improved the reliability of the results and thus facilitated better analyses of the relationship between environmental variables and growth. The annual cycle studies described a methodology to study the outcome of a regulation system that uses different environmental signals and how successful such systems would be in different climates. The mathematical treatment of light climate as a function of shading foliage gave us new tools to incorporate the community level influences on individual tree performance. The structural analysis of Scots pine showed both interesting connections between water conducting pathways and tree structure and geographical variation in the cross-sectional areas at different parts of the water conducting pathway. Also foliage mass–wood cross-sectional area relation increased in north to south gradient.

The model development was based on the following building blocks: i) carbon balance, ie. photosynthetic products are used for growth and maintenance, ii) nutrient balance, ie. nutrients are taken according the metabolic needs, iii) structural regularities determine the allocation of carbon to different compartments. and iiii) the interactions between trees are conveyd by extinction of light within canopy and reduction of nutrients in the soil. These corner stones of the model are rather easy to accept since they seem to correspond the functions of trees.

As process based models should describe realistically the growth and development of a stand, the first phase of testing is to study how well the model is able to reproduce various features of stand growth. The qualitative behaviour of the model is rather satisfactory. The closure of the stand, the patterns of height, diameter and volume growth are as expected and the dying of trees seems to be reasonable, the changes in north south direction are according expectations, etc. Only after we are satisfied with the qualitative behaviour of the model it makes sense to study its quantitative goodness. The quantitative behaviour is still limited to some extend. The lack of test stands which has been monitored for the whole rotation period is one major problem in the improvement of the model. This is why the quantitative judgement of the performance of the model is problematic. On the other hand, it is evident that the model is based on rather limited experimental data.

The requirement of unbiased estimates of stand development is often proposed for the models describing stand growth and development in rotation time scale. It is clear, that we cannot prove that our model is able to give unbiased estimates of growth during rotation time. This fact has been considered to be a severe shortcoming. The requirement of unbiased estimates for rotation time models is, however, unrealistic and shows misunderstanding of the content of unbiased estimates. Thus we do not consider this as relevant argumentation.

However, in the context of this work the ability to utilize the same model for different geographical regions was important. The models could be parametrized with fairly simple field measurements and readily available climate data. Even if the results were not perfect in these preliminary studies, they showed together with the results from the experimental work that our approach can be applied when utilizing process-based models for geographical analyses of growth.

Our co-operation is the first attemt to utilize the common functional and structural basis and their geographical variation in the analysis of growth and development of Scots pine stands. Our field measurements are limited and also some of the solutions of the technical details in the construction of the model should be carefully analysed and better solutions should be found. Despite these shortcomings, we are convinsed that the present approach is very promising. It enables utilization of structural and functional knowledge, gained in places of intensive research, in the analysis of growth and development of any stand. This opens new possibilities for growth research and also for applications in forestry practice.

Submission of Manuscripts Manuscripts should be submitted in triplicate to Acta Forestalia Fennica, Unioninkatu 40 A, FIN-00170 Helsinki, Finland. Detailed instructions to authors have last been printed in Acta Forestalia Fennica 244, are available from the editorial office, and can be found on Acta's WWW pages at http://www.metla.fi/publish/acta/

Publication Schedule Acta Forestalia Fennica is published intermittently, 3 to 6 numbers per year.

Subscriptions and Exchange Subscriptions and orders for back issues should be addressed to Academic Bookstore, Subscription Services, P.O. Box 23, FIN-00371 Helsinki, Finland, Phone +358 9 121 4242, Fax +358 9 121 4450. Subscription price for 1997 is 70 FIM per issue. Exchange inquiries should be addressed to the Finnish Society of Forest Science, Unioninkatu 40 B, FIN-00170 Helsinki, Finland, Phone +358 9 658 707, Fax +358 9 191 7619, E-mail sms@helsinki.fi

Statement of Publishers Acta Forestalia Fennica has been published since 1913 by the Finnish Society of Forest Science. In 1989 Acta Forestalia Fennica was merged with Communicationes Instituti Forestalis Fenniae, started in 1919 by the Finnish Forest Research Institute. In the merger, the Society and Forest Research Institute became co-publishers of Acta Forestalia Fennica. The Finnish Society of Forest Science is a nonprofit organization founded in 1909 to promote forest research. The Finnish Forest Research Institute, founded in 1917, is a research organization financed by the Ministry of Agriculture and Forestry.

Abstracting Articles in Acta Forestalia Fennica are abstracted and indexed in Agrindex, Biological Abstracts, Current Advances in Ecological Sciences, Current Advances in Plant Sciences, Ecological Abstracts, Forest Products Journal, Forestry Abstracts, International Bibliography of Periodical Literature, Life Sciences Collection.

ACTA FORESTALIA FENNICA
The Finnish Society of Forest Science
The Finnish Forest Research Institute

ISBN 951-40-1544-4
ISSN 0001-5636

Cover: Jarmo Koivunen